

TE
662
.A3
no.
FHWA-
RD-
78-157

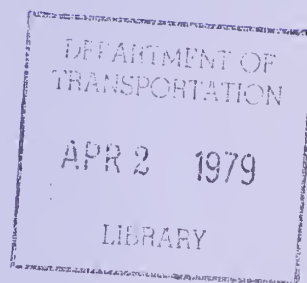
Report No. FHWA-RD-78-157

AN INVESTIGATION OF THE EFFECTIVENESS OF EXISTING BRIDGE DESIGN METHODOLOGY IN PROVIDING ADEQUATE STRUCTURAL RESISTANCE TO SEISMIC DISTURBANCES

Phase VI: Seismic Response of Bridges - Case Studies



October 1978
Final Report




Document is available to the public through
the National Technical Information Service,
Springfield, Virginia 22161

Prepared for
FEDERAL HIGHWAY ADMINISTRATION
Offices of Research & Development
Washington, D. C. 20590

FOREWORD

This report is the seventh in a series to result from research being conducted at the University of California-Berkeley for the Federal Highway Administration (FHWA), Office of Research, under Contract DOT-FH-11-7798. The report will be of interest to structural researchers and designers concerned with earthquake resistant design of highway bridges. It describes results from a series of dynamic analyses performed on three typical highway bridges.

Copies of the report are being distributed by FHWA transmittal memorandum. Additional copies may be obtained from the National Technical Information Service, 5285 Port Royal Road, Springfield, Virginia 22161.

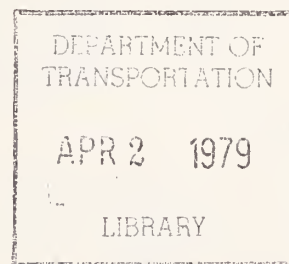

Charles F. Schettrey
Director, Office of Research
Federal Highway Administration

NOTICE

This document is disseminated under the sponsorship of the Department of Transportation in the interest of information exchange. The United States Government assumes no liability for its contents or use thereof. The contents of this report reflect the views of the contractor, who is responsible for the accuracy of the data presented herein. The contents do not necessarily reflect the official views or policy of the Department of Transportation. This report does not constitute a standard, specification, or regulation.

The United States Government does not endorse products or manufacturers. Trade or manufacturers' names appear herein only because they are considered essential to the object of this document.

1. Report No. FHWA-RD-78-157	2. Government Accession No.	3. Recipient's Catalog No.	
4. Title and Subtitle An Investigation of the Effectiveness of Existing Bridge Design Methodology in Providing Adequate Structural Resistance to Seismic Disturbances, Phase VI: Seismic Response of Bridges - Case Studies		5. Report Date October 1978	
		6. Performing Organization Code	
7. Author(s) Roy A. Imbsen, Richard V. Nutt, and Joseph Penzien		8. Performing Organization Report No. EERC-78/14	
9. Performing Organization Name and Address University of California Campus Research Office 118 California Hall Berkeley, California 94720		10. Work Unit No. (TRAIS) FCP 35A2012	
		11. Contract or Grant No. DOT-FH-11-7798	
12. Sponsoring Agency Name and Address Office of Research and Development Federal Highway Administration U.S. Department of Transportation Washington, D.C. 20590		13. Type of Report and Period Covered Phase VI Final Report	
		14. Sponsoring Agency Code S0820	
15. Supplementary Notes FHWA Contract Manager: James D. Cooper, HRS-11			
16. Abstract Presented are the results of six case studies conducted on each of three bridges (the Route 80 Onramp Undercrossing, the Northwest Connector Overcrossing, and the Southwest Connector Overcrossing designed by the California Department of Transportation) when subjected to strong seismic excitation. The dynamic responses of each bridge for separate excitations in the longitudinal and transverse directions were determined using the response spectral, linear time-history, and nonlinear time-history approaches. Maximum response values are interpreted in terms of current design procedures and code provision.			
17. Key Words Earthquake, Bridges, Seismic Analysis, Structural Analysis, Dynamic Behavior		18. Distribution Statement No restrictions. This document is available through the National Technical Information Service, Springfield, Virginia 22161.	
19. Security Classif. (of this report) Unclassified	20. Security Classif. (of this page) Unclassified	21. No. of Pages 186	22. Price



ACKNOWLEDGMENTS

The authors wish to express their appreciation and sincere thanks to the California Department of Transportation, Division of Structures, for their assistance in conducting this study. Special thanks go to Oris Degenkolb, who assisted in selecting the three candidate structures; James Gates and Ed Brunberg, who assisted in computer processing; and Robert Cassano and Guy Mancarti for their continued interest, encouragement and support of bridge seismic research.

The authors also wish to thank Engineering Computer Corporation for its support in allowing them time away from their regular duties and use of company facilities to conduct this study. Their financial assistance in preparing the final manuscript is also greatly appreciated. Special thanks to Joyce Fox for her dedication in typing this manuscript.

METRIC CONVERSION FACTORS

Approximate Conversions to Metric Measures

Symbol When You Know Multiply by To Find Symbol

LENGTH

in 2.5 centimeters
ft 30 centimeters
yd 0.9 meters
mi 1.6 kilometers

AREA

in² 6.5 square centimeters
ft² 0.09 square meters
yd² 0.8 square meters
mi² 2.6 square kilometers
acres 0.4 hectares

MASS (weight)

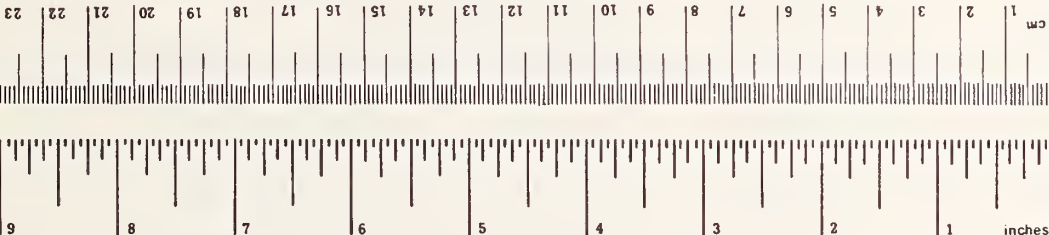
oz 28 grams
lb 0.45 kilograms
(2000 lb) 0.9 tonnes

VOLUME

tsp 5 milliliters
Tbsp 15 milliliters
fl oz 30 milliliters
cups 0.24 liters
pints 0.47 liters
quarts 0.95 liters
gallons 3.8 liters
cubic feet 0.03 cubic meters
cubic yards 0.76 cubic meters

TEMPERATURE (exact)

°F Fahrenheit temperature 5/9 (after subtracting 32) Celsius temperature °C



Approximate Conversions from Metric Measures

When You Know Multiply by To Find Symbol

LENGTH

millimeters 0.04 inches
centimeters 0.4 inches
meters 3.3 feet
kilometers 0.6 miles

AREA

square centimeters 0.16 square inches
square meters 1.2 square yards
square kilometers 0.4 square miles
hectares (10,000 m²) 2.5 acres

MASS (weight)

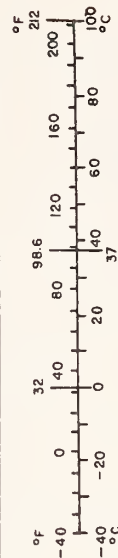
grams 0.035 ounces
kilograms 2.2 pounds
tonnes (1000 kg) 1.1 short tons

VOLUME

milliliters 0.03 fluid ounces
liters 2.1 pints
liters 1.06 quarts
liters 0.26 gallons
cubic meters 35 cubic feet
cubic meters 1.3 cubic yards

TEMPERATURE (exact)

°C Celsius temperature 9/5 (then add 32) Fahrenheit temperature °F



*1 in = 2.54 (exactly). For other exact conversions and more detailed tables, see NBS Misc. Publ. 286, Units of Weights and Measures, Price \$2.25, SD Catalog No. C13.1U-286.

TABLE OF CONTENTS

<u>Chapter</u>		<u>Page</u>
	ACKNOWLEDGMENTS.....	ii
	TABLE OF CONTENTS.....	iv
	LIST OF FIGURES.....	vi
	LIST OF TABLES.....	vii
1	INTRODUCTION.....	1
2	BRIDGE PROPERTIES.....	6
	2.1 Bridge 1 - Route 80 Onramp Undercrossing.....	7
	2.2 Bridge 2 - Northwest Connector Overcrossing.....	8
	2.3 Bridge 3 - Southwest Connector Overcrossing.....	9
3	METHODS OF ANALYSIS.....	22
	3.1 Description of Computer Program.....	22
	3.2 Seismic Excitation.....	24
	3.3 Modeling.....	25
4	RESULTS OF ANALYSIS.....	39
	4.1 Structure Period and Participation Factors.....	39
	4.2 Deadload Reactions.....	39
	4.3 Maximum Column Base Moments and Corresponding Shears.....	40
	4.4 Maximum Transverse Force in Shear Keys.....	41
	4.5 Maximum Deck Displacements.....	41

<u>Chapter</u>		<u>Page</u>
	4.6 Maximum Hinge Movements and Restrainer Forces.....	42
	4.7 Deck Displacement at First Yield.....	42
5	INTERPRETATION OF RESULTS.....	71
	5.1 Structure Periods and Participation Factors.....	71
	5.2 Deadload Reactions.....	73
	5.3 Maximum Column Base Moments and Corresponding Shears.....	74
	5.4 Maximum Transverse Force in Shear Keys.....	84
	5.5 Maximum Deck Displacements.....	87
	5.6 Maximum Hinge Movements and Restrainer Forces.....	92
6	CONCLUSIONS AND RECOMMENDATIONS.....	102
	6.1 Conclusions.....	102
	6.2 Recommendations.....	106
	REFERENCES.....	110
 <u>APPENDIX</u>		
A	Mode Shapes.....	A-1
B	Time History Plots of Selected Column Base Moments and Corresponding Deformations....	B-1
	Time History Plots.....	B-2
C	Time History Plots of Selected Expansion Joint Deformations.....	C-1
	Time History Plots.....	C-2

LIST OF FIGURES

<u>Figure No.</u>	<u>Description</u>	<u>Page</u>
2.1	Typical Bridge Expansion Joint.....	11
2.2	Bridge 1 - Route 80 On-Ramp Overcrossing.....	12
2.3	Bridge 2 - Northeast Connector Overcrossing.....	13
2.4	Bridge 3 - Southwest Connector Overcrossing.....	14
3.1	NEABS-YIELD Bridge Column Interaction Yield Surface Description.....	28
3.2	NEABS Hinge Idealization.....	29
3.3	S18+ Accelerograph.....	30
3.4	S18+ Response Spectrum.....	31
3.5	Bridge 1 - Structural Idealization.....	32
3.6	Bridge 2 - Structural Idealization.....	33
3.7	Bridge 3 - Structural Idealization.....	34

LIST OF TABLES

<u>Table No.</u>	<u>Description</u>	<u>Page</u>
2.1	Basic Characteristics of Bridges Selected for Parameter Study.....	15
2.2	Bridge 1 - Column Properties	16
2.3	Bridge 1 - Hinge Properties.....	17
2.4	Bridge 2 - Column Properties.....	18
2.5	Bridge 2 - Hinge Properties.....	19
2.6	Bridge 3 - Column Properties.....	20
2.7	Bridge 3 - Hinge Properties.....	21
3.1	Duration of Ground motion.....	35
3.2	Case Numbers.....	36
3.3	Bridge 1 - Column Yield Function Constants.....	37
3.4	Bridge 2 - Column Yield Function Constants.....	37
3.5	Bridge 3 - Column Yield Function Constants.....	38
4.1	Bridge 1 - Structural Period and Participation Factors	44
4.2	Bridge 1 - Deadload Forces at the Supports.....	45
	Bridge 1 - Maximum Column Moments and Corresponding Shears	
4.3	1) Due to Transverse Shock.....	46
4.4	2) Due to Longitudinal Shock.....	47
4.5	Bridge 1 - Maximum Transverse Force in Shear Keys for Transverse and Longitudinal Shocks.....	48
	Bridge 1 - Maximum Bridge Deck Displacements	
4.6	1) Due to Transverse Shock.....	49
4.7	2) Due to Longitudinal Shock.....	50
4.8	Bridge 1 - Maximum Hinge Separations and Restrainer Forces for Transverse and Longitudinal Shock.....	51

<u>Table No.</u>	<u>Description</u>	<u>Page</u>
4. 9	Bridge 1 - Deck Displacements at Initial Column Yielding.....	52
4.10	Bridge 2 - Structural Period and Participation Factors.....	53
4.11	Bridge 2 - Deadload Forces at the Supports.....	54
	Bridge 2 - Maximum Column Moments and Corresponding Shears	
4.12	1) Due to Transverse Shock.....	55
4.13	2) Due to Longitudinal Shock.....	56
4.14	Bridge 2 - Maximum Transverse Force in Shear Keys for Transverse and Longitudinal Shocks.....	57
	Bridge 2 - Maximum Bridge Deck Displacements	
4.15	1) Due to Transverse Shock.....	58
4.16	2) Due to Longitudinal Shock.....	59
4.17	Bridge 2 - Maximum Hinge Separations and Restrainer Forces for Transverse and Longitudinal Shock.....	60
4.18	Bridge 2 - Deck Displacements at Initial Column Yielding.....	61
4.19	Bridge 3 - Structural Period and Participation Factors.....	62
4.20	Bridge 3 - Dead Load Forces at the Supports.....	63
	Bridge 3 - Maximum Column Moments and Corresponding Shears	
4.21	1) Due to Transverse Shock.....	64
4.22	2) Due to Longitudinal Shock.....	65
4.23	Bridge 3 - Maximum Transverse Force in Shear Keys for Transverse and Longitudinal Shocks.....	66
	Bridge 3 - Maximum Bridge Deck Displacements	
4.24	1) Due to Transverse Shock.....	67
4.25	2) Due to Longitudinal Shock.....	68
4.26	Bridge 3 - Maximum Hinge Separations and Restrainer Forces for Transverse and Longitudinal Shock.....	69

<u>Table No.</u>	<u>Description</u>	<u>Page</u>
4.27	Bridge 3 - Deck Displacements at Initial Column Yielding.....	70
5.1	Bridge 1 - Column Flexural Yield Rotations.....	96
5.2	Bridge 1 - Maximum Local Bending Ductility Demands at the Column Bases.....	97
5.3	Bridge 2 - Column Flexural Yield Rotations.....	98
5.4	Bridge 2 - Maximum Local Bending Ductility Demands at the Column Bases.....	99
5.5	Bridge 3 - Column Flexural Yield Rotations.....	100
5.6	Bridge 3 - Maximum Local Bending Ductility Demands at the Column Bases.....	101

CHAPTER 1

INTRODUCTION

Bridges are important links in our surface transportation network because they provide the means for overcrossing both manmade and natural obstacles. It is crucial that they continue to function in this vital role following an earthquake when protection of lives and property depends on the efficient movement of emergency traffic. This requires that bridges maintain both structural integrity and accessibility.

1.1 BACKGROUND

Prior to the San Fernando earthquake of February 9, 1971 very little damage to reinforced concrete bridges resulted directly from seismically-induced vibrational effects. Most of the damage on a world-wide basis had been caused by:

- (1) tilting, settlement and overturning of substructures;
- (2) displacement of supports and anchor bolt breakage; and
- (3) settlement of approach fills and wingwall damage.

In California, the damage had been minimal, totaling approximately \$100,000, (1)* for the eleven most significant earthquakes (magnitudes 5.4 to 7.7) which occurred from 1933 to 1971. This general observation changed drastically, however, with the San Fernando earthquake (magnitude 6.6) which caused approximately \$6,500,000 damage to bridges, most of it due to vibration effects.

*Numerals in parentheses refer to reference numbers.

As a result of the San Fernando earthquake, there has been an increased public awareness of the potential of earthquake-induced damage to bridges. A reflection of this interest is a recognition of the need to design highway bridges that are more resistant to the damaging effects of seismic forces.

Immediately following the earthquake, the Office of Structures, California Department of Transportation (CALTRANS) recognized the need to develop a rational earthquake design criteria for bridges. Efforts were initiated to develop new earthquake design guidelines that would consider seismicity and the vibrational properties of both the bridge and the underlying soil. This effort provided the basis for a new national seismic bridge design code (2) that is currently accepted by the American Association of State Highway and Transportation Officials (AASHTO). This code is to a large degree a designer's response to the catastrophic types of failures experienced in the San Fernando earthquake.

The new code provides for seismic analysis by the equivalent static force method for simple structures. Response spectrum or transient analysis is required for more complex structures. CALTRANS, now a leader in the seismic design of bridges, is currently using 3 dimensional response spectrum modal analysis on a large number of their structures since they have found that the equivalent static force method is cumbersome to apply and generally yields unreliable results in most cases.

1.2 STATEMENT OF THE PROBLEM

Although the response spectrum dynamic analysis procedure is an improvement over previous bridge seismic design practice, there are limits to its applicability. Since postelastic behavior is not specifically accounted for in the overall response analysis, a ductility factor is applied to reduce the forces obtained from the linear response spectrum analysis. Because little is known about bridge ductility, the ductility factors used in bridge design have been extrapolated from research on building structures. Furthermore, the linear analysis does not account accurately for nonlinear behavior at expansion joint hinges, nor does it provide a means for assessing the redistribution of stress as yielding occurs in the ductile members. Further development and evaluation of bridge earthquake design methodology in the area of structural analysis has been limited by the unavailability of reliable analytical procedures for nonlinear seismic analysis of bridge structures.

1.3 OVERALL RESEARCH EFFORT

Following the San Fernando earthquake, the U. S. Department of Transportation, Federal Highway Administration, recognized the need for increased understanding of the behavior of bridge structures during earthquakes. A research project entitled An Investigation of the Effectiveness of Existing Bridge Design Methodology in Providing Adequate Structural Resistance to Seismic Disturbances was initiated at the Earthquake Engineering Research Center, University of California, Berkeley. This investigation consisted of the following six phases:

1. A thorough review of the world's literature on seismic effects on highway bridge structure, including damage to bridges during the San Fernando earthquake of February 9, 1971 (3).
2. An analytical investigation of the dynamic response of long multiple-span highway overcrossings of the type which suffered heavy damage during the 1971 San Fernando earthquake (4).
3. An analytical investigation of the dynamic response of short, single, and multiple span highway overcrossings of the type which suffered heavy damage during the 1971 San Fernando earthquake (5,6).
4. Detailed model experiments on a shaking table to provide dynamic response data similar to prototype behavior which was used to verify the validity of theoretical response predictions (7).
5. Correlation of dynamic response data obtained from shaking table experiments and theoretical response. Modification of analytical procedures as found necessary to achieve correlation (8).
6. Preparation of recommendations for changes in seismic design specifications and methodology as necessary to provide adequate protection of reinforced concrete highway bridges against severe damage in future earthquakes.

This report represents a part of Phase 6 of this investigation.

1.4 PHASE 6 RESEARCH OBJECTIVES

Recognizing the limitations inherent in using elastic analysis techniques to expand in the development of existing bridge design methodology, this phase of the project has been extended to apply the analytical capabilities developed and refined during this research effort to the problems currently confronting the practicing engineer. The analytical capabilities which have evolved through the various phases of this project now make it possible to evaluate the nonlinear behavior in the columns and expansion joint hinges. The objective of this case study is to compare the results of a time history analysis that considers the above nonlinear behavior with results from both a linear time history and response spectrum analysis. Based on this comparison the effectiveness of the current analytical approach as outlined in the seismic design recommendation can be evaluated. Also, the applicability of the nonlinear analysis capabilities to bridge design can be assessed. Extending this project in this manner will provide the profession with answers to some of the problems needed to continue development of the seismic design methodology and also demonstrate how other and future problems may be solved using the capabilities developed in this research effort.

CHAPTER 2

PROPERTIES OF THE BRIDGES

Three bridges which were designed by the California Department of Transportation were selected for this study. All three structures consist of curved concrete box girder decks cast monolithically with single column bents. The columns have shapes that were selected partially for architectural reasons. Two of the bridges have columns which are flared at the top. This limits yielding to the base of the column during an earthquake. Because of the length of the bridges, each structure has one or more intermediate expansion joints to accommodate temperature movement.

This type of structure is common in California and is typically used in freeway interchanges. During the San Fernando earthquake of 1971, some of the most spectacular failures involved this type of bridge (9). One of the primary causes of failure appeared to be the separation of expansion joint hinges. As a result all structures of this type designed since the earthquake, including the three used in this study, have been fitted with restrainers designed to prevent separation. These restrainers must be gapped to allow freedom of movement for temperature, etc. A typical expansion joint hinge of this type is shown in Figure 2.1.

In order to obtain a better understanding of the behavior of this type of bridge, each of the structures selected had a different fundamental period of vibration. A summary of some of the important

properties of these bridges is shown in Table 2.1. A short description giving the details of each bridge follows.

2.1 BRIDGE 1 - ROUTE 80 ONRAMP UNDERCROSSING

This bridge, which is shown in Figure 2.2, is a six span reinforced concrete box girder structure with one intermediate expansion joint located midway between the abutments. The total bridge length is 694 feet with span lengths of 100, 143, 117, 117, 117, and 100 feet. The bridge is on a relatively tight horizontal curve. The single column bents of constant cross-section are relatively short and stiff and approximately uniform in height. The principal axes of the columns are radial and tangent to the curved superstructure. Column properties and ultimate capacities are shown in Table 2.2. This bridge has the smallest fundamental period of the three bridges selected for the study.

The expansion joint hinges are typical California design with elastomeric bearing pads and steel cable restrainer units. Because of the curved alignment and relatively short deck length, the gaps in the restrainer units and the expansion joint seat are small. Properties of the expansion joint are shown in Table 2.3.

Northeast Connector Overcrossing Bridge is a hybrid structure consisting of both a conventionally reinforced concrete box girder section and a cast-in-place post tensioned prestressed concrete box girder section. A single intermediate expansion joint separates the two sections. The prestressed portion has longer span lengths and slightly taller columns. Since all columns are essentially the same shape, the prestressed section has a higher fundamental period of vibration than the conventionally reinforced section. This difference in period allows each section to respond somewhat independently during an earthquake. This structure has a period range which is between the other two structures selected.

The horizontal alignment of this bridge begins on a tangent and changes to a moderate curve in the fourth span. The span lengths are 108, 130, 130, 138, 192, 187.7, 172.3 and 80 feet. The total bridge length is 1138 feet. A schematic of this structure is shown in Figure 2.3.

The columns are octagonal in cross-section at the base and flared in the transverse direction at the top. Column properties and ultimate capacities are shown in Table 2.4. The principal axes of the columns are tangent and normal to the centerline of the superstructure.

The expansion joint hinge is typical of California designs. Four cable restrainer units, of eight cables each, are provided to prevent separation at the hinge. Elastomeric bearing pads provide for

temperature movement and support the load. Vertical restraining devices are provided to prevent vertical separation at the hinge. Concrete shear keys limit relative transverse movement at the expansion joint. The properties of this hinge are given in Table 2.5.

2.3 BRIDGE 3 - SOUTHWEST CONNECTOR OVERCROSSING

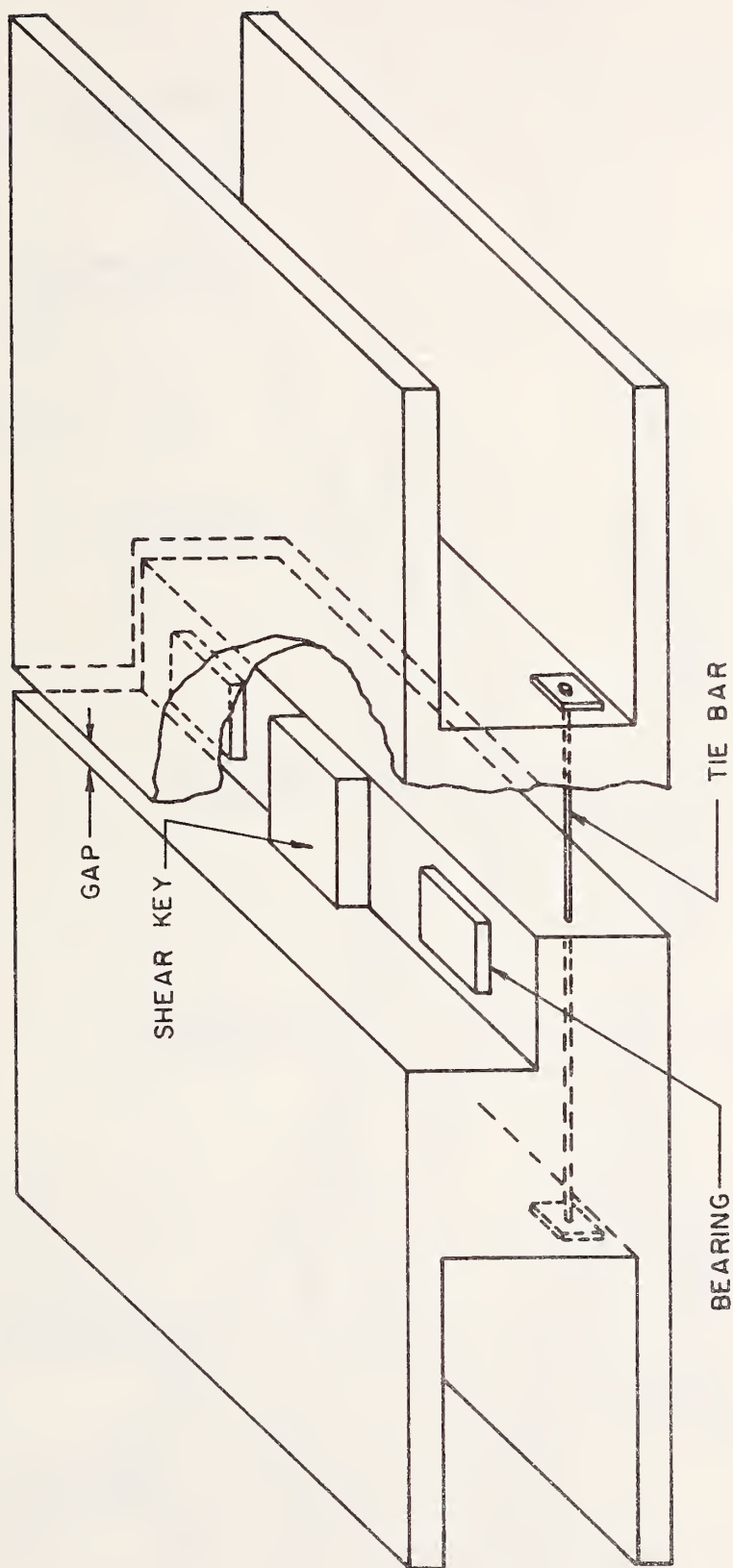
Southwest Connector is the largest of the three bridges studied. It also consists of both conventionally reinforced concrete and cast-in-place post tensioned prestressed concrete box girder sections. The single prestressed portion has longer span lengths but generally shorter column lengths than the two conventionally reinforced sections. The added mass of the deck carried by the columns in the prestressed section is offset by the decreased column height and thus the dynamic response of all sections are somewhat similar. The column heights are on the average much higher than the other two structures, and thus the fundamental period of this structure is the longest of the three bridges.

The total length of this bridge is 1410 feet with individual span lengths of 170, 205, 204.8, 134.3, 149.9, 125, 125, 155 and 141 feet. The horizontal alignment is a constant curve with a 1050' radius. Shown in Figure 2.4 is a schematic drawing of this bridge.

Single column bents ranging in height from just over 60 feet to nearly 86 feet support the structure. These columns have an elongated octagonal cross-section at the base with the strong axis in the transverse direction. The columns are flared in the transverse direction at the top for architectural reasons. Therefore, yielding

during an earthquake is confined to the base of the column. Column properties are shown in Table 2.6.

This structure has two different types of expansion joint hinges with similar displacement compatability and restraining properties. The first hinge which separates the prestressed section from one of the reinforced sections, was designed to allow post tensioning of the prestressed section after the hinge was in place. Greased neopreme strips were provided at bearing points in order to accomodate prestress shortening. The second hinge has 1/16" asbestos sheet packing inserted between the two steel bearing surfaces. Therefore, movement at both hinges takes place as sliding after a very small friction force is overcome. Both hinges are fitted with restrainer cables to prevent separation. Hinge properties are shown in Table 2.7.



TYPICAL BRIDGE EXPANSION JOINT

FIGURE 2.1

SUPERSTRUCTURE PROPERTIES

$L = 694.0 \text{ FT}$
 $A = 83.7 \text{ FT}^2$
 $I_x = 814.1 \text{ FT}^4$
 $I_y = 353.7 \text{ FT}^4$
 $I_z = 12868.8 \text{ FT}^4$
 $DL = 12.56 \text{ K/FT}$
 $E = 3000 \text{ KSI}$
 $R = 600 \text{ FT}$

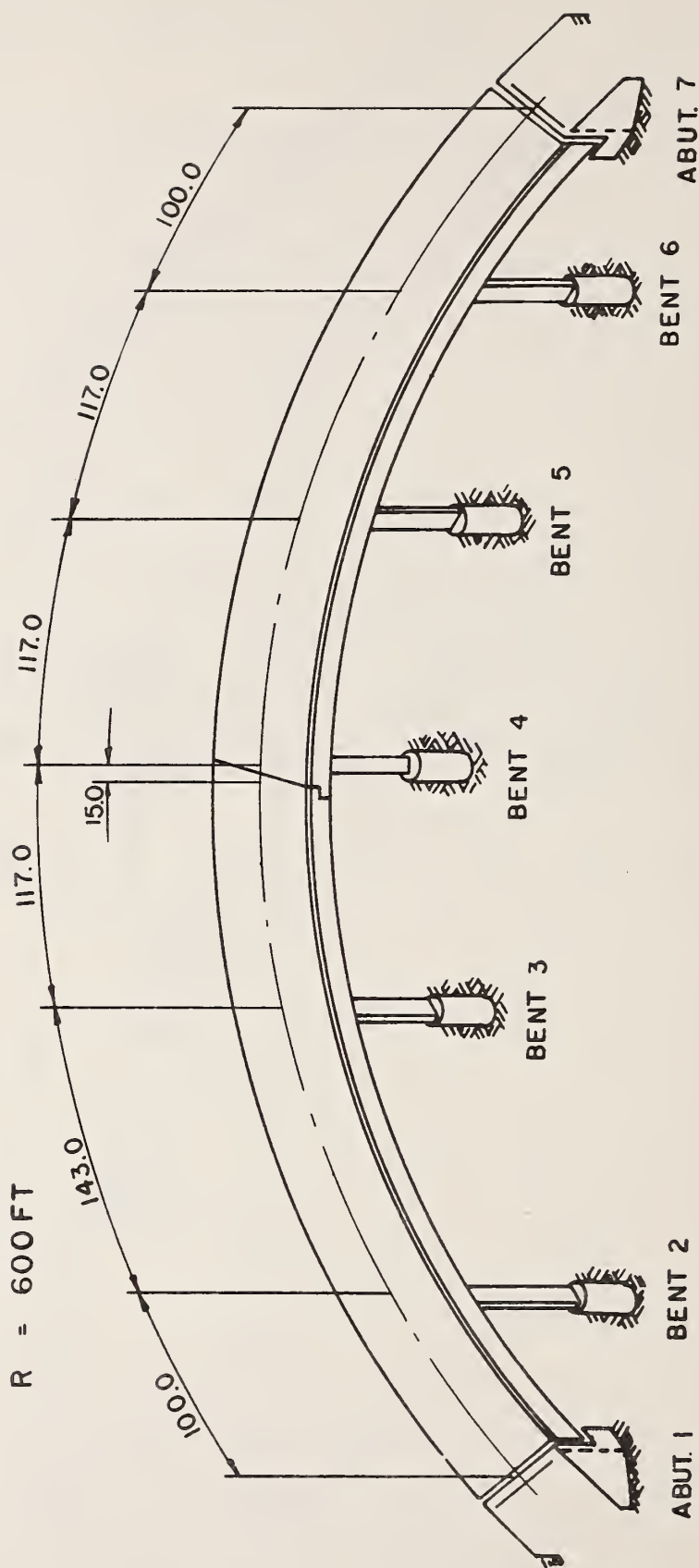


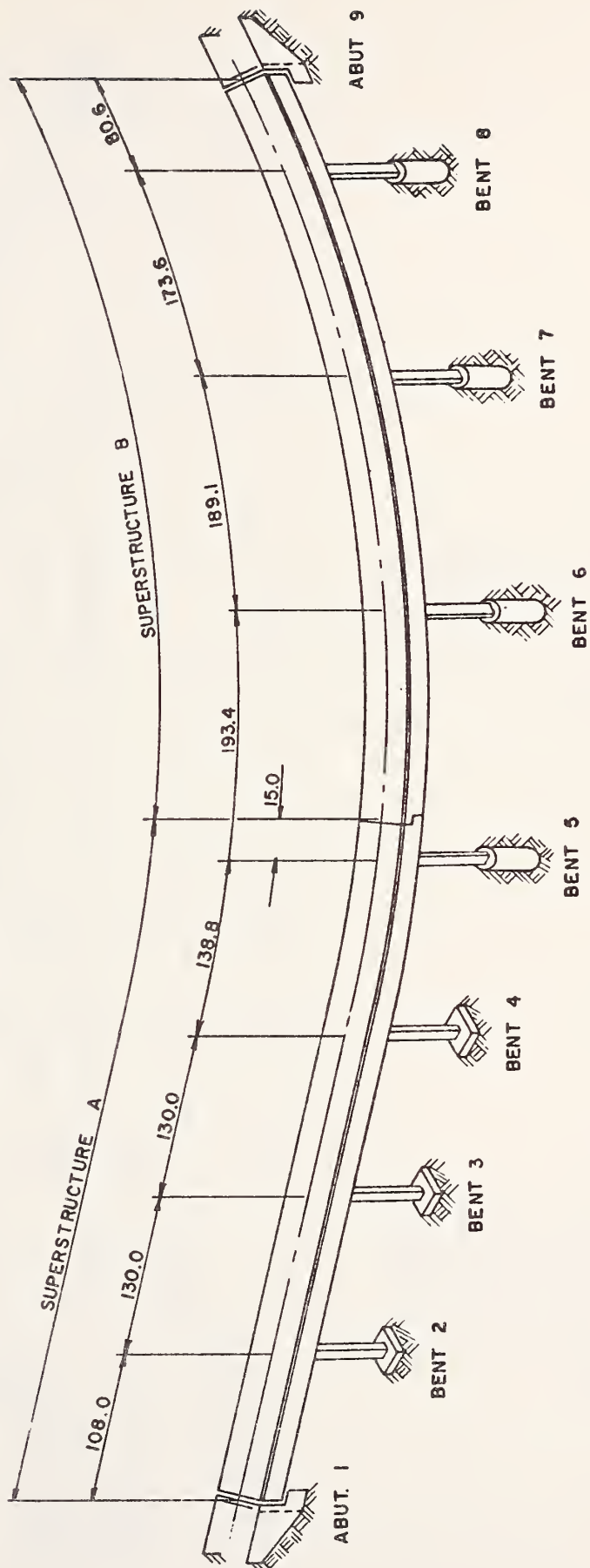
FIGURE 2.2

SUPERSTRUCTURE A

$L = 521.8 \text{ FT}$
 $A = 48.0 \text{ FT}^2$
 $I_x = 850.0 \text{ FT}^4$
 $I_y = 3130.5 \text{ FT}^4$
 $I_z = 381.4 \text{ FT}^4$
 $DL = 7.2 \text{ K/FT}$
 $E = 3000 \text{ KSI}$

SUPERSTRUCTURE B

$L = 621.7 \text{ FT}$
 $A = 54.5 \text{ FT}^2$
 $I_x = 850.0 \text{ FT}^4$
 $I_y = 3528.3 \text{ FT}^4$
 $I_z = 406.5 \text{ FT}^4$
 $DL = 8.175 \text{ K/FT}$
 $E = 3000 \text{ KSI}$
 $R = 1083 \text{ FT}$



BRIDGE 2
NORTHEAST CONNECTOR OVERCROSSING

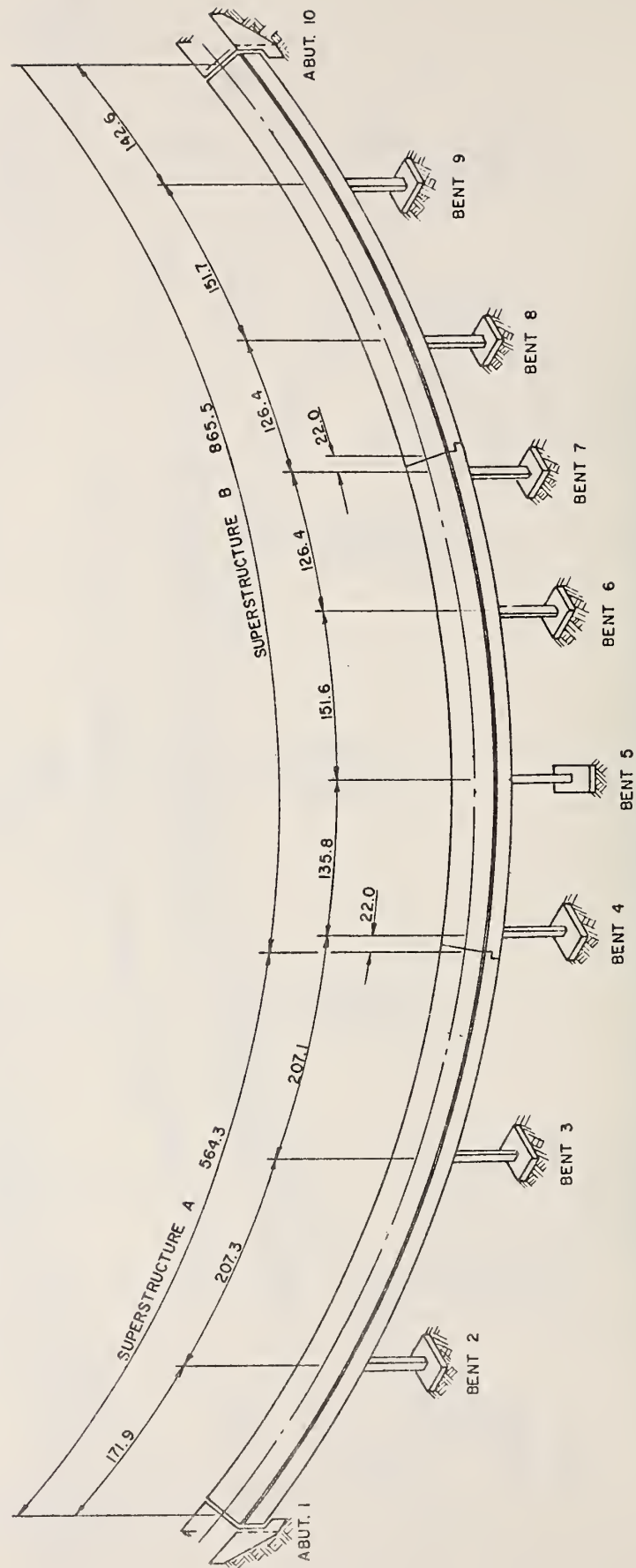
FIGURE 2.3

SUPERSTRUCTURE A

$A = 81.3 \text{ FT}^2$
 $I_x = 1000 \text{ FT}^4$
 $I_y = 9713.5 \text{ FT}^4$
 $I_z = 664.6 \text{ FT}^4$
 $DL = 12.195 \text{ K/FT}$
 $E = 3000 \text{ KSI}$
 $R = 1062 \text{ FT}$

SUPERSTRUCTURE B

$A = 75.5 \text{ FT}^2$
 $I_x = 980 \text{ FT}^4$
 $I_y = 9152.9 \text{ FT}^4$
 $I_z = 640.0 \text{ FT}^4$
 $DL = 11.325 \text{ K/FT}$
 $E = 3000 \text{ KSI}$
 $R = 1062 \text{ FT}$



BRIDGE 3
SOUTHWEST CONNECTOR OVERCROSSING

FIGURE 2.4

Bridge			Curve Radius (ft)	No. Col. Per Bent	Column Lengths (ft)		Hinges		Periods of the First 20 Modes (Sec)	
Name	No.	Length (ft)			Min.	Max.	No. Location	Span	Max.	Min.
Rte 80 On-Ramp Undercrossing	1	694	600	1	24.3	26.3	1	3	.40	.07
Northeast Conn. Undercrossing	2	1138	1075	1	25.1	49.4	1	5	1.11	.15
Southwest Conn. Undercrossing	3	1410	1050	1	60.7	85.6	2	3,7	1.94	.21

TABLE 2.1 - Basic Characteristics of Bridges Selected
for Parameter Study

			ULTIMATE CAPACITY		
Bent No.	Length* (ft)	Steel Area (in ²)	Axial P _o (kips)	Long. Moment My _o (k-ft)	Trans. Moment Mz _o (k-ft)
2	24.30	108	17,600	9310	12870
3	24.30	108	17,600	9310	12870
4	24.30	108	17,600	9310	12870
5	25.30	108	17,600	9310	12870
6	26.30	108	17,600	9310	12870

*From top of footing to neutral axis of deck

TABLE 2.2 - Bridge 1 - Column Properties

EXPANSION JOINT HINGE LOCATION

SPAN 3

Number of Restrainer Units	2
Transverse Location of Restrainer Units	<u>+</u> 12.88
Restrainer Gap (Nominal)	.10 FT
Axial Stiffness of Restrainer Unit	1224 K/FT
Axial Yield Force of Restrainer Unit	352 K/FT
Expansion Joint Seat Gap (Nominal)	.08 FT
Coefficient of Friction of Bearings	.4
Total Shear Stiffness of Bearings	700 K/FT

TABLE 2.3 - Bridge 1 - Hinge Properties

			ULTIMATE CAPACITY		
Bent No.	Length* (ft)	Steel Area (in ²)	Axial P _o (kips)	Long. Moment My _o (k-ft)	Trans. Moment Mz _o (k-ft)
2	36.5	112.3	16,348	10,340	10,340
3	41.9	84.2	15,230	8,010	8,010
4	47.7	84.2	15,230	8,010	8,010
5	25.1	140.4	17,470	12,600	12,600
6	44.38	112.3	16,348	10,340	10,340
7	49.4	112.3	16,348	10,340	10,340
8	36.3	93.6	15,600	8,800	8,800

*From top of footing to neutral axis of deck.

TABLE 2.4 - Bridge 2 - Column Properties

EXPANSION JOINT HINGE LOCATION

SPAN 5

Number of Restrainer Units	4
Transverse Location of Restrainer Units From Bridge Centerline	$\begin{array}{c} + 9.73 \text{ FT} \\ \pm 4.83 \text{ FT} \\ \hline \end{array}$
Restrainer Gap (Nominal)	.27 FT
Axial Stiffness of Restrainer Unit	1073 K/FT
Axial Yield Force of Restrainer Unit	352 K
Expansion Joint Seat Gap (Nominal)	.21 FT
Coefficient of Friction of Bearings	.4
Total Shear Stiffness of Bearings	484 K/FT

TABLE 2.5 - Bridge 2 - Hinge Properties

			ULTIMATE CAPACITY		
Bent No.	Length* (ft)	Steel Area (in ²)	Axial P _o (kips)	Long. Moment My _o (k-ft)	Trans. Moment Mz _o (k-ft)
2	60.7	480	35,830	38,580	47,470
3	71.0	480	35,830	38,580	47,470
4	85.6	480	35,830	38,580	47,470
5	84.0	480	35,830	38,580	47,470
6	79.6	400	32,630	34,430	42,530
7	75.6	400	32,630	34,430	42,530
8	67.84	320	29,430	29,800	37,030
9	64.6	320	29,430	29,800	37,030

*From top of footing to neutral axis of deck.

TABLE 2.6 - Bridge 3 - Column Properties

EXPANSION JOINT HINGE LOCATION

SPAN 3

SPAN 7

Number of Restrainer Units	4	4
Transverse Location of Restrainer Units	± 11.63 FT ± 3.88 FT	± 13.50 FT ± 7.50 FT
Restrainer Gap (Nominal)	.33 FT	.25 FT
Axial Stiffness of Restrainer Unit	2217 K/FT	1224 K/FT
Axial Yield Force of Restrainer Unit	308 K	440 K
Expansion Joint Seat Gap (Nominal)	.20 FT	.20 FT
Coefficient of Friction Bearings	.05	.05
Total Shear Stiffness of Bearings	10^{10}	10^{10}

TABLE 2.7 - Bridge 3 - Hinge Properties

3.1 DESCRIPTION OF COMPUTER PROGRAMS

Three different types of analyses were performed on each of the three bridges selected for this study. A response spectrum (10), modal analysis was performed because this is the approach currently being used at the California Department of Transportation (CALTRANS) and appears at the present to be the most desirable from a design implementation point of view. A linear time history, which is the most sophisticated type of analysis available to the bridge designer at CALTRANS, was also performed. The nonlinear dynamic analysis capabilities (4,8), which are the result of previous research efforts of this research project, were used for comparisons with currently used and available linear analysis techniques.

The linear analysis capabilities of STRUDL (STRuctural Design Language) which is the main analytical tool available to CALTRANS, were used to perform the response spectrum and linear time history analyses. STRUDL is a well known general purpose computer program for static and dynamic analysis of linear structural systems. The MCAUTO proprietary version (12) was used along with bridge STRUDL input code generating facilities STRUBAG (STRUDL Bridge Analysis Generator), developed in-house at CALTRANS.

The nonlinear analysis was performed by the NEABS (Nonlinear Earthquake Analysis of Bridge Systems) program. This computer

program uses a step-by-step integration procedure which assumes piecewise linear behavior over each increment of time. Either the linear or constant acceleration method can be chosen. The linear acceleration method was used for this study. Loading was input as rigid support accelerations. The program element library has the following linear and nonlinear element types:

- . Linear elastic truss elements
- . Linear elastic and elasto-plastic straight beam elements
- . Linear elastic circularly curved beam elements
- . Linear elastic and bi-linear boundary spring elements
- . Linear and nonlinear expansion joint elements

The two nonlinear parameters considered for this study were the yielding of the single column bents, and the nonlinearity of the expansion joint hinges.

The yielding of columns is limited to axial and flexural yielding along an interaction yield surface. The yield surface for a typical bridge column is shown in Figure 3.1. The parameters which define this surface are calculated using a separate computer program called YIELD (4). The ultimate capacity of the column in shear is considered to be infinite. Thus, there is no reduction in shear values due to yielding.

The nonlinear behavior of the expansion joint hinges are modeled using the expansion joint element shown in Figure 3.2. In this

expansion joint hinge, the restrainers are assumed inactive until movement at the joint is sufficient to take up the gaps which are normally placed in the restrainer anchorages to allow for normal movements of the joint. When the restrainers are active, they behave in an ideally elasto-plastic manner. Closure of the hinge is limited by stiff impact springs activated after a seat gap is taken up. This represents banging of the two adjacent superstructure sections. The effect of bearing pads is also included in the expansion joint element. The vertical and shear stiffnesses of the pads can be represented by springs. Sliding of the pads when the coefficient of friction is overcome is also considered.

A linear dynamic analysis program BSAP (Bridge Structural Analysis Program), also developed as a part of the six phase project, uses linear elements, and has an input format similar to NEABS. As a check on the NEABS model, a BSAP problem was run for each bridge using input data similar to that used by NEABS. The results of a frequency analysis on BSAP were then compared with STRUDL frequency results as a means of spotting errors in the input.

3.2 SEISMIC EXCITATION

Rigid support motion was used for all of the bridges. The S18+ time history ground motion developed by Seed and Idress (14) for a simulated 8+ Richter magnitude earthquake was used. The response spectrum used was generated on STRUDL for 5 percent damping. The time history ground motion and corresponding response spectrum are shown in Figures 3.3 and 3.4 respectively. This ground motion was applied to the bridges in the two orthogonal

directions. The longitudinal motion was in a direction parallel to a straight line between the abutments. The transverse motion was perpendicular to the longitudinal.

Because of the costs involved in nonlinear analysis and because of prior tests to determine the most critical time after onset of the earthquake attack, some of the analyses were not allowed to run for the entire duration of ground motion. Table 3.3 shows the duration of ground motion used for each analysis.

With three types of analysis for each of the three bridges studied and ground motion in two directions, the total number of cases examined amounted to 18. These cases are numbered for convenience as shown in Table 3.4.

3.3 MODELING

The bridge decks and columns were modeled with space frame members. Masses in the deck were lumped at the quarter points. Column masses were lumped at the third points. For simplicity, the base of each column was assumed fixed at the footing. A typical structure idealization showing the location of lumped masses is shown for each bridge in Figures 3.5, 3.6 and 3.7.

A structure generation program was used to develop the STRUDL model. This program models the freedom of movement at the abutments and the hinges by using member releases in a short member at these locations.

This is done to insure that the superstructure mass is lumped on the proper portion of the superstructure. The curved portion of the superstructure is modeled with straight space frame members at the chords since STRUDL does not have curved members.

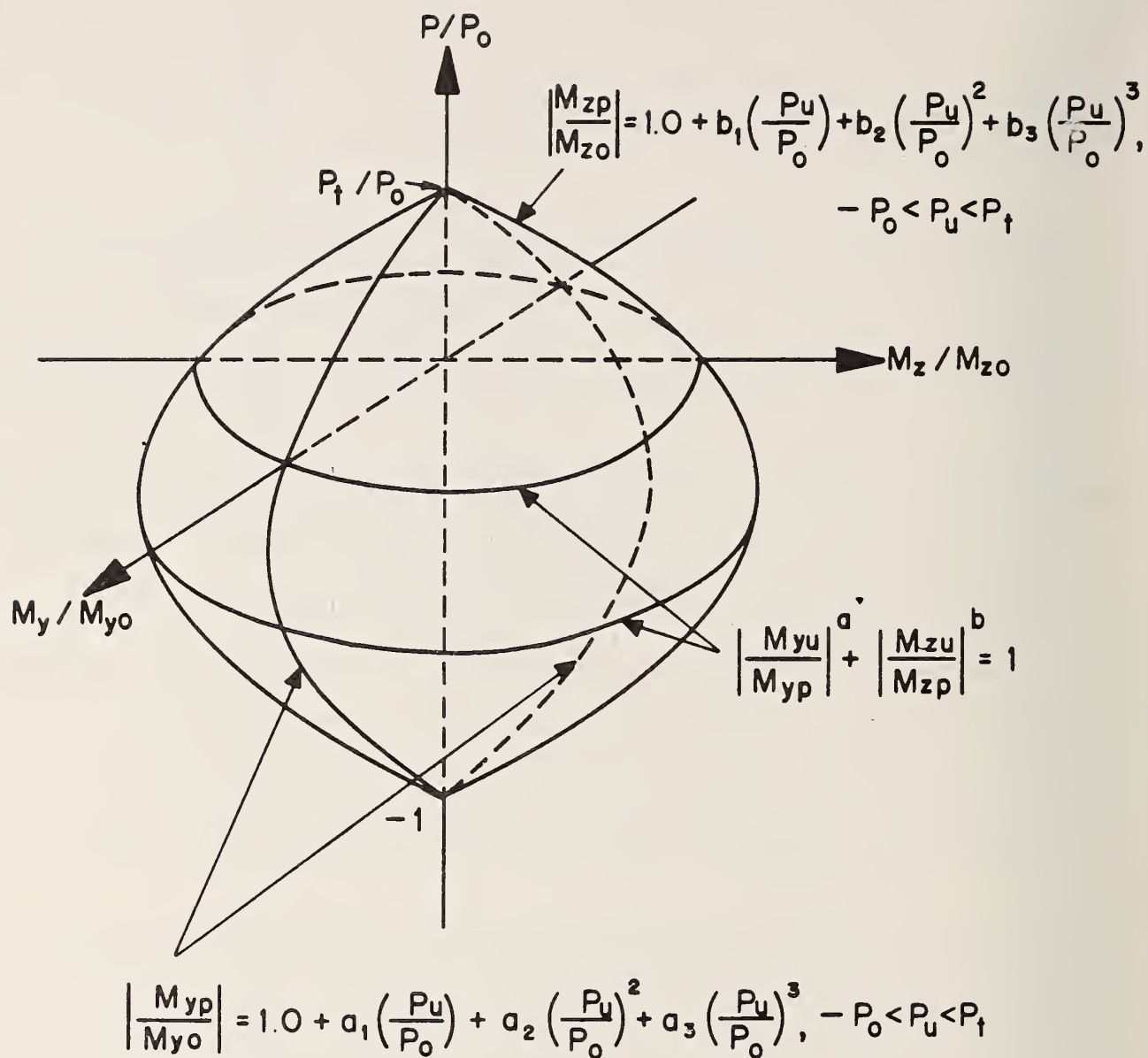
The hinge for STRUDL is modeled by releasing member axial forces, and transverse and longitudinal bending forces at the hinge. The effect of restrainers is represented by placing transversely eccentric space frame members between both sections of the superstructure as shown in Figures 3.5, 3.6 and 3.7. This idealization assumes no gap and both tension and compression at the restrainers.

The basic assemblage of members for BSAP and NEABS is similar to that used for STRUDL with a few exceptions. First, the curved superstructure is represented by circularly curved beam members. Secondly, the freedom at the abutments and the expansion joint hinge are modeled with special foundation spring elements and expansion joint elements. These elements make it unnecessary to use short space frame members to insure proper lumping of the mass.

The NEABS expansion joint element has several nonlinear parameters that must be input. Design values shown on the plan drawings for tie and seat gaps were used. In actuality, these values will vary depending on such factors as temperature and shrinkage. Cable restrainer stiffnesses were calculated assuming an effective Young's modulus of 13,800 kips per square inch. The yield force in a typical 3/4 inch restainer was taken as 30.6 kips. The shear stiffness of elastomeric bearing pads was calculated based on an assumed

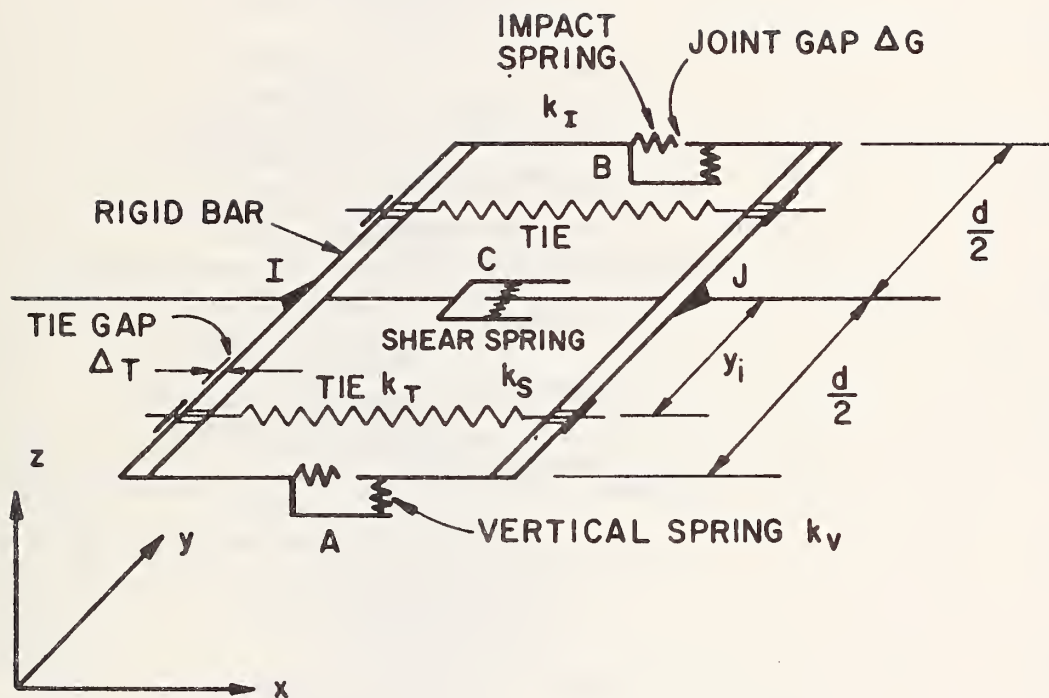
shear modulus of 135 psi. The coefficient of sliding friction was assumed to be 0.4. For lubricated sliding steel plates, the shear stiffness was assumed to be very high and the friction very low. For the purposes of modeling impacting of the superstructure, the impact spring was assumed to have the axial stiffness of the shortest adjacent section of superstructure.

Nonlinear column elements were used at locations where column yielding might be expected. Nonlinear columns were modeled on NEABS by inputting parameters obtained from a separate column analysis computer program called YIELD. In addition to maximum values for axial force and bending, normalized constants which define the yield surface are required. The values for these constants are shown for the three bridges in Tables 3.3, 3.4 and 3.5.



NEABS/YIELD BRIDGE COLUMN INTERACTION
YIELD SURFACE DESCRIPTION

FIGURE 3.1



NEABS HINGE IDEALIZATION

FIGURE 3.2

S.I.8 + RECORD GENERATED BY SEED AND IDRISS

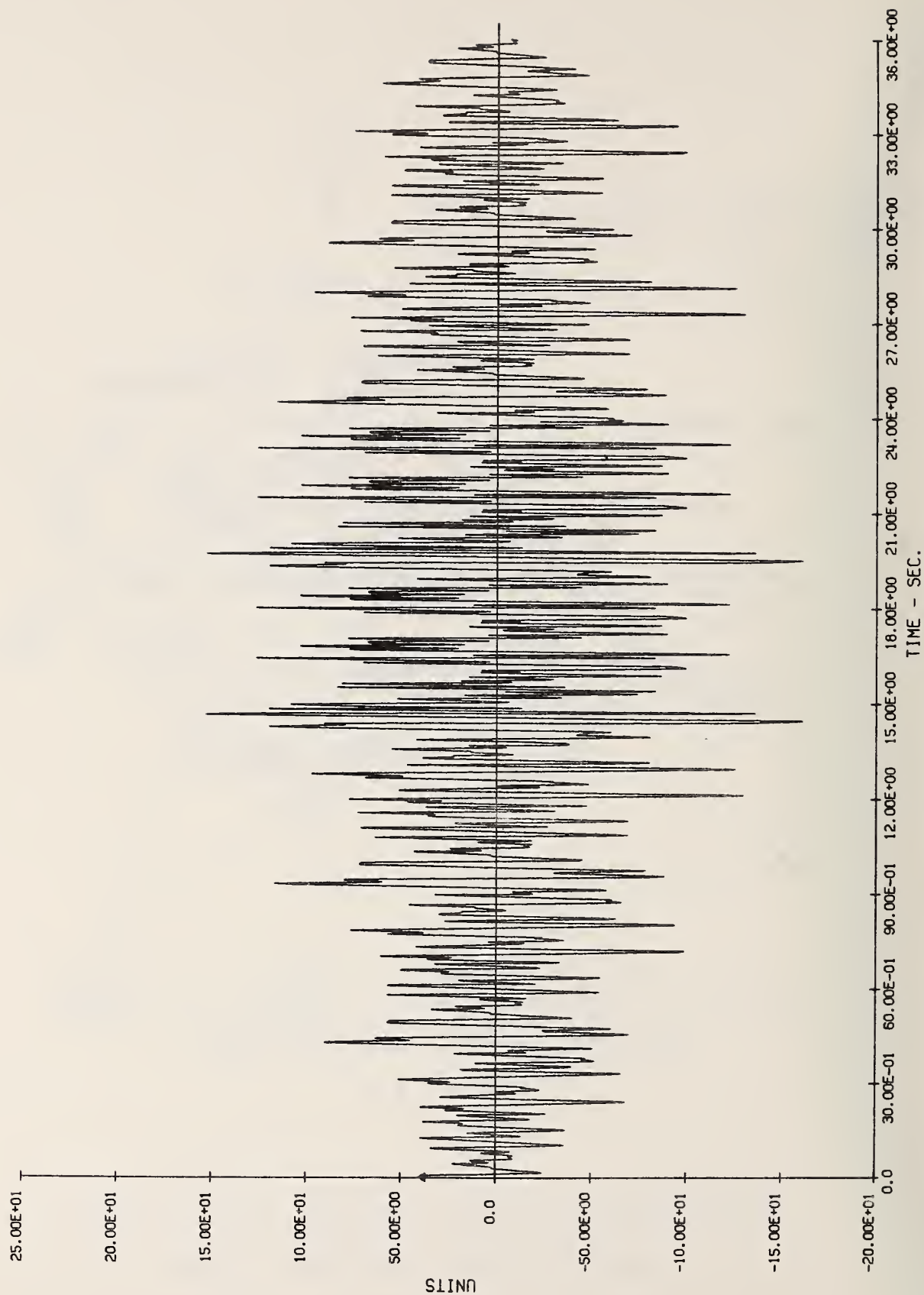


FIGURE 3.3

RESPONSE SPECTRUM FOR S18 +
GROUND MOTION
5% DAMPING

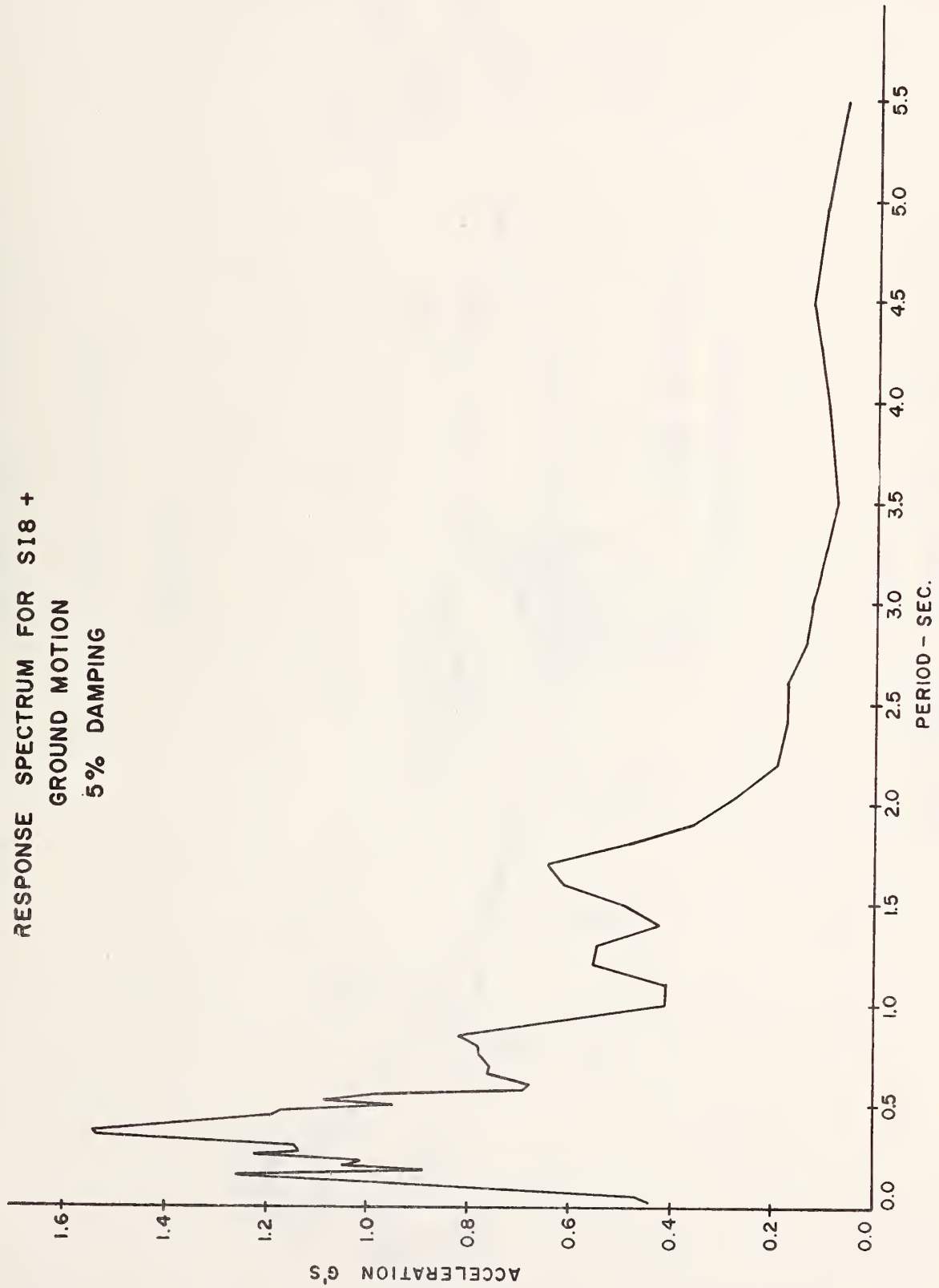
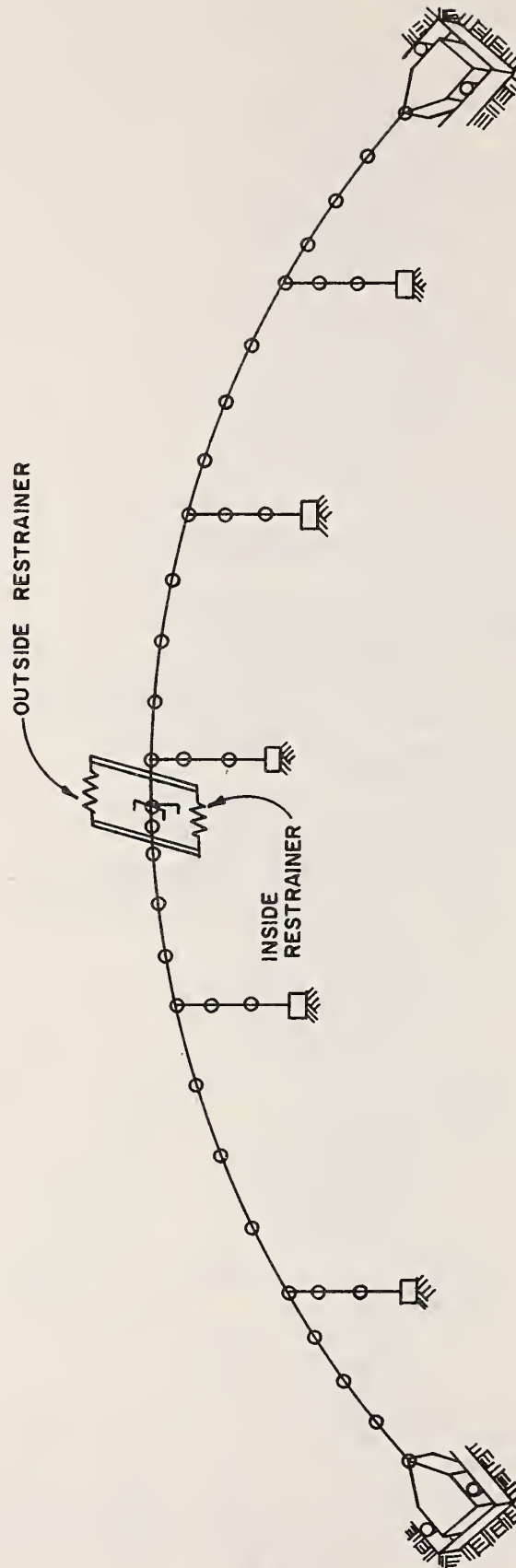
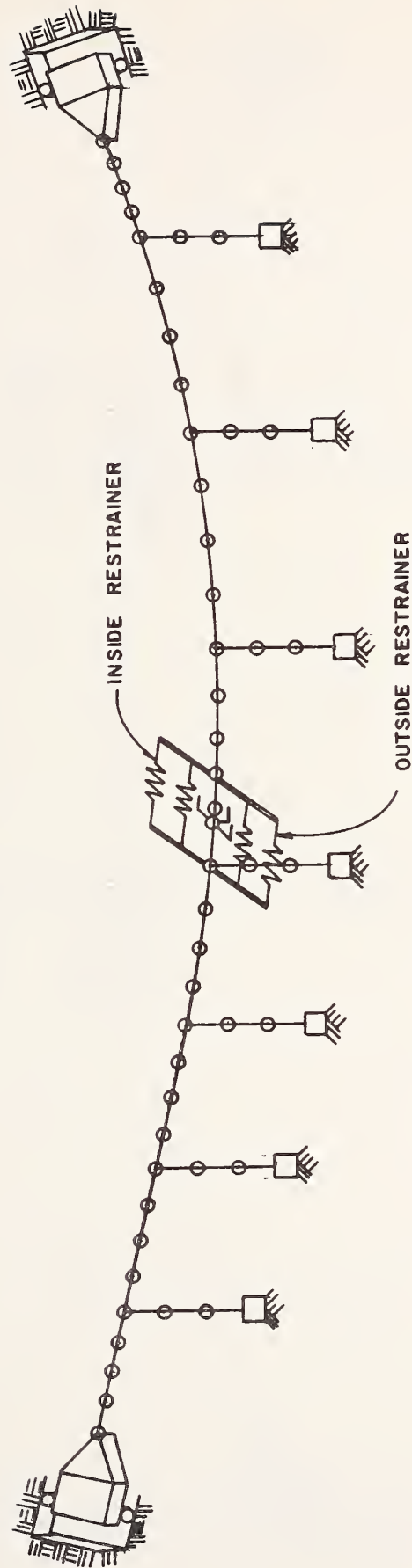


FIGURE 3.4



BRIDGE 1
ROUTE 80 ON-RAMP

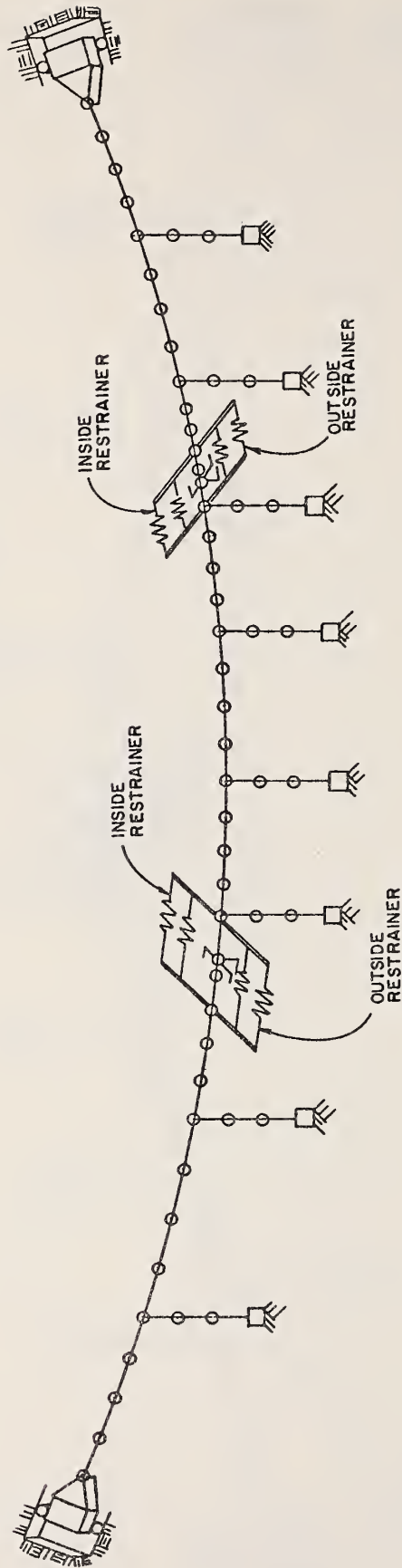
FIGURE 3.5



BRIDGE 2

NORTHEAST CONNECTOR OVERCROSSING

FIGURE 3.6



BRIDGE 3
SOUTHWEST CONNECTOR OVERCROSSING

FIGURE 3.7

		Duration of Sl8+ Ground Motion (Sec)					
Analysis Description	Computer System Used	Bridge 1		Bridge 2		Bridge 3	
		Long.	Trans.	Long.	Trans.	Long.	Trans.
Free Vibration	BSAP STRUDL	--	--	--	--	--	--
Response Spectrum (RMS)	BSAP STRUDL	36	36	36	36	36	36
Time History Nonlinear Columns and Expansion Joint	NEABS	20	20	30	30	30	30

TABLE 3.1 - Duration of Ground Motion

Bridge	Analysis					
	Response Spectrum		Linear Time History		Nonlinear Time History	
	Trans. Excitation	Long. Excitation	Trans. Excitation	Long. Excitation	Trans. Excitation	Long. Excitation
1	1	2	3	4	5	6
2	7	8	9	10	11	12
3	13	14	15	16	17	18

TABLE 3.2 - Case Numbers

Bent No.	a	a ₁	a ₂	a ₃	b	b ₁	b ₂	b ₃
2 to 6	1.0	-3.307	-4.764	-0.457	1.0	-3.216	-4.897	-0.681

TABLE 3.3 - Bridge 1 - Yield Function Constants
for the Columns

Bent No.	a	a ₁	a ₂	a ₃	b	b ₁	b ₂	b ₃
2,6,7	1.0	-2.670	-4.366	-0.696	1.0	-2.670	-4.366	-0.696
3,4	1.0	-3.507	-5.115	-0.608	1.0	-3.507	-5.115	-0.608
5	1.0	-2.165	-3.933	-0.768	1.0	-2.165	-3.933	-0.768
8	1.0	-3.174	-4.818	-0.644	1.0	-3.174	-4.818	-0.644

TABLE 3.4 - Bridge 2 - Yield Function Constants
for the Columns

Bent No.	a	a ₁	a ₂	a ₃	b	b ₁	b ₂	b ₃
2,3,4,5	1.0	-0.916	-2.817	-0.901	1.0	-1.225	-3.613	-1.388
6,7	1.0	-1.158	-3.189	-1.031	1.0	-1.272	-3.419	-1.146
8,9	1.0	-1.504	-3.663	-1.159	1.0	-1.371	-3.237	-0.866

TABLE 3.5 - Bridge 3 - Yield Function Constants
for the Columns

CHAPTER 4

RESULTS OF ANALYSIS

The results from the three different analyses of each bridge are summarized in the tables which follow. Similar component results are tabulated for each bridge. The following is a brief description of the types of results given.

4.1 STRUCTURE PERIOD AND PARTICIPATION FACTORS

The structure period for the first modes of vibration were determined using both STRUDL and BSAP. The participation factors, which are from the STRUDL program, are defined as

$$(PF) = [\emptyset]^T [M] (N) \quad 4.1$$

where $[\emptyset]$ is the matrix of eigenvectors, normalized with respect to unit mass, $[M]$ is the system inertia matrix, and (N) are rigid body vectors which relate the motion at each joint to support motion. Participation factors are useful in determining the coupling effects and the relative participation of each mode for a shock in a given direction.

4.2 DEADLOAD REACTIONS

The deadload reactions at the base of the columns are calculated by the NEABS program prior to the nonlinear dynamic analysis. The structure is analyzed as a space frame to determine deadload member forces. These values are used internally by NEABS since the effect of deadload must be considered in determining nonlinear response. For an elastic analysis, this is

not necessary, however. Therefore, in order to make a meaningful comparison of results, it was necessary to add deadload member forces to the earthquake member forces derived from an elastic analysis. The deadload reactions and corresponding moments are given at the base of the column in the local coordinate system where longitudinal is defined as tangent or parallel to the superstructure and transverse is radial or perpendicular to the superstructure.

4.3 MAXIMUM COLUMN BASE MOMENT AND CORRESPONDING SHEAR

The maximum column base moments and shears are compared for the three types of analyses. Deadload moments and shears are added to the results for the elastic analysis. The yield moments shown on the chart were taken from the interaction yield surface for the column assuming a vertical reaction equal to the deadload reaction.

The moments and shears are given in the local coordinate system. The earthquake ground accelerations are applied in the global coordinate system. A longitudinal earthquake is applied in a direction parallel to a straight line between the abutments. A transverse excitation is 90° to the longitudinal. The application of individual shocks in the two orthogonal horizontal directions to determine maximum member forces is the current design practice. There is no current provision to superimpose the earthquake effects of the two horizontal directions or the vertical direction. The coupling effects that are reported in these results suggest

that the seismic design provisions for bridges should consider the effect of simultaneously applying components in three orthogonal directions.

Response spectrum results are the root-mean-square (RMS), of the individual modal responses. The values presented for both the response spectrum and linear time history analysis are all time maximums that do not necessarily occur within the column at the same time. These values envelop the worst condition and would more than likely be used under the current seismic design criteria by the bridge designer in designing the column. The nonlinear moment results represent maximum values traced on the yield surface and would be of no direct use to the designer, except to verify the current assumed values of ductility demands.

4.4 MAXIMUM TRANSVERSE FORCE IN SHEAR KEYS

The maximum transverse shear forces in the shear keys at the abutment and the hinges are given. Members connected to the abutments are considered fixed in the transverse direction for both the linear and nonlinear analysis. The intermediate hinges are connected with horizontal members having displacement compatibility in the transverse direction for the linear analyses. For the nonlinear model a stiff spring is used to connect the members, meeting at the hinge, in the transverse direction.

4.5 MAXIMUM DECK DISPLACEMENTS

The maximum horizontal displacement of the deck at points over the supports are tabulated. The results are maximum for each

location and each direction and do not necessarily occur at the same time. All results are given in the global coordinate system which was defined earlier.

4.6 MAXIMUM HINGE MOVEMENT AND RESTRAINER FORCES

The maximum hinge movements are given at the location of the hinge restrainers which are closest to the left and right edges of the superstructure deck. For the elastic analysis, the movements are given as absolute values and may represent either closing or separation at the expansion joints. The maximum corresponding restrainer forces are tabulated for these restrainer movements. For the elastic analyses the restrainer forces are absolute values and may be either tension or compression. The nonlinear analysis, however, considers the fact that compression cannot exist in the restrainer. In addition, the effect of a tie gap and restrainer yield force are included. Therefore, the nonlinear analysis is the most rational approach to determining the actual forces in the restrainers. As before, all values are maximum and may not occur at the same time.

4.7 DECK DISPLACEMENT AT FIRST YIELD

The deck displacements at the first sign of yielding in one or more of the columns have been tabulated in Tables 4.9, 4.18 and 4.27 from the nonlinear time history analyses. These displacements occur over the bents and are given in the global coordinate system.

In addition to the results presented in this section, the following items are included in the appendices:

Appendix A: Mode shape plots for first
10 modes of each bridge

Appendix B: Time history plots of selected
column forces and nonlinear
displacements

Mode	Period (Sec)		Participation Factor		
	STRU DL	BSAP	X (Long.)	Y (Vert.)	Z (Trans.)
1	0.399	0.398	1.6	26.8	28.7
2	0.371	0.371	83.3	- 0.8	-75.3
3	0.367	0.367	55.6	- 6.5	115.2
4	0.340	0.340	-66.5	0.2	3.2
5	0.309	0.309	-30.4	4.5	- 3.3
6	0.294	0.294	73.6	0.3	2.6
7	0.261	0.261	- 3.9	- 9.5	- 5.1
8	0.240	0.239	4.3	14.6	-34.4
9	0.234	0.233	-15.8	-22.7	4.0
10	0.221	0.222	17.0	-74.8	- 4.8

TABLE 4.1 - Bridge 1 - Structure Period
and Participation Factors

Location	Axial Force (kips)	Trans. Shear (kips)	Long. Shear (kips)	Torsional Moment (kip-ft)	Long. Moment (kip-ft)	Trans. Moment (kip-ft)
Abut 1	0	3	418	-247	0	0
Bent 2	1802	20	161	- 6	-1377	210
Bent 3	1827	27	-161	- 4	1160	332
Bent 4	1389	8	172	9	- 950	281
Bent 5	1618	22	-136	14	1484	283
Bent 6	1633	9	- 37	8	622	71
Abut 7	0	3	418	-247	0	0

TABLE 4.2 - Bridge 1 - Deadload Forces at the Supports

Bent No.	Direction of Shear and Moment	Yield Moment*	CASE NO.		
			1 (R.S.)	3 (L.T.H.)	5 (N.T.H.)
2	Trans.	16,457	22689 # (1040)+	28802 (1312)	14941 (688)
	Long.	12,002	31253 (2306)	17395 (1388)	9396 (762)
3	Trans.	16,497	44593 (1978)	55713 (2484)	16754 (727)
	Long.	12,033	3670 (2671)	8420 (672)	4514 (404)
4	Trans.	16,748	53254 (2368)	62014 (2721)	16536 (791)
	Long.	11,465	6117 (660)	2167 (328)	2867 (222)
5	Trans.	16,148	44185 (1907)	51336 (2208)	16329 (708)
	Long.	11,768	11855 (903)	10597 (801)	5335 (708)
6	Trans.	16,175	24186 (1029)	27032 (1133)	14405 (605)
	Long.	11,789	14528 (964)	14641 (979)	7843 (562)

*Moment Corresponding to Deadload
#Maximum Column Base Moment (kip-ft)
+Maximum Column Base Shear (kips)

TABLE 4.3 - Bridge 1 - Maximum Column Moments and Corresponding Shears Due to Transverse Shock

Bent No.	Direction of Shear and Moment	Yield Moment*	CASE NO.		
			2 (R.S.)	4 (L.T.H.)	6 (N.T.H.)
2	Trans.	16,457	15,468# (733)+	9773 (519)	6457 (330)
	Long.	12,002	33,216 (2469)	35739 (2662)	12331 (1019)
3	Trans.	16,497	26,988 (1221)	9112 (471)	6724 (301)
	Long.	12,033	31,398 (2349)	37207 (2807)	12293 (1031)
4	Trans.	15,748	29,440 (1292)	7626 (339)	3727 (162)
	Long.	11,465	16,721 (1333)	23334 (1716)	11980 (929)
5	Trans.	16,148	25,902 (1140)	15317 (727)	9102 (428)
	Long.	11,768	21,956 (1826)	28932 (2258)	11975 (428)
6	Trans.	16,175	15,139 (663)	11640 (548)	7657 (347)
	Long.	11,789	16,802 (1180)	22250 (1477)	12107 (318)

*Moment Corresponding to Deadload
#Maximum Column Base Moment (kip-ft)
+Maximum Column Base Shear (kips)

TABLE 4.4 - Bridge 1 - Maximum Column Moments and Corresponding Shears Due to Longitudinal Shock

CASE	LOCATION		
	Abutment 1 (kips)	Abutment 7 (kips)	Hinge Span 3 (kips)
1	234	330	803
3	260	336	936
5	379	430	363
2	188	265	475
4	252	316	229
6	178	240	N.A.

TABLE 4.5 - Bridge 1 - Maximum Transverse Force
in Shear Keys for Transverse and Longitudinal Shocks

Location	Global Direction	Case No.		
		1 (R.S.)	3 (L.T.H.)	5 (N.T.H.)
Abut. 1	Trans.	.0665	.0373	.0284
	Long.	.1014	.0555	.0435
Bent 2	Trans.	.0763	.1012	.0637
	Long.	.1146	.0236	.0242
Bent 3	Trans.	.1293	.1711	.1100
	Long.	.1307	.0088	.0243
Bent 4	Trans.	.1623	.1903	.1390
	Long.	.0109	.0068	.0224
Bent 5	Trans.	.1503	.1730	.1090
	Long.	.0116	.0039	.0217
Bent 6	Trans.	.1032	.1134	.0747
	Long.	.0258	.0201	.0238
Abut. 7	Trans.	.0403	.0408	.0296
	Long.	.0597	.0603	.0453

TABLE 4.6 - Bridge 1 - Maximum Bridge Deck Displacements Due to Transverse Shock, in feet

Location	Global Direction	Case No.		
		2 (R.S.)	4 (L.T.H.)	6 (N.T.H.)
Abut 1	Trans.	.0702	.0731	.0609
	Long.	.1067	.1119	.0934
Bent 2	Trans.	.0770	.0551	.0367
	Long.	.1074	.1273	.1066
Bent 3	Trans.	.0880	.0274	.0156
	Long.	.1132	.1390	.1165
Bent 4	Trans.	.0895	.0218	.0115
	Long.	.0686	.0960	.0870
Bent 5	Trans.	.0846	.0425	.0270
	Long.	.0676	.0960	.0870
Bent 6	Trans.	.0632	.0393	.0347
	Long.	.0637	.0919	.0820
Abut. 7	Trans.	.0417	.0554	.0481
	Long.	.0632	.0845	.0737

TABLE 4.7 - Bridge 1 - Maximum Bridge Deck Displacements Due to Longitudinal Shocks, in feet

CASE	Max. Hinge Movement (ft)		Max. Restrainer Force (kips)	
	Inside Unit (Rt)	Outside Unit (Lt)	Inside Unit (Rt)	Outside Unit (Lt)
1	.1224	.1307	149	159
3	.0123	.0220	15	27
5	.0432	.0481	0	0
2	.1249	.1315	152	160
4	.1124	.1158	137	141
6	.0824	.0836	0	0

TABLE 4.8 - Bridge 1 - Maximum Hinge Separations and Restrainer Forces Due to Longitudinal and Transverse Shocks

Location	Transverse Excitation		Longitudinal Excitation	
	Trans. Displacement	Long. Displacement	Trans. Displacement	Long. Displacement
Abut 1	-.0116	.0178	.0227	-.0348
Bent 2	-.0349	.0048	.0073	-.0426
Bent 3	-.0518	-.0011	-.0028*	-.0461*
Bent 4	-.0541*	.0012*	-.0009	-.0383
Bent 5	-.0512	.0006	.0014	-.0392
Bent 6	-.0360	-.0049	-.0061	-.0374
Abut 7	-.0120	-.0184	-.0200	-.0306

*Bent where first yielding occurs -
all results are from nonlinear
time history analysis.

TABLE 4.9 - Bridge 1 - Deck Displacements
at Initial Column Yielding, in feet

Mode	Period (Sec)		Participation Factor		
	STRU DL	BSAP	X (Long.)	Y (Vert.)	Z (Trans.)
1	1.107	1.046	-23.9	0.5	-116.2
2	0.792	0.790	28.1	1.5	- 86.3
3	0.673	0.674	-59.2	-18.5	9.7
4	0.634	0.607	-11.7	5.2	- 3.9
5	0.574	0.574	-114.6	3.4	12.8
6	0.500	0.500	6.1	-36.1	3.0
7	0.433	0.430	15.8	- 0.7	1.9
8	0.399	0.398	-56.7	34.7	-12.8
9	0.385	0.385	34.8	69.5	16.6
10	0.368	0.358	0.2	0.9	-41.5

TABLE 4.10 - Bridge 2 - Structure Period
and Participation Factor

Location	Axial Force (kips)	Trans. Shear (kips)	Long. Shear (kips)	Torsional Moment (kip-ft)	Long. Moment (kip-ft)	Trans. Moment (kip-ft)
Abut 1	0	- 2	296	97	0	0
Bent 2	1164	18	- 52	13	914	389
Bent 3	1150	11	- 38	11	758	352
Bent 4	1219	4	- 51	- 3	983	268
Bent 5	1236	7	151	-64	-854	530
Bent 6	1964	5	- 63	13	2522	119
Bent 7	1733	12	- 76	15	1965	218
Bent 8	1383	11	126	-12	-794	-133
Abut 9	0	3	146	480	0	0

TABLE 4.11 - Bridge 2 - Dead Load Forces at the Supports

Bent No.	Direction of Shear and Moment	Yield Moment*	CASE NO.		
			7 (R.S.)	9 (L.T.H.)	11 (N.T.H.)
2	Trans.	12,080	15849# (560)	15129 (548)	10431 (366)
	Long.	12,080	4783 (271)	5706 (325)	6707 (310)
3	Trans.	9,900	25511 (807)	25092 (790)	10263 (322)
	Long.	9,900	3897 (197)	4581 (233)	3961 (177)
4	Trans.	10,000	20442 (567)	19990 (542)	10398 (322)
	Long.	10,000	3935 (196)	4610 (238)	3138 (160)
5	Trans.	14,340	21471 (878)	23699 (850)	14488 (642)
	Long.	14,340	6081 (496)	8881 (679)	5509 (442)
6	Trans.	13,020	23636 (708)	27045 (806)	13169 (391)
	Long.	13,020	8444 (327)	9279 (367)	8120 (351)
7	Trans.	12,770	21761 (600)	23668 (645)	12848 (362)
	Long.	12,770	4710 (198)	5135 (214)	8062 (364)
8	Trans.	10,950	14751 (601)	13863 (533)	10592 (391)
	Long.	10,950	10748 (696)	10868 (612)	9544 (647)

*Moment Corresponding to Deadload
#Maximum Column Base Moment (kip-ft)
+Maximum Column Base Shear (kips)

TABLE 4.12 - Bridge 2 - Maximum Column Moments and Corresponding Shears Due to Transverse Shock

Bent No.	Direction of Shear and Moment	Yield Moment*	CASE NO.		
			8 (R.S.)	10 (L.T.H.)	12 (N.T.H.)
2	Trans.	12,030	6893 # (270)+	6322 (238)	6044 (267)
	Long.	12,080	12569 (724)	16508 (938)	12162 (679)
3	Trans.	9,900	9253 (299)	9024 (297)	7312 (239)
	Long.	9,900	9856 (505)	12976 (650)	10302 (510)
4	Trans.	10,000	7348 (206)	6701 (187)	5446 (144)
	Long.	10,000	10501 (535)	13252 (662)	10493 (552)
5	Trans.	14,430	9665 (434)	9698 (498)	7453 (301)
	Long.	14,340	16079 (1143)	21212 (1548)	14891 (1106)
6	Trans.	13,020	7214 (250)	6369 (209)	8036 (247)
	Long.	13,020	21001 (1040)	21931 (996)	13162 (693)
7	Trans.	12,770	5831 (190)	4952 (152)	6023 (155)
	Long.	12,770	14910 (645)	18304 (788)	12943 (590)
8	Trans.	10,950	6194 (282)	4374 (204)	4233 (137)
	Long.	10,950	23930 (1462)	26589 (1558)	11652 (890)

*Moment Corresponding to Deadload
#Maximum Column Base Moment (kip-ft)
+Maximum Column Base Shear (kips)

TABLE 4.13 - Bridge 2 - Maximum Column Moments and Corresponding Shears Due to Longitudinal Shock

CASE	LOCATION		
	Abutment 1 (kips)	Abutment 9 (kips)	Hinge Span 5 (kips)
7	162	265	524
9	186	237	484
11	203	254	509
8	89	76	249
10	76	73	180
12	43	84	93

TABLE 4.14 - Bridge 2 - Maximum Transverse Force
in Shear Keys for Transverse and Longitudinal Shocks

Location	Global Direction	Case No.		
		7 (R.S.)	9 (L.T.H.)	11 (N.T.H.)
Abut 1	Trans.	.0072	.0093	.0063
	Long.	.0279	.0339	.0274
Bent 2	Trans.	.1931	.1845	.1498
	Long.	.0413	.0487	.0376
Bent 3	Trans.	.3996	.3911	.3290
	Long.	.0825	.0908	.0733
Bent 4	Trans.	.4175	.4081	.3383
	Long.	.0849	.0945	.0696
Bent 5	Trans.	.1384	.1579	.1379
	Long.	.0340	.0391	.0338
Bent 6	Trans.	.4235	.4845	.4167
	Long.	.0917	.1035	.1741
Bent 7	Trans.	.4707	.5150	.4002
	Long.	.0970	.1046	.1642
Bent 8	Trans.	.1780	.1762	.1758
	Long.	.0350	.0311	.0864
Abut. 9	Trans.	.0353	.0383	.0503
	Long.	.0688	.0756	.0976

TABLE 4.15 - Bridge 2 - Maximum Bridge Deck Displacements Due to Transverse Shock, in feet

Location	Global Direction	Case No.		
		8 (R.S.)	10 (L.T.H.)	12 (N.T.H.)
Abut. 1	Trans.	.0191	.0259	.0271
	Long.	.0838	.1142	.1184
Bent 2	Trans.	.0801	.0728	.0605
	Long.	.0823	.1103	.1173
Bent 3	Trans.	.1407	.1336	.1221
	Long.	.0862	.1050	.1226
Bent 4	Trans.	.1439	.1330	.1332
	Long.	.0865	.1009	.1184
Bent 5	Trans.	.0583	.0600	.0516
	Long.	.0774	.1006	.1105
Bent 6	Trans.	.1138	.1108	.1445
	Long.	.1647	.1961	.2097
Bent 7	Trans.	.1252	.1093	.1327
	Long.	.1526	.1930	.2100
Bent 8	Trans.	.1025	.0837	.0721
	Long.	.1447	.1811	.1843
Abut. 9	Trans.	.0734	.0852	.0853
	Long.	.1506	.1758	.1656

TABLE 4.16 - Bridge 2 - Maximum Bridge Deck Displacements Due to Longitudinal Shocks, in feet

CASE	Max. Hinge Movement (ft)		Max. Restrainer Force (kips)	
	Inside Unit (Rt)	Outside Unit (Lt)	Inside Unit (Rt)	Outside Unit (Lt)
7	.1229	.0863	131	92
9	.1417	.0939	151	100
11	.1752	.2221	0	0
8	.1539	.1511	164	161
10	.1938	.1876	207	200
12	.2186	.2111	0	0

TABLE 4.17 - Bridge 2 - Maximum Hinge Separations and Restrainer Forces Due to Longitudinal and Transverse Shocks

Location	Transverse Excitation		Longitudinal Excitation	
	Trans. Displacement	Long. Displacement	Trans. Displacement	Long. Displacement
Abut 1	.0019	.0083	-.0145	-.0637
Bent 2	.0173	.0047	-.0018	-.0657
Bent 3	.0293	.0019	-.0004	-.0653
Bent 4	.0438	-.0016	-.0143	-.0603
Bent 5	.0463	-.0024	-.0178	-.0567
Bent 6	.2381*	.0745*	-.0481*	-.1244*
Bent 7	.2503	.0731	-.0637	-.1244
Bent 8	.0842	.0192	-.0014*	-.1005*
Abut 9	.0080	-.0155	.0418	-.0811

*Bent where first yielding occurs -
all results are from nonlinear
time history analysis.

TABLE 4.18 - Bridge 2 - Deck Displacements
at Initial Column Yielding, in feet

Mode	Period (Sec)		Participation Factor		
	STRU DL	BSAP	X (Long.)	Y (Vert.)	Z (Trans.)
1	1.943	1.938	2.0	0.1	-185.1
2	1.538	1.534	88.4	0.3	69.5
3	1.364	1.371	194.6	- 0.7	- 24.9
4	1.099	1.096	16.2	- 0.7	- 71.2
5	.819	0.822	16.9	- 0.9	- 15.8
6	.791	0.790	-37.0	2.0	- 12.8
7	.761	0.759	3.5	16.1	- 2.5
8	.588	0.587	-13.6	-30.6	- 8.3
9	.580	0.578	-12.2	0.6	- 33.3
10	.546	0.548	1.2	-11.1	- 3.0

TABLE 4.19 - Bridge 3 - Structure Period
and Participation Factors

Location	Axial Force (kips)	Trans. Shear (kips)	Long. Shear (kips)	Torsional Moment (kip-ft)	Long. Moment (kip-ft)	Trans. Moment (kip-ft)
Abut 1	0	1	764	810	0	0
Bent 2	2983	3	36	- 22	-667	-220
Bent 3	3213	6	- 38	29	769	- 63
Bent 4	2422	-4	- 7	- 1	501	- 42
Bent 5	2200	3	- 31	2	1051	94
Bent 6	2191	3	12	- 7	-140	43
Bent 7	1788	-1	17	- 7	-297	-110
Bent 8	2048	-1	14	- 22	-680	-162
Bent 9	2380	1	12	- 8	-701	-104
Abut 10	0	-2	603	-424	0	0

TABLE 4.20 - Bridge 3 - Dead Load Forces at the Supports

Bent No.	Direction of Shear and Moment	Yield Moment*	CASE NO.		
			13 (R.S.)	15 (L.T.H.)	17 (N.T.H.)
2	Trans.	51,080	34442 # (694)+	33228 (705)	28614 (587)
	Long.	40,800	34289 (1135)	32899 (1086)	17674 (562)
3	Trans.	51,260	56044 (962)	49342 (842)	43250 (725)
	Long.	40,900	19717 (578)	19543 (572)	12744 (382)
4	Trans.	50,600	59538 (921)	64609 (1109)	50517 (760)
	Long.	40,500	7872 (176)	6872 (151)	7482 (169)
5	Trans.	50,380	45178 (645)	50355 (806)	45827 (658)
	Long.	40,350	7855 (201)	6181 (159)	6814 (174)
6	Trans.	45,520	35593 (511)	35912 (551)	34489 (524)
	Long.	36,620	10165 (276)	9684 (264)	7922 (225)
7	Trans.	45,070	34258 (576)	31097 (596)	30552 (569)
	Long.	36,290	12058 (325)	10367 (286)	10034 (265)
8	Trans.	39,990	30915 (550)	31140 (560)	28780 (538)
	Long.	32,400	13255 (397)	11798 (353)	11623 (346)
9	Trans.	40,370	16494 (306)	19665 (382)	15584 (299)
	Long.	32,730	15939 (489)	15639 (478)	14039 (427)

*Moment Corresponding to Deadload
#Maximum Column Base Moment (kip-ft)
+Maximum Column Base Shear (kips)

TABLE 4.21 - Bridge 3 - Maximum Column Moments and Corresponding Shears Due to Transverse Shock

Bent No.	Direction of Shear and Moment	Yield Moment*	CASE NO.		
			14 (R.S.)	16 (L.T.H.)	18 (N.T.H.)
2	Trans.	51,080	16123 # (359)+	19126 (436)	16615 (382)
	Long.	40,800	47534 (1571)	46756 (1542)	40701 (1383)
3	Trans.	51,260	19877 (390)	18913 (367)	18172 (350)
	Long.	40,900	37068 (1081)	38943 (1132)	39252 (1146)
4	Trans.	50,600	14495 (255)	16177 (325)	14397 (287)
	Long.	40,500	23557 (559)	26979 (646)	22389 (531)
5	Trans.	50,380	8234 (123)	6194 (944)	7307 (106)
	Long.	40,350	26810 (676)	30188 (759)	23787 (593)
6	Trans.	45,520	25793 (406)	20997 (345)	19497 (309)
	Long.	36,620	29149 (777)	30862 (819)	26196 (691)
7	Trans.	45,070	41158 (720)	33065 (583)	29227 (522)
	Long.	36,290	30604 (826)	29822 (812)	25630 (693)
6	Trans.	39,990	38130 (698)	32777 (611)	27171 (509)
	Long.	32,400	37041 (1125)	31771 (963)	31169 (953)
9	Trans.	40,370	20324 (378)	18513 (350)	15053 (287)
	Long.	32,730	40699 (1266)	31499 (979)	30486 (956)

*Moment Corresponding to Deadload
#Maximum Column Base Moment (kip-ft)
+Maximum Column Base Shear (kips)

TABLE 4.22 - Bridge 3 - Maximum Column Moments and Corresponding Shears Due to Longitudinal Shock

CASE	LOCATION			
	Abutment 1 (kips)	Abutment 10 (kips)	Hinge Span 3 (kips)	Hinge Span 7 (kips)
13	372	242	400	192
15	375	301	430	232
17	331	248	396	257
14	297	257	314	267
16	284	289	337	258
18	266	258	246	196

TABLE 4.23 - Bridge 3 - Maximum Transverse Force
in Shear Keys for Transverse and Longitudinal Shocks

Location	Global Direction	Case No.		
		13 (R.S.)	15 (L.T.H.)	17 (N.T.H.)
Abut 1	Trans.	.3098	.2890	.1694
	Long.	.3919	.3668	.2196
Bent 2	Trans.	.6001	.5321	.4137
	Long.	.2643	.2955	.1684
Bent 3	Trans.	1.0630	.9517	.8291
	Long.	.1851	.1411	.3032
Bent 4	Trans.	1.5483	1.6401	1.5974
	Long.	.1613	.1183	.1893
Bent 5	Trans.	1.2420	1.3241	1.2400
	Long.	.1474	.0965	.1762
Bent 6	Trans.	.9011	.8636	.8477
	Long.	.1658	.1272	.1934
Bent 7	Trans.	.7105	.6773	.7065
	Long.	.2203	.2121	.2527
Bent 8	Trans.	.5151	.5257	.4838
	Long.	.1832	.1710	.2274
Bent 9	Trans.	.3020	.3444	.3043
	Long.	.1467	.1269	.1670
Abut 10	Trans.	.1437	.1407	.1339
	Long.	.1834	.1787	.1736

TABLE 4.24 - Bridge 3 - Maximum Bridge Deck Displacements Due to Transverse Shock, in feet

Location	Global Direction	Case No.		
		14 (R.S.)	16 (L.T.H.)	18 (N.T.H.)
Abut 1	Trans.	.4112	.3926	.4294
	Long.	.5250	.5018	.5567
Bent 2	Trans.	.3373	.2203	.2617
	Long.	.6107	.6526	.7393
Bent 3	Trans.	.3262	.2588	.2134
	Long.	.6877	.7765	.8399
Bent 4	Trans.	.2673	.2931	.2646
	Long.	.6373	.7157	.6196
Bent 5	Trans.	.2000	.1343	.1945
	Long.	.6344	.6976	.6149
Bent 6	Trans.	.5686	.4188	.3818
	Long.	.6260	.7089	.6177
Bent 7	Trans.	.7899	.5498	.4764
	Long.	.6108	.7206	.6184
Bent 8	Trans.	.6632	.4395	.4402
	Long.	.5241	.6016	.5948
Bent 9	Trans.	.4907	.2953	.3456
	Long.	.4956	.4845	.4850
Abut 10	Trans.	.3919	.2972	.2812
	Long.	.5041	.3835	.3645

TABLE 4.25 - Bridge 3 - Maximum Bridge Deck Displacements Due to Longitudinal Shocks, in feet

CASE	SPAN 3				SPAN 7			
	Maximum Hinge Movement (ft)		Maximum Hinge Restrainer Force (kips)		Maximum Hinge Movement (ft)		Maximum Hinge Restrainer Force (kips)	
	Inside Unit (Lt)	Outside Unit (Rt)	Inside Unit (LT)	Outside Unit (Rt)	Inside Unit (Lt)	Outside Unit (Rt)	Inside Unit (Lt)	Outside Unit (Rt)
13	.0555	.1493	120	325	.1331	.0964	160	114
15	.0559	.1488	124	330	.1445	.1004	177	123
17	.4524	.2927	271	0	.2772	.2726	31	21
14	.1132	.1186	209	213	.0882	.1185	105	146
16	.0710	.1453	157	322	.1079	.0996	132	122
18	.4347	.3955	219	135	.2838	.3048	40	65

TABLE 4.26 - Bridge 3 - Maximum Hinge Separations and Restrainer Forces Due to Longitudinal and Transverse Shocks

Location	Transverse Excitation		Longitudinal Excitation	
	Trans. Displacement	Long. Displacement	Trans. Displacement	Long. Displacement
Abut 1	.1269	.1646	.3316	.4299
Bent 2	.2576	.0790	.1381*	.5580*
Bent 3	.7188	-.1114	-.0107	.6272
Bent 4	1.4437*	-.0101*	-.0325	.5013
Bent 5	1.1837	.0036	.1123	.4931
Bent 6	.8224	-.0260	.2029	.4988
Bent 7	.4898	-.0975	.2208	.5016
Bent 8	.2416	.0539	.1287	.4145
Bent 9	.1104	-.0103	-.0267	.3367
Abut 10	.0433	-.0561	-.1792	.2323

*Bent where first yielding occurs -
all results are from nonlinear
time history analysis.

TABLE 4.27 - Bridge 3 - Deck Displacements
at Initial Column Yielding, in feet

CHAPTER 5

INTERPRETATION OF RESULTS

5.1 STRUCTURE PERIOD AND PARTICIPATION FACTORS

There is very good agreement between the STRUDL and BSAP results for the structure period of the first ten modes of vibration for each of the three bridges. STRUDL uses the Householder-Ortega-Wielandt method to solve the eigenvalue problem. BSAP solves the eigenvalue problem by either a determinant search solution or a subspace iteration solution depending on the number of degrees of freedom. Bridges 1 and 2 were solved using the determinant search algorithm and Bridge 3 was solved using the subspace iteration technique.

The principal difference between the two structural idealizations was that the bridge deck for STRUDL consisted of straight space frame members and BSAP employed curved space frame members. The close agreement in the structural periods indicates that the straight member model yields satisfactory results for column design with the discretizations used here, which are normally used to simulate the inertia effects of the bridge deck for a dynamic analysis. The mode shape plots for the first ten modes of vibration for each of the three bridges studied are included in Appendix A. The participation factors tabulated represent the extent to which an earthquake motion directed in the referenced coordinate directions tends to excite response in the given mode of vibration.

5.1.1 BRIDGE 1

The structure periods shown in Table 4.1 for the first 10 modes of vibration are concentrated in a range from 0.40 to 0.22 seconds. The participation factors also shown in Table 4.1 together with the mode shape plots for the second and third modes, shown on pages A-1 and A-2, indicate that there is coupling in the two horizontal directions. This coupling effect is more pronounced for this bridge due to the high degree of curvature of the deck. The periods of the two modes differ by only 0.004 seconds. Both periods result in near peak response for the S18+ earthquake, thus indicating that these modes will simultaneously contribute substantially to the total response of this bridge. The signs of the participation factors for the second and third modes of vibration indicate out of phase response due to a transverse excitation.

The first mode of vibration is coupled in both the vertical and horizontal directions. As shown on the plot for this mode, the vertical response predominates to the left of the intermediate hinge where the span lengths are somewhat unbalanced.

The large degree of coupling in this bridge indicates that bridge design criteria should consider a method for combining the response due to motion in the three orthogonal directions for this type of bridge or for structures with similar coupling effects.

5.1.2 BRIDGE 2

The structure periods recorded in Table 4.10 for the first ten modes of vibration for Bridge 2 range from 1.05 to 0.36 seconds. The first two modes are coupled in the horizontal direction with the predominant response being in the transverse direction to the right of the hinge for the first mode and to the left of the hinge for the second mode, as illustrated by the mode shape plots shown on page A-6. This behavior is due to the combined effect of a relatively stiff column at Bent 5 and a discontinuity caused by the nearby hinge. The third mode is coupled in all three directions with the predominant response being in the longitudinal direction. Here again the coupling between the three coordinate directions draws attention to the importance of including multi-directional input motions.

5.1.3 BRIDGE 3

The periods tabulated in Table 4.19 for the first ten modes of vibration for Bridge 3 range from 1.94 to 0.57 seconds. Here the first mode is predominantly a transverse mode with very little coupling in the other directions. The second mode is coupled in the two horizontal directions with approximately equal participation. The third mode responds predominantly due to an earthquake in the X direction. Note that in this case the seventh mode is the first mode responding to a vertical input motion.

5.2 DEADLOAD REACTIONS

The column deadload axial reactions tabulated in Tables

4.2, 4.11 and 4.20 respectively, for the three bridges selected for this study, are equal to approximately 10% of the ultimate axial load capacity of the columns. This is generally the case for most bridge structures. The presence of small transverse deadload moments is due to the curvature of the superstructures. The longitudinal deadload moments are generally quite small for most cases except for Bridge 2 which has large longitudinal deadload moments at Bents 6 and 7. These moments are approximately 20% of the ultimate moment capacity of the column. This is due to the unbalanced span lengths and the discontinuity caused by the intermediate hinge.

5.3 MAXIMUM COLUMN BASE MOMENTS AND CORRESPONDING SHEARS

The maximum transverse and longitudinal bending moments at the base of the column are tabulated separately for both the transverse and longitudinal shocks. The corresponding column shears, enclosed in parentheses, are shown below the bending moments. The moments are tabulated for the response spectrum, linear time history, and nonlinear time history analyses. The maximum transverse and longitudinal bending moments recorded for a single time history analysis do not necessarily occur at the same time. The values shown are the individual maximum components that occurred during the time history analysis. These values would generally be used by the designers. Although this is somewhat conservative, the design loads would envelop the maximum loading case. When designing a column with response spectrum analysis results, designers generally use the individual RMS values for bending

moment in the two orthogonal directions. This is also generally conservative but will envelop the maximum instantaneous loading conditions.

The yield moments tabulated in the transverse and longitudinal directions correspond to the axial deadload forces. The maximum moments occurring during the nonlinear analysis include the effect of both deadload and the axial forces imposed by the time history motion. The maximum moments tabulated for the nonlinear analysis vary from the tabulated yield moments because of the instantaneous axial force and corresponding orthogonal moment.

The maximum local or rotational ductility demands tabulated in Tables 5.2, 5.4 and 5.6 for Bridges 1, 2 and 3 respectively were computed using the same basic approach used by Tseng and Penzien (4). The column flexural yield rotation and corresponding assumed hinge lengths are shown in Tables 5.1, 5.2 and 5.3 respectively for the three bridges considered.

5.3.1 TRANSVERSE SHOCK

The case studies considered are described in Chapter 3 and summarized in Table 3.2. The odd number cases correspond to the transverse shocks. For the curved bridges considered herein, the transverse direction is taken normal to a chord connecting the abutments. Seismic loads applied in the transverse direction generally yield the highest column moment in single column bent due to the cantilever bending of the column. This case is generally given additional consideration in design (10), due to the potential instability, i.e., lack of redundant members, in the transverse direction by reducing the allowable ductility force reduction factor.

5.3.1.1 Bridge 1 (Cases 1, 3 and 5)

The maximum bending moments and corresponding shears at the base of the column of Bridge 1 due to a transverse shock are reported in Table 4.3. The response spectrum RMS results for the transverse bending moments are less than the results of the linear time history for all the columns. The differences range from 21 percent at Bent 2 to 11 percent at Bent 6. These differences in the transverse bending moment are the result of replacing the effects of the time domain by a statistical averaging technique. When two modes of vibration occur close together, near peak on the response spectrum, the two modal results should be added algebraically.

The difference between response spectrum RMS results and linear time history results for longitudinal moment is somewhat erratic.

The response spectrum results for the longitudinal moment are generally greater, except at Bent 3 where they are less by 63 percent. The maximum difference occurs at Bent 2 where the response spectrum result is 94 percent larger than the moment obtained from the linear time history analysis. Since there is no consistent pattern, the possibility of using some other means of statistically combining the response spectrum modal results seems somewhat remote. Furthermore, if the current design practice is modified to include the combination of a percentage of the results for an orthogonal horizontal motion, realistic results would be virtually impossible for this type of bridge with a response spectrum approach.

The nonlinear time history analysis results reported in Table 5.2 indicate that yielding has occurred in all the columns due to the transverse motion. The time history plot of nonlinear transverse deformations at the base of the column at Bent 4 due to transverse motion is included in the Appendix on page B-2. Column flexural yield rotations were calculated using the values shown in Table 5.1.

Although the maximum rotational ductility demand of 3.2 at Bent 4 is far below the ductility generally considered to be available in the column, the time history plot of nonlinear deformation indicates that there have been several excursions into the nonlinear range. With this degree of cyclic yielding, it is likely that considerable structural damage will take place with a resulting degradation in column stiffness. This raises a question about the validity of maximum ductility demand as a measure of a structure's

ability to withstand damage from seismic loadings. It also points to the importance of considering stiffness degradation in the analysis.

The reduction in moments derived from the linear time history analysis indicates that a ductility reduction factor of between 3 and 4 would have yielded a similar column design for this seismic loading. However, current practice is to use a reduction factor of 3 for single column bents multiplied by a risk factor of 2 for structures in this period range. This would have resulted in a column moment capacity below the value used in the nonlinear analysis. With the amount of cyclic yielding that occurred in Case 5, it is doubtful that the structure as analyzed would have performed satisfactorily during the SI8+ earthquake, much less a weaker structure.

One of the main reasons for the extensive cyclic yielding of this structure was its relatively short period range which resulted in a greater number of nonlinear excursions. Yet current practice specifies a risk reduction for short period structures. Nonlinear results for this bridge indicate this practice should be reevaluated.

When the columns yield, column shears are reduced in order to satisfy statics. In addition, shear force is transferred to the rigid abutments through the superstructure. By considering the reduction in summation of the shear forces caused by yielding of

the columns, the overall force level is reduced by a factor of approximately 2.5 for this bridge.

5.3.1.2 Bridge 2 (Cases 7, 9 and 11)

As shown in Table 4.12, the response spectrum RMS values and the linear time history results for both the transverse and longitudinal moments agree quite well for Bridge 2 subjected to transverse motion. With the exception of Bent 6, the response spectrum analysis yields RMS results that are within 10 percent of time history and thus can be used with some degree of confidence for design purposes.

The column flexural yield rotations are calculated using the values shown in Table 5.3. The nonlinear analysis results reported in Table 5.4 indicate that yielding has occurred in all the columns due to the transverse shock. The maximum difference in moments occurs at Bent 3 where the moments determined by the linear analysis are 2.5 times larger than the maximum moment determined by the nonlinear analysis. It is also interesting to note that while this column has a large rotational ductility demand, Bent 6 has a larger demand, but a moment reduction factor of only slightly over 2. The rotational ductility demands for both of these columns are greater than Bent 4 in Bridge 1, yet the moment reduction is considerably less. In addition, the degree of cyclic yielding shown on the time history plot of nonlinear deformations on page B-17 of the Appendix indicates that Bent 6 of Bridge 2 is less likely to be damaged to the same extent as Bent 4 of

Bridge 1. Therefore, the rotational ductility demands do not seem to be a good indication of the ability of a structure to withstand earthquake loading, or of the amount of moment capacity reduction that is justified, even for two columns within the same bridge.

The overall reduction in the summation of shear forces is approximately 1.6 due to yielding in the columns. This is less than the reduction in Bridge 1 where there was more energy dissipation due to yielding.

5.3.1.3 Bridge 3 (Cases 13, 15 and 17)

The results obtained for Bridge 3 by the response spectrum analysis agree quite well with the linear time history analysis as shown in Table 4.21. It appears for this bridge, that response spectrum results are adequate for design. As can be seen from the nonlinear deformations shown in Table 5.6, only Bent 4 has yielded due to the transverse ground motion. The yield moments in Bent 4 are approximately three-fourths the moments from an elastic analysis. The remaining column moments are reduced, but to a much smaller degree. This small reduction is due to a reduced response caused by the energy dissipation in Bent 4, and the hinge action which plays a role in this case.

5.3.2 LONGITUDINAL SHOCK

The even numbered cases correspond to the longitudinal shocks. The longitudinal direction is parallel to the chord

connecting the abutments. Generally the longitudinal ground motion is not as critical as the transverse. This is because of the following factors:

- . The columns participate more uniformly because they are connected by an axially rigid deck.
- . The continuity of the columns and the superstructure allow the columns to carry more shear force without flexural yielding.
- . The effect of other loading conditions such as deadload, liveload, temperature movement, etc. tend to affect the design of columns in this direction more than in the transverse direction.

The continuity of the superstructure with the substructure makes the resisting system for longitudinal loads more redundant. This is reflected in the design code by higher allowable ductility force reduction factors.

For highly curved structures such as those studied, longitudinal ground motion can produce significant overturning forces radial to the deck. The interaction of radial and tangential moments can be critical.

5.3.2.1 Bridge 1 (Cases 2, 4 and 6)

The maximum bending moments and corresponding shears at the base of the columns of Bridge 1 due to longitudinal shock are shown in Table 4.4. The response spectrum RMS results for longitudinal moment are approximately 30 percent less than those predicted by a linear time history analysis. The RMS transverse moments are in some cases several times greater than the linear time history results. In Bent 4, for example, the response spectrum analysis predicts a transverse moment nearly twice as large as the longitudinal moment. This structure, because of its close periods and degree of coupling, is particularly unsuitable for analysis by the response spectrum method.

The relatively uniform maximum rotational ductility demands shown in Table 5.2 show the relatively uniform participation of all the columns due to longitudinal ground motion. Notice that the two columns supporting an approximately equal weight section to the left of the hinge have a greater ductility demand than the three columns to the right. The plot in Appendix B on page B-7 shows a much more desirable history of yielding at Bent 5 for longitudinal ground motion than was experienced for transverse motion. Notice that for this case, where approximately equal columns participate equally in resisting the load, the maximum rotational ductility demands are approximately proportional to the moment reductions at the columns. Unfortunately, this uniformity of response is not typical of bridge structures.

5.3.2.2 Bridge 2 (Cases 8, 10 and 12)

The response spectrum RMS longitudinal moments shown in Table 4.13 are generally 30% less than the linear time history moments. It was found that a PRMS combination of modal responses yielded much more realistic results than it did for several of the other cases.

The maximum ductility demands for longitudinal ground motion given in Table 5.4 indicate the difference in response of the structural sections to either side of the expansion joint hinge. For example, Bent 8 which is approximately equal in height (and thus stiffness) to Bent 2, has more than twice the rotational ductility demand even though the ultimate capacities are not significantly different. This illustrates the difficulties inherent in trying to predict the distribution and magnitude of ductility demands from a linear analysis.

5.3.2.3 Bridge 3 (Cases 14, 16 and 18)

The maximum column moments and corresponding shears for Bridge 3 subjected to longitudinal ground motion are reported in Table 4.22. The RMS response spectrum moments are generally in fairly good agreement with the linear time history results and are thus acceptable for use in design.

The nonlinear rotational deformations and maximum rotational ductility demands reported in Table 5.6 indicate that yielding occurred in only 2 columns. The plot of nonlinear longitudinal

displacements for Bents 2 and 3 are shown on pages B-33 and B-37 respectively. Notice that Bent 3 yields only once at approximately 20 seconds. The linear time history analysis would seem to indicate that yielding would not occur. Since yielding occurs in Bent 2 prior to yielding in Bent 3, as do banging and restrainer takeup at the hinge in Span 3, it is apparent that the yielding in Bent 3 is caused by nonlinear behavior elsewhere in the structure. Again, this illustrates the difficulties in using a linear analysis to predict nonlinear behavior.

5.4 MAXIMUM TRANSVERSE FORCE IN THE SHEAR KEYS

The shear forces that occur during an earthquake at the abutments and hinges are somewhat more critical in that these forces must be resisted by nonductile components such as shear keys. The problem of obtaining realistic forces at these locations using a linear analysis is compounded by the fact that yielding in the ductile components results in a redistribution of the forces to the stiffer nonductile components. Transverse motion controls here as is generally the governing case for design.

5.4.1 BRIDGE 1 (Cases 1 thru 6)

The maximum shear key forces are tabulated in Table 4.5. The response spectrum values are slightly less than the time history for the transverse shock for Cases 1 and 3. For Case 5, the nonlinear analysis results are larger by 46 percent and 28 percent at Abutments 1 and 7 respectively. The increase in shear force

can be attributed to the yielding in the columns and the redistribution of the force to the abutments. The shear force at the intermediate hinge as determined by the response spectrum analysis is less than that obtained from the linear time history analysis by about 14 percent which corresponds to the difference obtained in column moments in the span adjacent to the span containing the hinge. The nonlinear analysis, however, indicates a reduction in force level by a factor of 2.6 at the hinge which corresponds to the overall reduction of 2.5 previously mentioned for the overall structure. The tabulated shear forces due to the longitudinal shocks are less than those obtained for the transverse shock and consequently would not govern for design, but do however, indicate that there is coupling.

5.4.2 BRIDGE 2 (Cases 7 thru 12)

Here again, the shear forces due to transverse shocks are the greatest. This structure is somewhat unusual however, because of the way the bents influence the overall response. In particular, the bent nearest the hinge is very stiff in relation to the other bents due to the shorter column length. Because of this and the difference between the vibrational characteristics of the two sections of bridge on either side of the hinge, this bent tends to behave almost like an abutment. This can be seen by observing the first two mode shapes which are shown in Appendix A on Page A-6.

When column yielding occurs, the lateral force, although reduced as a whole, tends to be redistributed toward the stiffer abutment, and in this case the hinge located near a very stiff bent.

5.4.3 BRIDGE 3 (Cases 13 to 18)

Both the longitudinal and transverse shocks cause significant transverse forces in the shear keys at the abutment and hinges. This is due to the fact that the structure is a long extended curved structure with shear keys having components in both directions and to the presence of two intermediate expansion joint hinges. These factors cause considerable coupling between longitudinal and transverse motion of the bridge.

The response spectrum results for the transverse shock are generally less than those for the linear time history, with differences varying from 1 percent at Abutment 1 and increasing to 20 percent at Abutment 10. The differences in shear key forces are more pronounced at the hinge in Span 7 and at Abutment 10. This is due to the method of combining the modes which represent maximum response in this section of the bridge. This phenomenon is not as pronounced for the longitudinal shock where the difference at Abutment 10 is 12 percent.

The nonlinear time history results for a transverse shock are consistently lower than the linear time history with the exception of the hinge in Span 7. The amount of column yielding in this

bridge is much less than in the other two structures. Aside from this yielding, the principal difference between the linear and nonlinear time histories is the nonlinear behavior of the expansion joint hinges. Since the yielding of columns is localized, the redistribution of force is minimal. The overall force is reduced, however, thus resulting in a reduction in shear key forces.

5.5 MAXIMUM DECK DISPLACEMENTS

RMS combinations of modal results for the response spectrum analysis yield results for deck displacements that are in disagreement with the linear time history results in many cases. These differences are more pronounced in bridges where substantial modal responses occur in two or more modes. The displacements from the nonlinear analyses are generally lower than the linear results. This is just opposite to what might be expected since yielding is generally thought to produce greater deformations. However, the energy dissipation caused by column yielding reduces the response and consequently the net displacements. There are exceptions, however, where the additional deformation at a column yielding exceeds the deformations calculated by the linear analysis. This usually occurs just at initial yielding when the reduction in displacement due to energy dissipation is less than the energy contained in the system.

5.5.1 BRIDGE 1 (Cases 1 - 6)

The maximum deck displacements due to a transverse shock (Cases 1, 2 and 5) are shown in Table 4.6. The response

spectrum displacements at the bents in the transverse direction are consistently less than the values obtained from the linear time history analysis. This is because there are three modes, with closely spaced periods, which are all responding to this transverse excitation. It is very likely that the peak modal responses will all tend to occur simultaneously. The RMS value of the modal responses will therefore yield lower displacements. For longitudinal displacement due to the same shock, the response spectrum RMS values vary drastically with displacements being less than the linear time history. This is again due to the small differences in periods and the degree of coupling between the longitudinal and transverse directions in this bridge.

The nonlinear deck displacements in the transverse direction due to the transverse shock are from between 27 percent and 37 percent less than the linear time history. This reduction in displacement is caused by the reduction in response due to energy dissipation in the columns. The displacements that occurred during the first excursion into the nonlinear range at 4.40 seconds exceed the values reported by the linear analysis at the same time. This is due to the increased deformation caused initially by yielding. With succeeding reversals in the direction of the ground acceleration, however, energy dissipation and reduction in the elastic restoring forces occurs in the column, and thus the maximum response of the structure is reduced. It will be noted that there is a small but significant increase in the longitudinal displacements at Bents

3, 4 and 5. This is due to the fact that these three bents have significant deadload moments due to unbalanced span lengths. During initial yielding of these bents, rotational deformations occur which tend to relieve the longitudinal deadload moments. This occurs even with relatively small earthquake longitudinal moment components. Once this yielding has occurred, subsequent column yielding will be due entirely to earthquake forces. Thus the rotational deformations due to longitudinal deadload moments cause permanent nonlinear deformations in the structure resulting in a biased seismic response in the longitudinal direction. This results in the increased longitudinal displacement as seen in the results.

The maximum deck displacements due to a longitudinal shock (Cases 2, 4 and 6), are shown in Table 4.7. The longitudinal displacement values for the response spectrum are also consistently less than the linear time history. This difference is less to the left of the hinge where mode 2 dominates the longitudinal motion. For transverse displacements due to longitudinal shock, the response spectrum analysis does not at all agree with the linear time history results. This is also due to the fact that the periods are close together and out of phase coupling exists between the second and third modes of vibration.

The nonlinear displacements in the longitudinal direction due to longitudinal earthquake are also less than the displacements

resulting from a linear time history analysis. The displacements on the left side of the hinge, Bents 2 and 3 are reduced more than those to the right of the hinge, Bents 4 thru 6. This is due in part to the increased yielding and energy dissipation and the compensating effects of the unbalanced moments in the bents to the left of the hinge. The larger deadload moments to the right of the hinge have an effect on these displacements by a biased longitudinal motion, although it is not as obvious as in the previous example. This biased effect caused by releasing of deadload moments may also be the reason why the difference in deck displacement is less than the transverse displacements due to transverse earthquake. Since transverse deadload moments are relatively small, the transverse displacements are not affected and therefore they do not experience a reduction similar to the longitudinal displacements.

5.5.2 BRIDGE 2 (Cases 7 thru 12)

The maximum deck displacements due to a transverse shock (Cases 7, 9 and 11) are shown in Table 4.15. This shock produces results which are similar to Bridge 1. The overall response for the nonlinear analysis is less than the response for the linear analysis due to the energy dissipation. In general, the displacements for the nonlinear analysis are less except the longitudinal displacements to the right of the hinge where they are larger than the displacements for the linear analysis. This is due again to the same phenomenon that occurred for Bridge 1

in that the effects of the larger unbalanced deadload moments to the right of the hinge cause the structure to have a biased movement as the moments are released during the nonlinear column deformation.

The maximum deck displacements due to a longitudinal shock (Cases 8, 10 and 12) are shown in Table 4.16. For this shock the displacements for the nonlinear analysis are larger than the linear analysis and the transverse displacements are less. The increase is approximately 17 percent at Bents 3 and 4. For the remaining bents, the difference varies from 1.8 to 9.8 percent.

The increased differences at Bents 3 and 4 can be explained by the fact that the maximum displacement occurs relatively early in the earthquake, shortly after the column first yields. The effect of energy dissipation during the short time between first yield and maximum response is insufficient to overcome the effect of increased displacement due to inelastic deformation. The increase in the remainder of the longitudinal displacements is due to the deadload moment effect discussed earlier.

5.5.3 BRIDGE 3 (Cases 13 thru 18)

The maximum deck displacements due to transverse and longitudinal shocks are shown in Tables 4.24 and 4.25 respectively. For the transverse shock, the deck displacements are generally less for the nonlinear analysis due to the energy dissipation in the column yielding at Bent 4. Since the column at Bent 4 is the

only column that yielded, there is some elastic response in the nonlinear model which exceeds the elastic response in the linear model. This occurs in the columns adjacent to the column that has yielding.

For the longitudinal shock, yielding occurs in the columns at Bents 2 and 3. The nonlinear deck displacements are larger than the linear in the first frame where this yielding occurs. Since the yield moments are very close to the moments obtained in the linear analysis, the anticipated energy absorption will be minimal. The remaining displacements are generally less for the nonlinear analysis, except in the last frame where the differences are influenced by the tie bar gap at the intermediate expansion joint hinge.

5.6 MAXIMUM HINGE MOVEMENTS AND RESTRAINING FORCES

The assumptions inherent in the elastic analysis approach currently used and generally available to the bridge designer limits the modeling capabilities at the intermediate expansion joint hinge. The idealizations currently used are approximate in that the restrainer unit must take compression as well as tension and the gaps provided for temperature movements are ignored. The banging effects caused by closing of the seat gap and yielding of the tie bar cannot be incorporated into the model. These assumptions imposed by the limitations of an elastic analysis have been of major concern to the bridge designer both in the effects

on the overall response of the structure and the localized effects on the restrainer units. Basically, the designer's viewpoint has been that the assumptions inherent in this approach will not have a significant effect on the overall response and will yield results in the restrainer unit that are approximate. These forces are then checked against a minimum of 25 percent of the deadload of the smallest frame.

5.6.1 BRIDGE 1 (Cases 1 thru 6)

The maximum hinge separations and corresponding restrainer forces due to both longitudinal and transverse shocks are recorded in Table 4.8. The response spectrum results are 6 to 10 times larger than the elastic time history for the transverse shock. These large differences are due to the out of phase response that occurs between the second and third modes of vibration. Each mode having a substantial contribution to the total response of the system is not added algebraically as in the time history analysis. Contrary to this, however, the results for the longitudinal motion agree quite well, the results agreeing within 10 percent for both the inside and outside restrainer units. The longitudinal motion is generally the one that controls and for this bridge is less the 542 kips obtained using the minimum as specified by the code provisions.

The nonlinear analysis yielded no restrainer law forces indicating that the temperature gap of 0.1 foot in the restrainer was not taken up in either the transverse or longitudinal motions.

Time history plots of the expansion joint movements at the right and left of edge of deck for both the transverse and longitudinal motions are included in Appendix C pages C-2 to C-5 respectively. The tie gap and seat gap are also superimposed on the plots. The plots indicate that the hinge movements are almost large enough to cause forces in the restrainers. Also, the seat gaps are closed up to yield only a minimum amount of banging action at the hinge. The plots of expansion joint movement for the transverse motion indicates the tendency of the joint to open due to the non-linear behavior occurring in the bridge. This biased movement would be more pronounced with additional column yielding or sliding of the expansion joint bearing. Considering the number of excursions of the columns into the nonlinear range for this low period structure, and the probable reduction in column stiffness, the biased opening at the hinge to yield forces in the restrainers is very probable. The actual magnitude of these forces would require additional analytical studies with the capability of including stiffness degradation in the columns. Assuming, however, that the columns could maintain their integrity and that stiffness degradation in the post-elastic cycles is not significant, the present minimum code requirements appear to be conservative.

5.6.2 BRIDGE 2 (Cases 7 thru 12)

The maximum hinge separations and corresponding restrainer forces due to both longitudinal and transverse shocks are recorded in Table 4.17. For this bridge, the response spectrum and linear time history analysis agree quite well; within

15 percent for the transverse motion and 20 percent for the longitudinal motion. The longitudinal motion yields the largest forces which are less than the minimum 235 kips required by the code.

The nonlinear analysis results, similar to those obtained for Bridge 1, indicate that the restrainer forces are zero. This structure has fewer excursions into the nonlinear range and thus the nonlinear analysis, performed with the assumed perfectly elastic-plastic column behavior, can be considered to be a more accurate simulation for this bridge. The nonlinear analysis here again indicates that the current minimum requirements of the code and the results obtained using the elastic analysis are conservative.

5.6.3 BRIDGE 3 (Cases 13 thru 18)

The maximum hinge separations and corresponding restrainer forces for the hinge in Spans 3 and 7 for both transverse and longitudinal motion are recorded in Table 4.26. The response spectrum and linear time history analysis generally agree. The nonlinear analysis yields restrainer forces which are generally less than those obtained from the linear analysis, with the exception of the inside unit at the hinge in Span 3. The force obtained in this restrainer unit can be attributed to the yielding of the column in Bents 2 and 3. The non-uniform yielding of the columns here results in larger restrainer forces. The nonlinear

analysis indicates that for structures with more than one intermediate hinge the restrainer forces are affected by the non-uniform yielding in the columns. Both the elastic analysis results agree quite well and are equal to or less than the minimum code requirements of 324 kips and 282 kips for the hinges in Spans 3 and 7 respectively.

Bent No.	E (k/ft ²)	I _y (long.) (ft ⁴)	M _{yp} (k-ft)	h _y (ft)	θ_y (rad. $\times 10^{-3}$)	I _z (ft ⁴)	M _{zp} (k-ft)	h _z (ft)	θ_z (rad. $\times 10^{-3}$)
2 to 6	432,000	72.9	12,000	7.0	1.715	142.9	16,000	5.0	1.633

TABLE 5.1 - Bridge 1
Column Flexural Yield Rotations

Location	Maximum Nonlinear Rotational Distortion		Maximum Rotational Ductility Demand	
	Trans. Shock (Rad.x10 ⁻³)	Long. Shock (Rad.x10 ⁻³)	Trans. Shock	Long Shock
Bent 2	1.337	3.176	1.79	2.86
Bent 3	2.456	3.238	2.50	2.89
Bent 4	3.588	1.781	3.20	2.04
Bent 5	2.625	2.155	2.58	2.26
Bent 6	.989	1.729	1.59	2.01

TABLE 5.2 - Bridge 1 - Maximum Local Bending Ductility Demands at the Column Bases

Bent No.	E (k/ft ²)	I _y (Long.) (ft ⁴)	M _{yp} (k-ft)	h _y (ft)	θ_y (rad. $\times 10^{-3}$)	I _z (ft ⁴)	M _{zp} (k-ft)	h _z (ft)	θ_z (rad. $\times 10^{-3}$)
2, 6, 7	432,000	70.9	12,500	6.0	2.204	10.9	12,500	6.0	2.204
3, 4	432,000	70.9	10,000	6.0	1.763	70.9	10,000	6.0	1.763
5	432,000	70.9	14,340	6.0	2.528	70.9	14,340	6.0	2.528
8	432,000	70.9	10,950	6.0	1.931	70.9	10,950	6.0	1.931

TABLE 5.3 - Bridge 2
Column Flexural Yield Rotations

Location	Maximum Nonlinear Rotational Distortion		Maximum Rotational Ductility Demand	
	Trans. Shock (Rad.x10 ⁻³)	Long. Shock (Rad.x10 ⁻³)	Trans. Shock	Long Shock
Bent 2	.035	.945	1.02	1.43
Bent 3	4.205	.819	3.39	1.46
Bent 4	2.874	.715	2.63	1.41
Bent 5	1.363	2.097	1.54	1.82
Bent 6	5.946	2.622	3.70	2.19
Bent 7	3.736	2.067	2.70	1.94
Bent 8	2.301	4.285	2.19	3.22

TABLE 5.4 - Bridge 2 - Maximum Local Bending Ductility Demands at the Column Bases

Bent No.	E (k/ft ²)	I _y (Long.) (ft ⁴)	M _{yp} (k-ft)	h _y (ft)	θ_y (rad. ^{.3}) $\times 10^{-3}$	I _z (ft ⁴)	M _{zp} (k-ft)	h _z (ft)	θ_z (rad. ^{.3}) $\times 10^{-3}$
2, 3, 4, 5	432,000	106.9	40,500	6.0	4.736	182.7	51,000	8.0	4.652
6, 7	432,000	106.9	36,500	6.0	4.268	182.7	45,500	8.0	4.151
8, 9	432,000	106.9	32,500	6.0	3.800	182.7	40,000	8.0	3.649

TABLE 5.5 - Bridge 3
Column Flexural Yield Rotations

Location	Maximum Nonlinear Rotational Distortion		Maximum Rotational Ductility Demand	
	Trans. Shock (Rad.x10 ⁻³)	Long. Shock ₋₃ (Rad.x10 ⁻³)	Trans. Shock	Long. Shock
Bent 2	0	3.779	1.0	1.80
Bent 3	0	1.551	1.0	1.33
Bent 4	2.981	0	1.64	1.0
Bent 5	0	0	1.0	1.0
Bent 6	0	0	1.0	1.0
Bent 7	0	0	1.0	1.0
Bent 8	0	0	1.0	1.0
Bent 9	0	0	1.0	1.0

TABLE 5.6 - Bridge 3 - Maximum Local Bending Ductility Demands at the Column Bases

CONCLUSIONS AND RECOMMENDATIONS

6.1 CONCLUSIONS

6.1.1 DYNAMIC CHARACTERISTICS OF BRIDGES

Accurately predicting the response of complex bridge structures to strong earthquake motions requires the use of sophisticated nonlinear dynamic analysis computer programs not generally available to the bridge design engineer. The complex nonlinear behavior that occurs in bridges subjected to earthquakes is currently accounted for by reducing the results from a linear analysis by an assumed ductility factor. This does not account for the redistribution of forces due to nonlinear behavior nor does it predict the areas of maximum ductility demand.

The current methods generally used for the prediction of linear forces include equivalent static force, response spectrum analysis, or a linear time history analysis. The equivalent static force method is somewhat limited in that it can be applied only to simple structures with a single, predetermined mode of vibration. For the more complex structures requiring three dimensional analysis, such as the three bridges selected for this study, a more sophisticated computer analysis of response is required. While the use of elastic dynamic analysis for design is a substantial improvement over past practice and may in some instances suffice, it should not, however, be viewed as the ultimate tool for use in bridge design in highly seismic regions. Nonlinear analysis techniques which include the nonlinear behavior of column yielding, hinge discontinuity, foundations and energy absorptions should be implemented into design in these critical regions.

The two structure idealizations used in this study employ straight members and curved members for the superstructure. From this it is apparent that straight members yield nearly identical results because of the discretization of mass normally used at the quarter points.

Because of the coupling effects of the modes and contributions of several modes, three dimensional analysis is required to accurately predict the response of horizontally curved bridges. This also implies that the effect of excitation from orthogonal directions should be superimposed on the results for a shock in one direction.

6.1.2 RESPONSE SPECTRUM ANALYSIS

The response spectrum method generally appears to be satisfactory for the seismic design of bridges. Of the three structures tested, one of the bridges had two modes of vibration with approximately equal periods. In this case, the RMS combination for modal results from a response spectrum analysis did not agree with the linear time history as explained in Chapter 5.

6.1.3 OBSERVED NONLINEAR BEHAVIOR OF BRIDGES

The nonlinear behavior of bridge structures, as observed in the analysis of the three structures used in this study, indicates that redistribution of forces and location and magnitude of maximum ductility demands cannot be accurately predicted by an elastic analysis. The first excursion into the nonlinear range produced displacements in excess of those determined by the linear analysis. With succeeding excursions, however, the nonlinear

displacements were reduced, illustrating the effects of energy absorption due to the nonlinear action in the columns. The maximum displacements for the nonlinear analysis were less than the linear analysis results where there was yielding throughout the structure. When localized yielding occurred, however, the maximum displacements were sometimes greater. Therefore, it is almost impossible to predict nonlinear effects from a linear analysis.

6.1.3.1 Columns

The maximum rotational ductility demands are less than those currently assumed to be available for design. For one of the structures examined, however, the total accumulative yielding that occurred was much larger than the other structures which had comparable or larger ductility demands. Therefore, the maximum ductility demands as they are currently conceived do not indicate the maximum damage potential or the amount of energy absorption required by the structure during a maximum credible earthquake.

Classical ductility reduction factors for seismic loadings derived for simple elasto-plastic systems by equating elastic and inelastic response in terms of energy or deflection do not apply for the complex bridge systems examined in this study.

The current provisions for the design of maximum positive girder moment due to deadload and live load do not include the effects of relieving the deadload moment capacity of the column caused by formation of plastic hinges during an earthquake.

Variable column stiffnesses cause the redistribution of force to the other columns. This results in non-uniform yielding of the columns.

This could result in high ductility demands at isolated locations during an earthquake of even moderate intensity.

6.1.3.2 Abutments

The redistribution of forces due to columns yielding results in an increased force in the nonductile shear keys at the abutments. The current AASHTO seismic design provisions in which the response spectrums are reduced by ductility factors will yield forces in nonductile components such as shear keys which are far below the forces actually experienced.

6.1.3.3 Expansion Joints

Non-uniform yielding of bridge columns results in larger restrainer forces in structures having more than one intermediate hinge. The minimum code requirements of 25 percent and the forces obtained from an elastic analysis for Bridge 3 are larger than that obtained for the nonlinear analysis; however, the existence of a larger force in the restrainer at Bent 3 suggests that large forces could occur in bridges containing more than one intermediate hinge. For structures containing one intermediate hinge, the current approach for restrainer design at the expansion joint appears to be conservative.

The overall response of the structures examined do not appear to be significantly affected by the nonlinear behavior at the expansion joint hinges. The tie bar gaps and expansion joint seat gaps normally required for temperature considerations preclude their effects until column yielding and energy dissipation have occurred in the columns. Also, the possibility of inserting a practical energy

absorption device at the intermediate expansion joints to reduce the response of a structure or to limit the damage in a column is limited by this type of behavior. Transverse shear key forces at intermediate hinges are reduced due to the column yielding on structures that have approximately uniform column stiffness.

6.2 RECOMMENDATIONS

6.2.1 DESIGN PRACTICE AND CODE PROVISIONS

Based on the comparison of results from the three types of analyses used in this study, it is recommended that consideration be given to the following suggested changes in seismic design practice and/or code provisions:

- a. The response spectrums currently used in the AASHTO specification should be revised so as not to include the reduction for ductility. Ductility reductions should be made on an individual component basis.
- b. Seismic design provisions should consider the simultaneous application of earthquake motion in the three component directions since there is coupling between the component directions within each mode of vibration.
- c. The PRMS combination of modal contributions resulting from a response spectrum analysis was an improvement for bridges analyzed using the response spectrum technique and may potentially be used for bridges having two modes of vibration with approximately equal periods.

- d. Some means of evaluating the total damage potential to a bridge should be employed as an indicator of the severity of the seismic motion. This could be accomplished by summing the total ductility demands or the total energy dissipation during the time history of motion.
- e. Seismic design provisions should establish some threshold of yielding for moderate earthquakes expected to occur several times during the expected life of the bridge. The need for this aspect of seismic design becomes more prevalent when consideration is given to the unequal distribution of ductility demands in a structure having non-uniform column stiffnesses.
- f. The seismic design should provide for an increase of approximately 1.5 to 2 in the forces at the abutments derived from an elastic analysis if yielding in the columns is anticipated.
- g. Design provision for combining girder moments due to dead and liveloads should include the effects of deadload moment redistribution due to possible relief of deadload moments at the location of a plastic hinge in a column during an earthquake.
- h. The use of intermediate hinges should be avoided if possible in bridges located in areas of high seismicity.

i. Nonlinear computer capabilities such as those developed in the earlier phases of this project should be modified for use by the practicing engineer and disseminated to the engineering profession so they can be used to:

1. study the seismic behavior of bridges
2. expand on the current seismic design code provisions
3. analyze complex structures

6.2.2 FUTURE STUDIES

The questions raised by this study indicate the need for future studies in the following areas:

- a. Stiffness Degradation - The effect of stiffness degradation on the nonlinear dynamic response should be considered in future bridge studies.
- b. Energy Absorption - The important role of inelastic energy absorption in the columns and expansion joint restrainers should be studied. Special attention should be given to developing a clearer understanding of the concept of ductility and how it relates to bridge design so that elastic analysis techniques may be used by the bridge designer. Of special concern is the problem of defining the "damage potential" of an earthquake on a particular structure.

- c. Restrainer Units - Non-uniform yielding and ductility demands in the columns result in larger forces at the restrainer units for bridges with more than one intermediate hinge. These effects should be studied further to investigate the current minimum specification in the code and if elastic analysis techniques currently used can predict these restrainer forces.
- d. Response Spectrum Analysis - Special studies to improve the results gained from a response spectrum analysis are needed. The determination of the most effective means of combining modal results for a particular bridge is especially needed.

The computer capabilities developed as a part of earlier phases of this project such as BRISOT (5,6) and NEABS (4,8) represent powerful research tools. They may be effectively used for studying special problems related to bridge design and analysis, and for analyzing bridge response due to past and future earthquakes. Because of their potential for advancing the state of knowledge, these computer capabilities should be continually improved and enhanced to provide researchers and engineers with an effective means for analytically studying bridge seismic behavior.

REFERENCES

1. Gates, J., "California's Seismic Design Criteria for Bridges," *Journal of the Structural Division*, ASCE, Vol. 102, No. ST12, Proc. Paper No. 12636, December 1976, pp 2301-2313.
2. *Interim Specifications Bridges*, Section 2, 1975, American Association of State Highway and Transportation Officials.
3. Iwasaki, T., Penzien, J. and Clough, R. "Literature Survey-Seismic Effects on Highway Bridges," Report No. EERC 71-11, Earthquake Engineering Research Center, University of California, Berkeley, November 1972.
4. Tseng, W. S., and Penzien, J., "Analytical Investigations of the Seismic Response of Long Multiple Span Highway Bridges," Report No. EERC 73-12, Earthquake Engineering Research Center, University of California, Berkeley, June 1973.
5. Chen, M. C., and Penzien, J., "Analytical Investigations of Seismic Response of Short, Single, or Multiple Span Highway Bridges," Report No. EERC 75-4, Earthquake Research Engineering Center, University of California, Berkeley, January 1975.
6. Chen, M. C., and Penzien, J., "Nonlinear Soil-Structures Interaction of Skew Highway Bridges," Report No. UCB/EERC 77/24, Earthquake Engineering Research Center, University of California, Berkeley, August 1977.

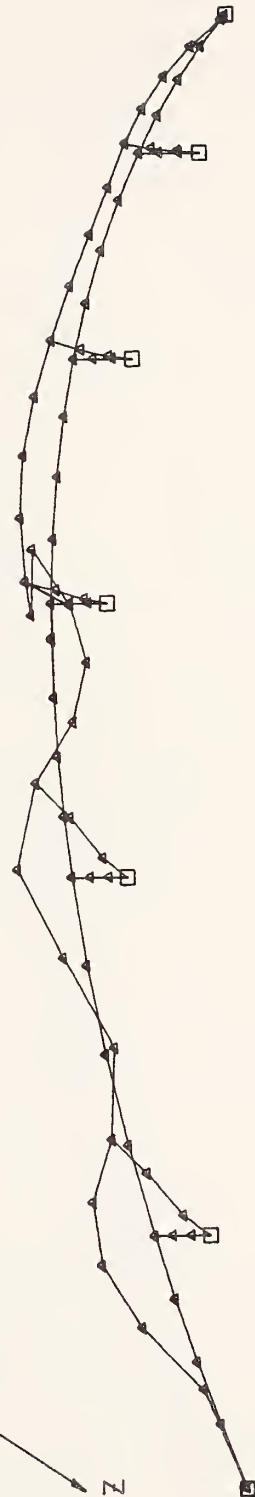
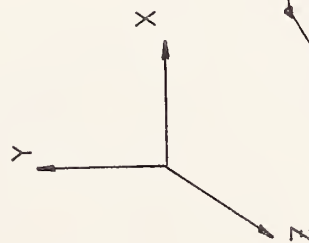
7. Williams, D., and Godden, W. G., "Experimental Model Studies on the Seismic Response of High Curved Overcrossing," Report No. EERC 76-18, Earthquake Engineering Research Center, University of California, Berkeley, June 1976.
8. Kawashima, K., and Penzien, J., "Correlative Investigations on Theoretical and Experimental Dynamic Behavior of a Nodal Bridge Structure," Report No. EERC 76-26, Earthquake Engineering Research Center, University of California, Berkeley, July 1976.
9. Fung, G., LeBeau, R., Klein, E., Belvedere, J., Goldschmidt, A., "Field Investigation of Bridge Damage in the San Fernando Earthquake," State of California, Division of Highways, Bridge Department, 1971.
10. "Bridge Planning Design Manual," Vol. 1, Sect. 2-16, April 1977, California Department of Transportation, Office of Structures.
11. Logcher, R. D., Flachsbarth, B. B., Hall, E. J., Power, C. M., Wells, R. A., and Ferrante, A. J., "ICES STRUDL II The Structural Design Language, Engineering User's Manual, Volume 1, Frame Analysis," MIT Department of Civil Engineering Report R68-91, November 1968.
12. "STRUDL, STRUDL DYNAL and STRUDL Plots," by Mc Auto and Multi-systems, Inc.

13. "STRUBAG - Instructions to Users" by California Department of Transportation, Division of Structures.
14. Seed, H. B., Idriss, I. M., "Rock Motion Accelerograms for High Magnitude Earthquakes," Earthquake Engineering Research Center Report EERC 69-7, 1969, University of California, Berkeley.

Mode Shapes



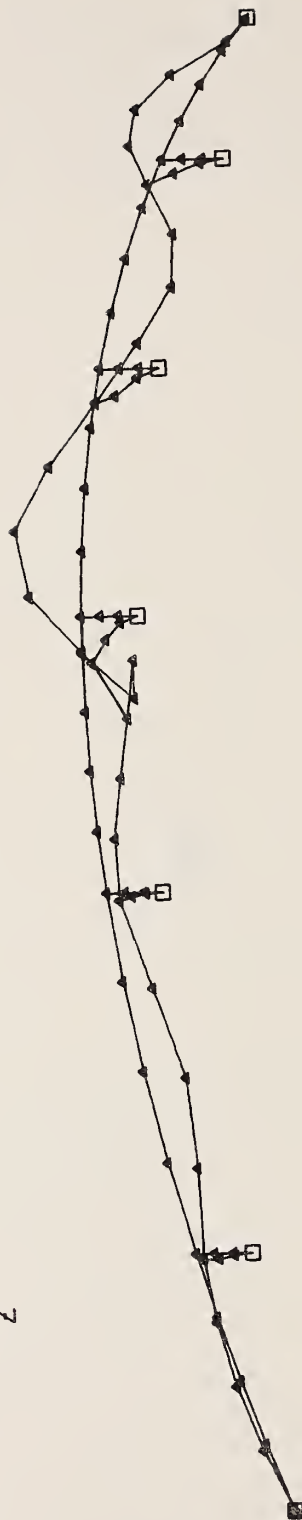
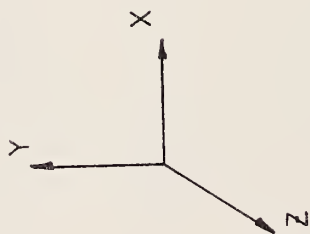
MODE 1



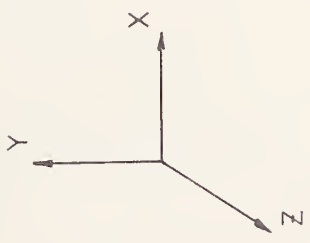
MODE 2
BRIDGE 1



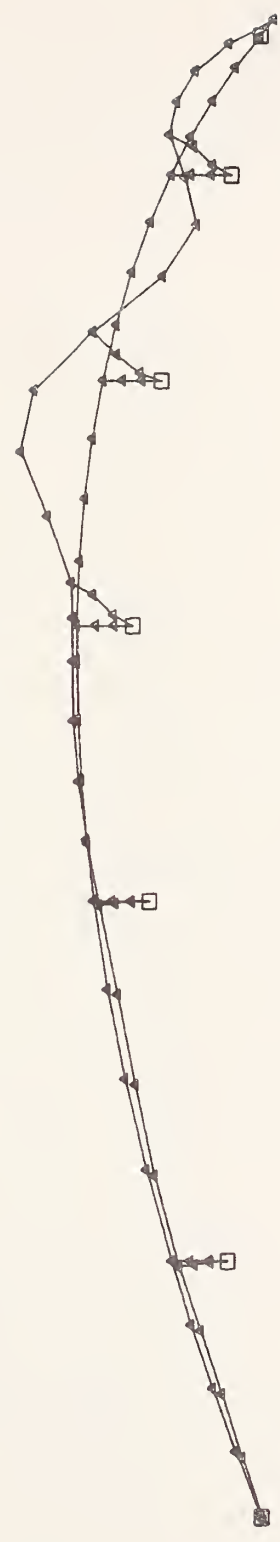
MODE 3



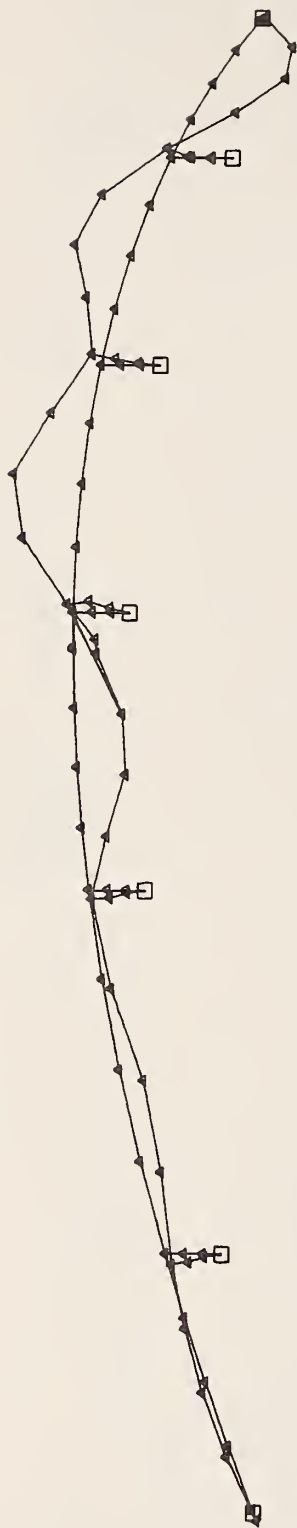
MODE 4
BRIDGE 1



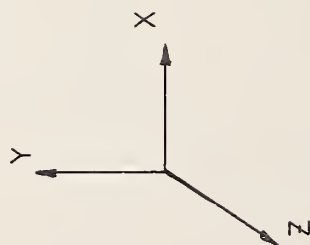
MODE 5



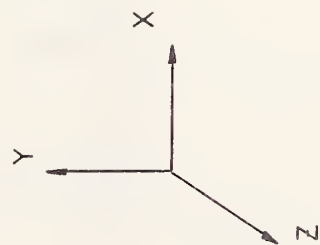
MODE 6
BRIDGE 1



MODE 7



MODE 8
BRIDGE 1



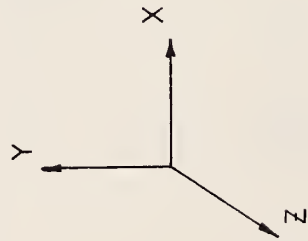
MODE 9



MODE 10
BRIDGE 1



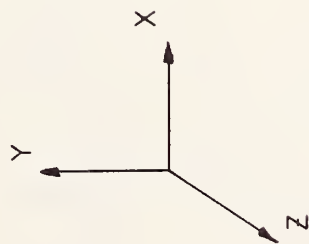
MODE 1



MODE 2
BRIDGE 2



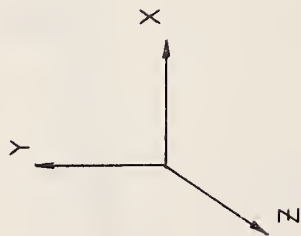
MODE 3



MODE 4
BRIDGE 2



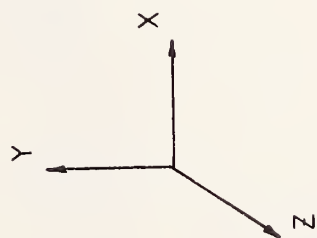
MODE 5



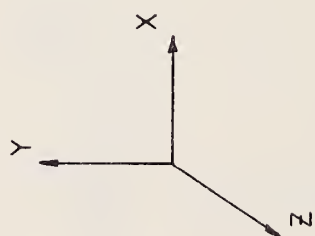
MODE 6
BRIDGE 2



MODE 7



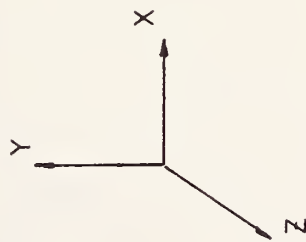
MODE 8
BRIDGE 2



MODE 9



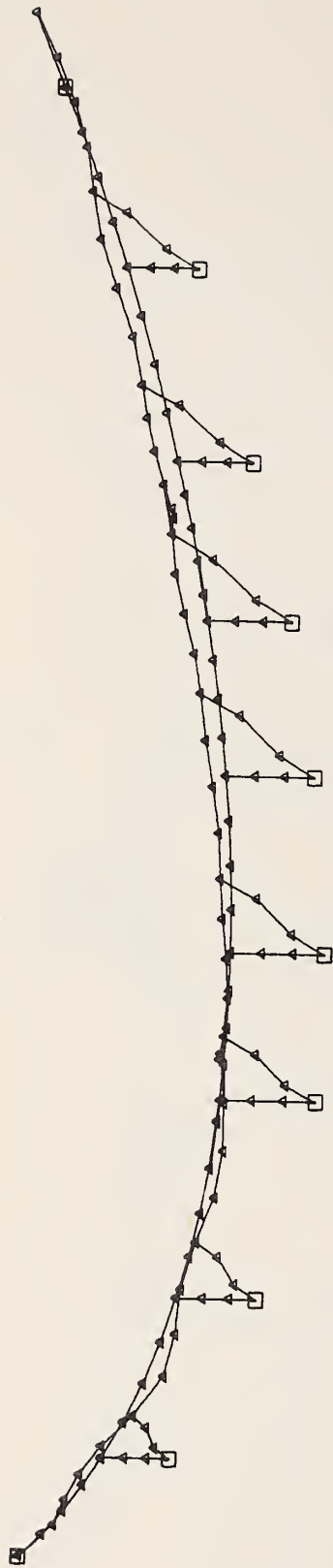
MODE 10
BRIDGE 2



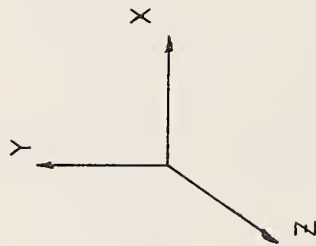
MODE 1



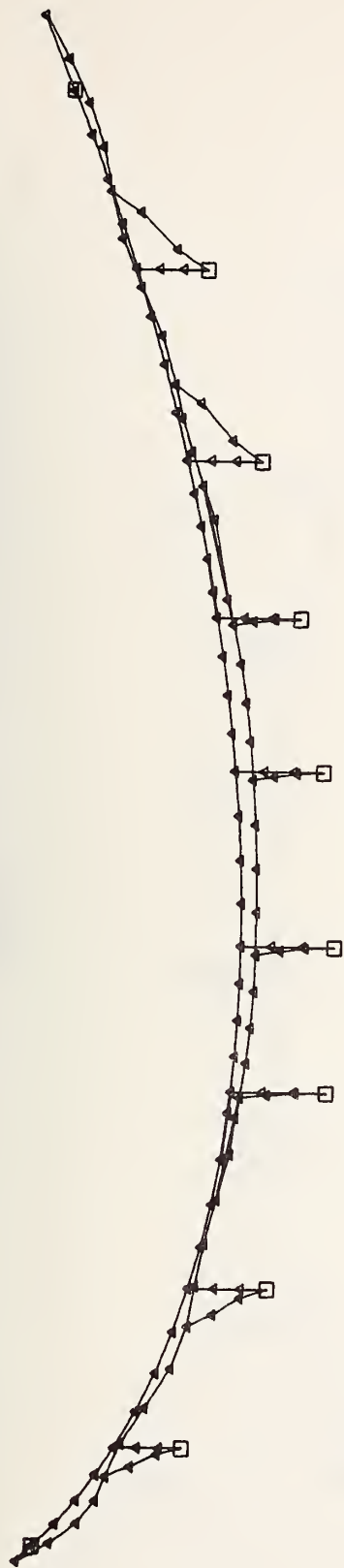
MODE 2
BRIDGE 3



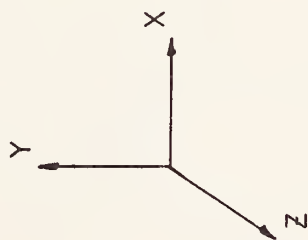
MODE 3



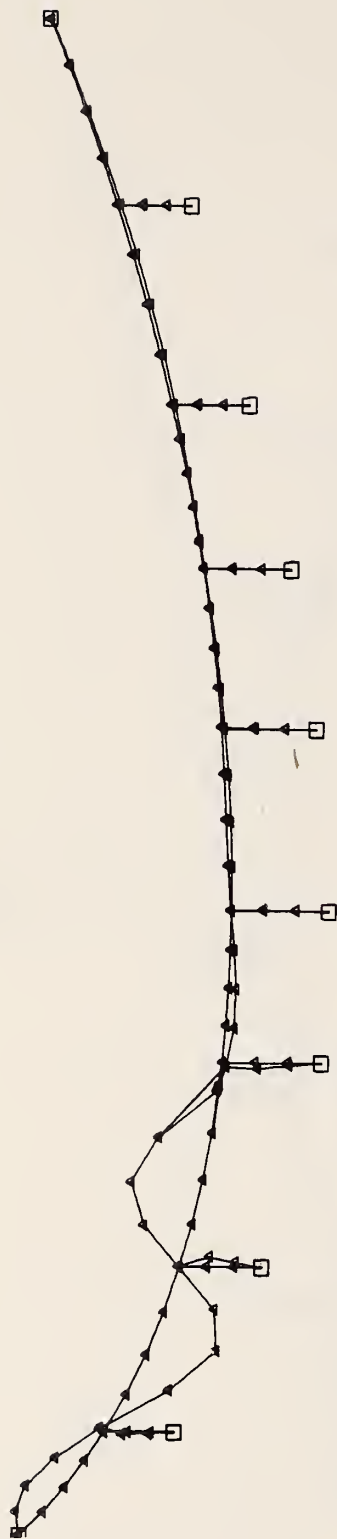
MODE 4
BRIDGE 3



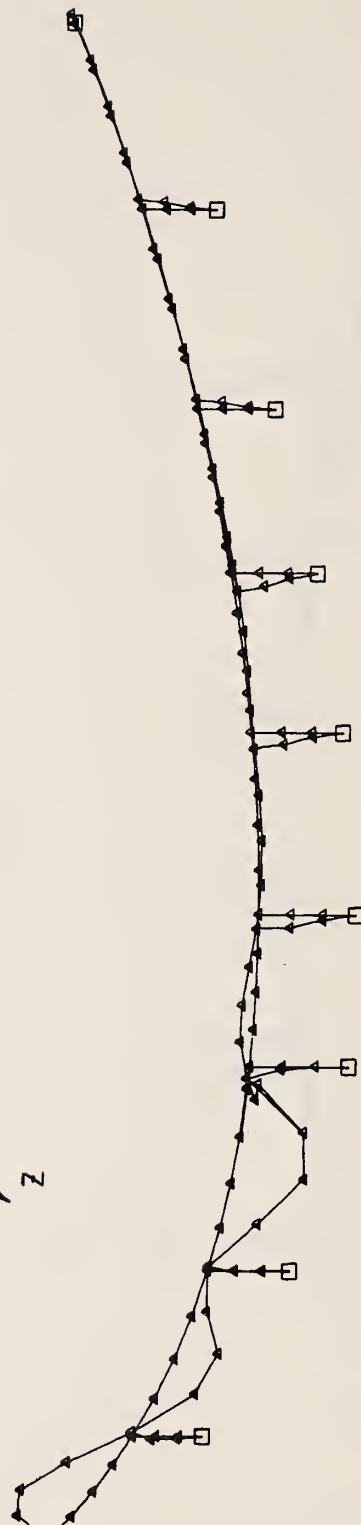
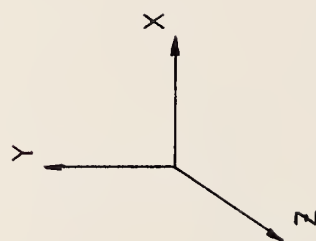
MODE 5



MODE 6
BRIDGE 3

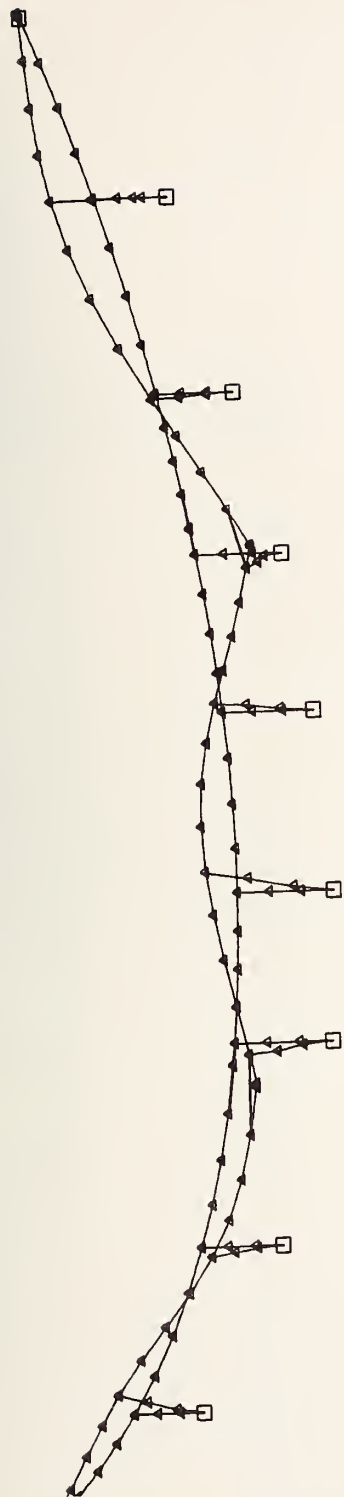


MODE 7

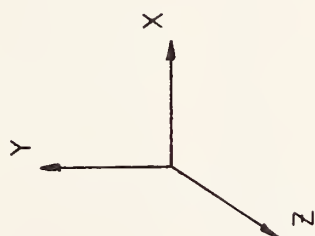


MODE 8

BRIDGE 3



MODE 9



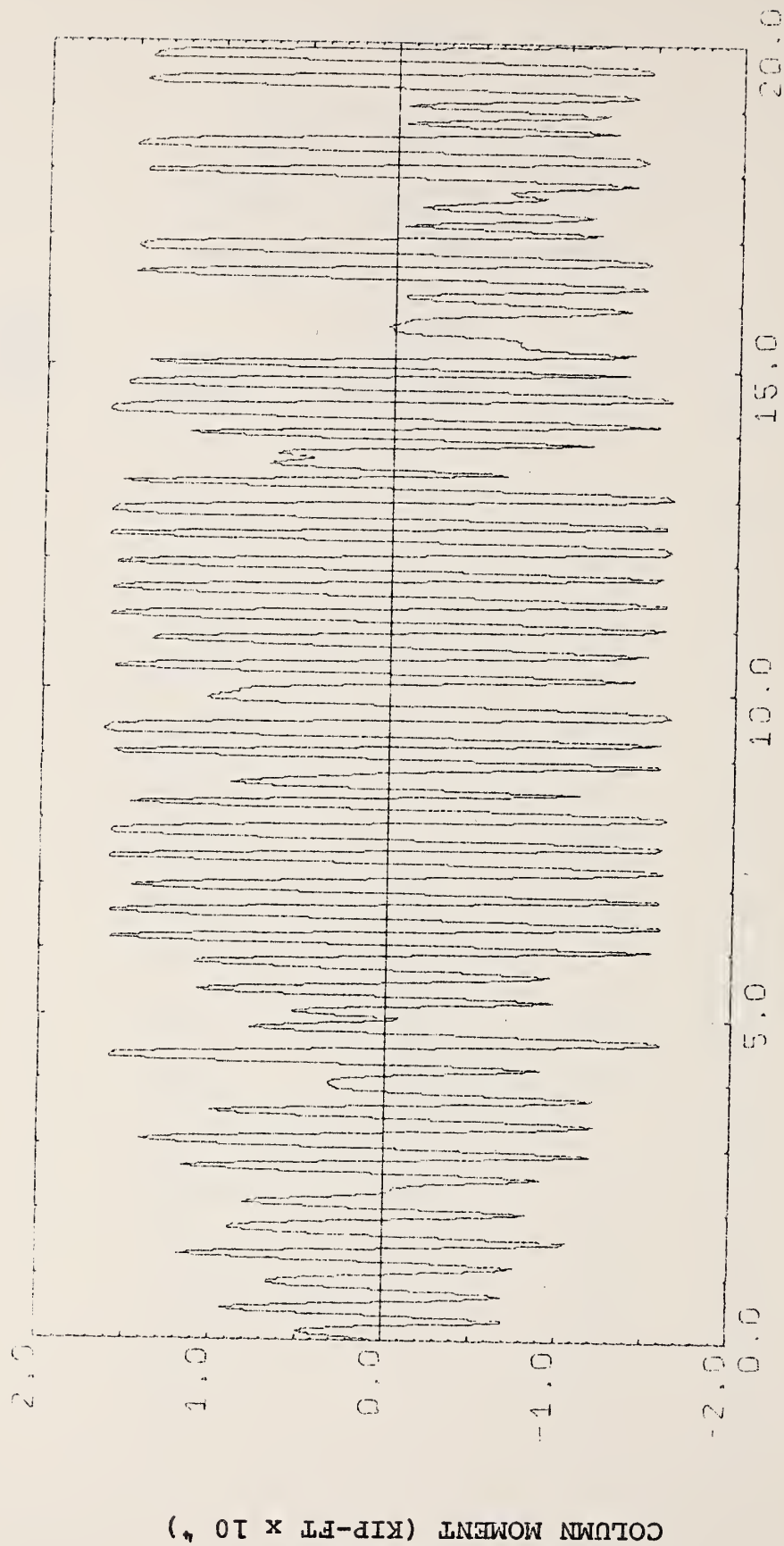
MODE 10
BRIDGE 3

APPENDIX B

NEABS

Time History Plots of Selected Column Base Moments and Corresponding Deformations

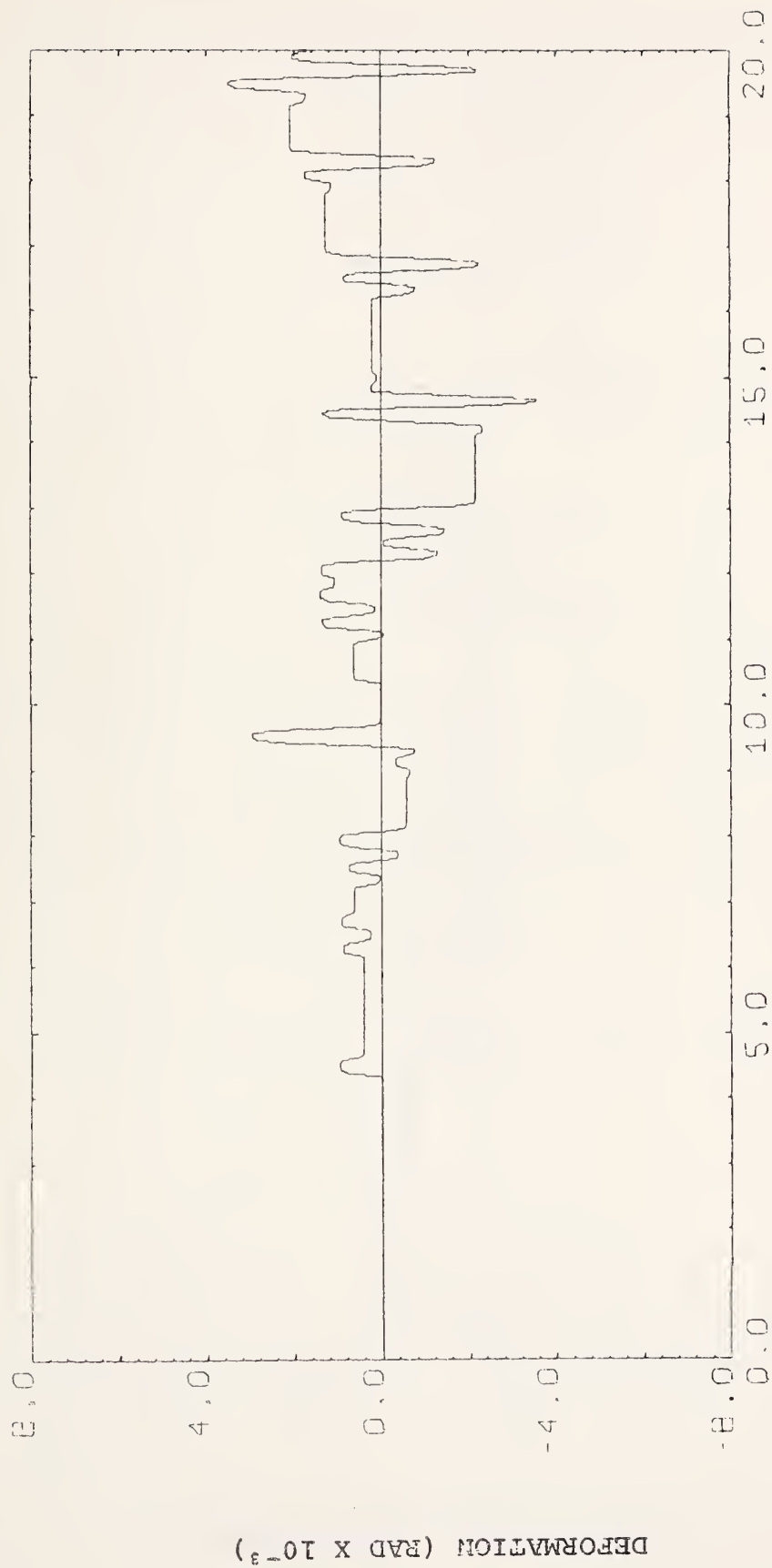
<u>Bridge</u>	<u>Case</u>	<u>Bent</u>	<u>Direction of Bending</u>	<u>Moment</u>	<u>Nonlinear Rotational Deformation</u>
1	5	4	T	B- 2	B- 3
1	5	4	L	B- 4	B- 5
1	6	4	L	B- 6	B- 7
1	6	4	T	B- 8	B- 9
2	11	5	T	B-10	B-11
2	11	5	L	B-12	B-13
2	11	6	T	B-14	B-15
2	11	6	L	B-16	B-17
2	12	5	T	B-18	B-19
2	12	5	L	B-20	B-21
2	12	6	T	B-22	B-23
2	12	6	L	B-24	B-25
3	17	4	T	B-26	B-27
3	17	4	L	B-28	B-29
3	18	2	T	B- 30	B-31
3	18	2	L	B-32	B-33
3	18	3	T	B-34	B-35
3	18	3	L	B-36	B-37



TIME (SEC)

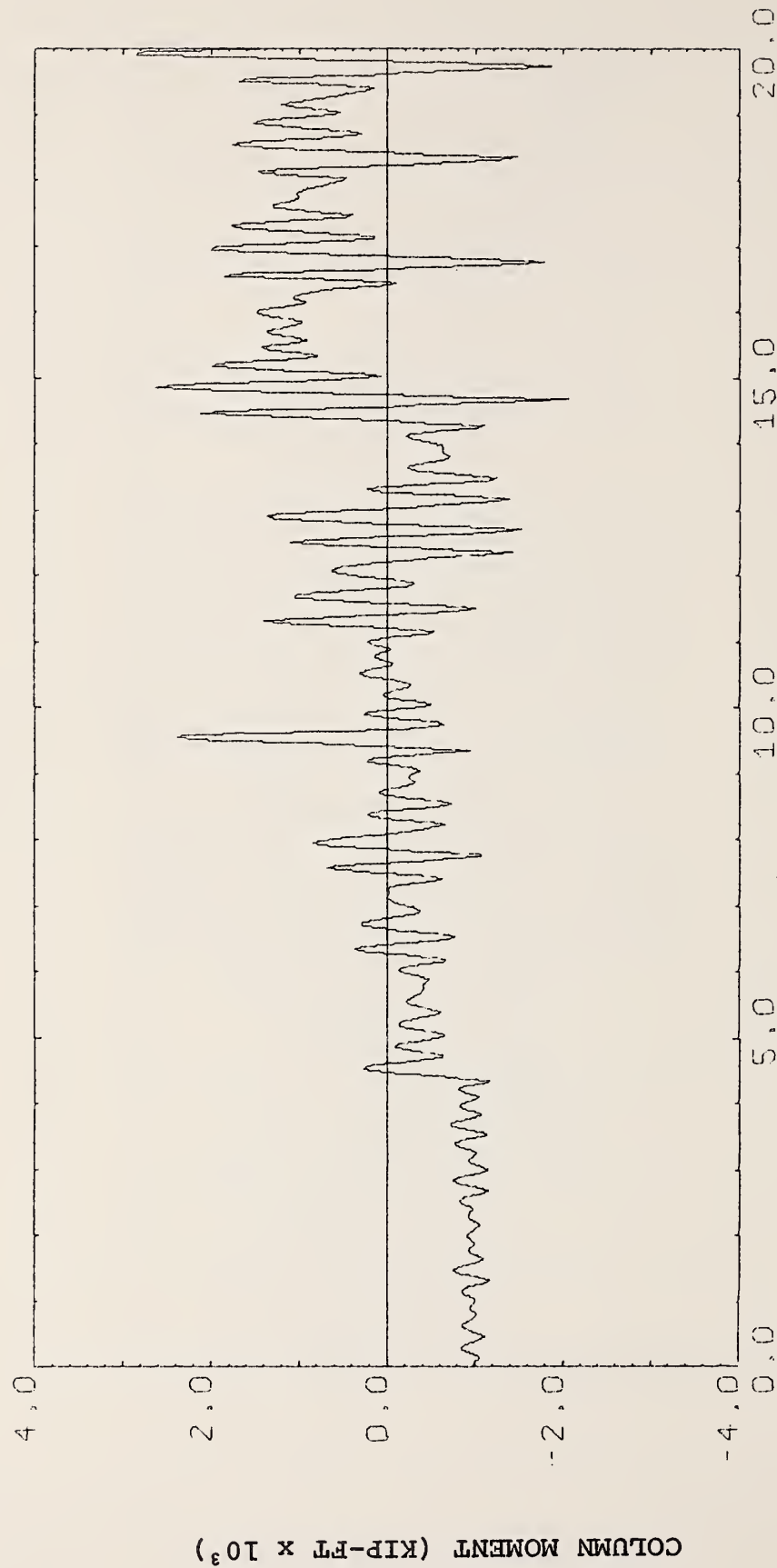
Transverse Moment at Base of Column - Bent 4

Bridge 1 - Case 5



Nonlinear Transverse Rotational Deformation at Base of Column - Bent 4

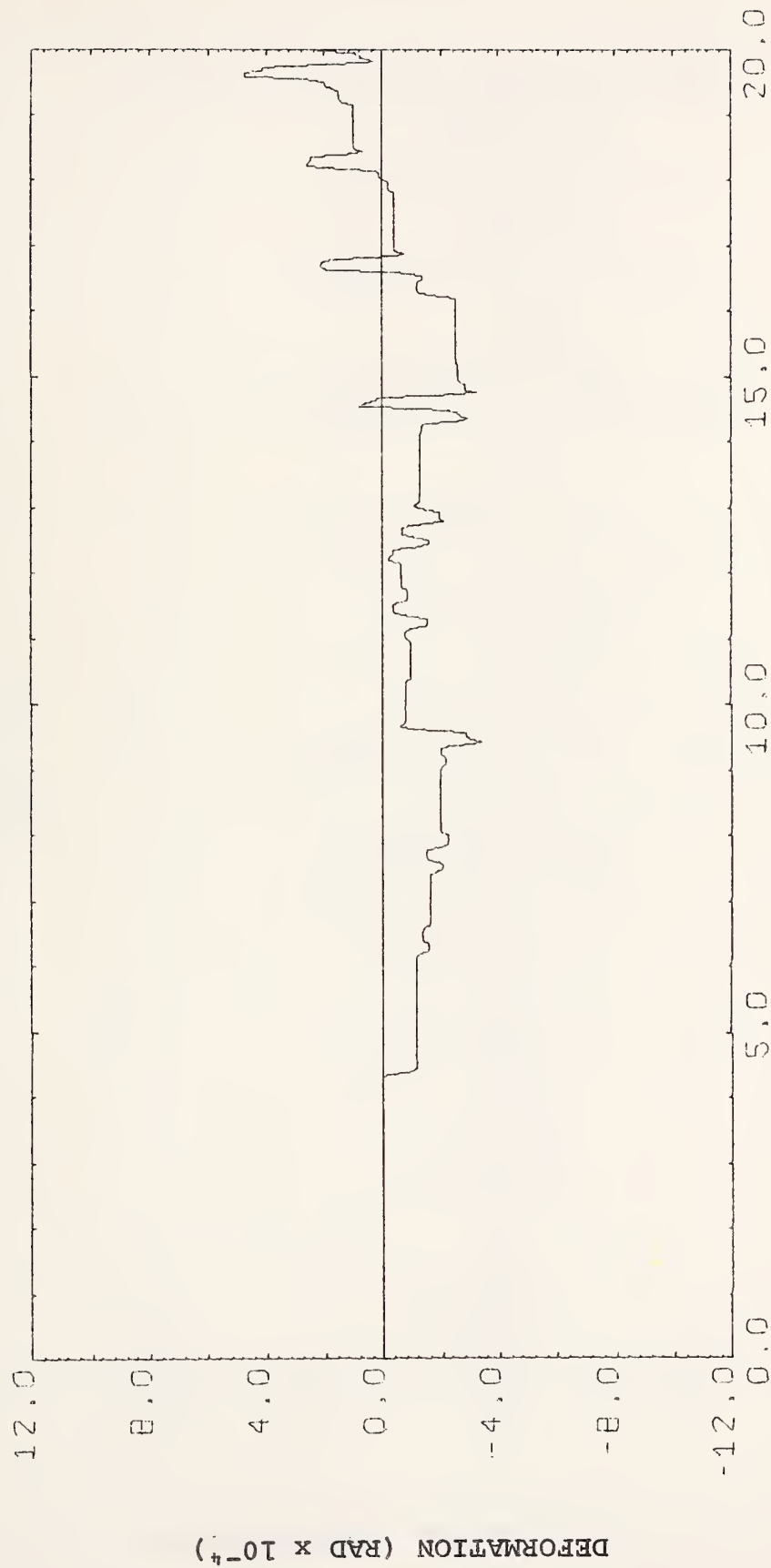
Bridge 1 - Case 5



TIME (SEC)

Longitudinal Moment at Base of Column - Bent 4

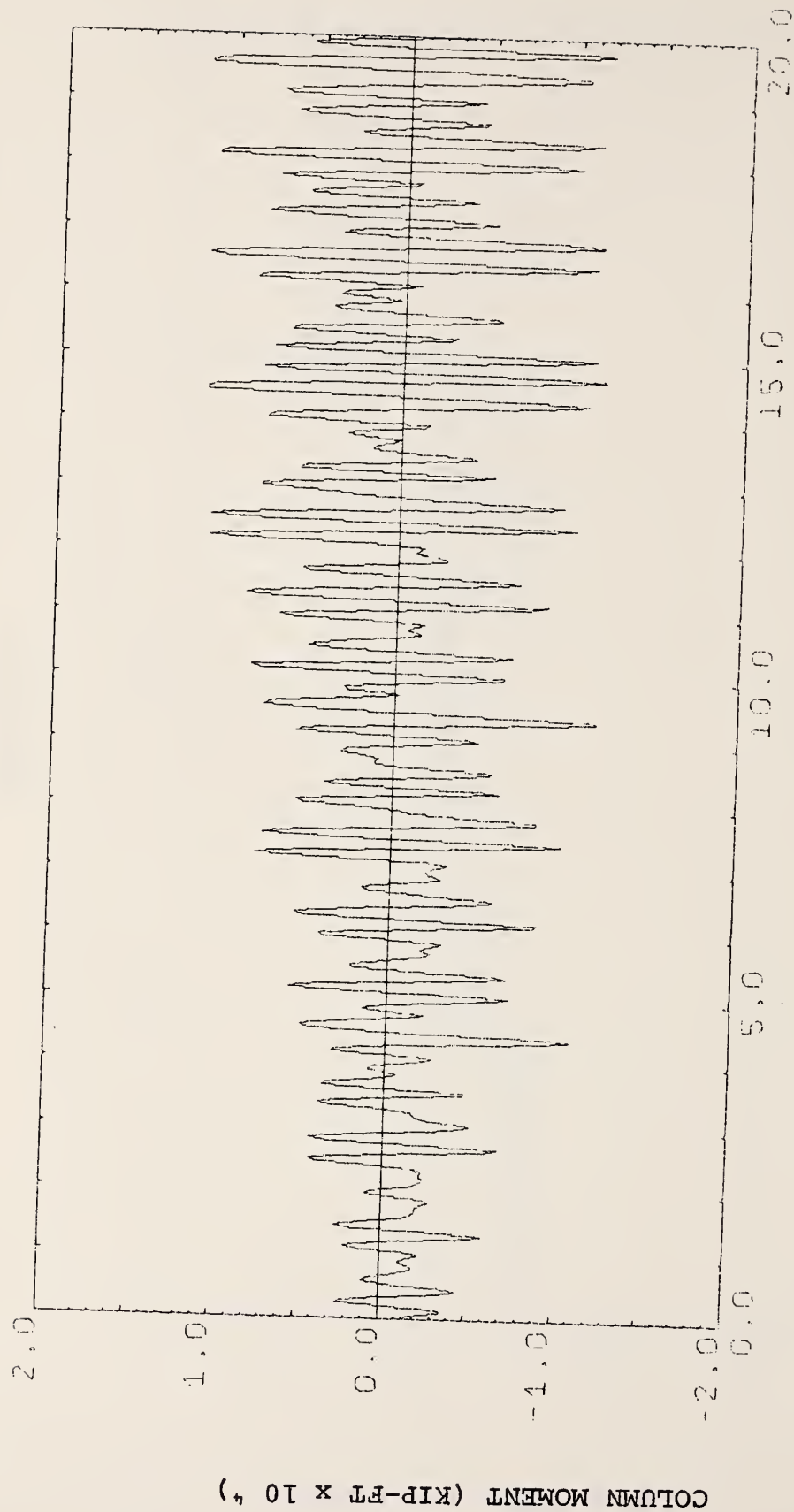
Bridge 1 - Case 5



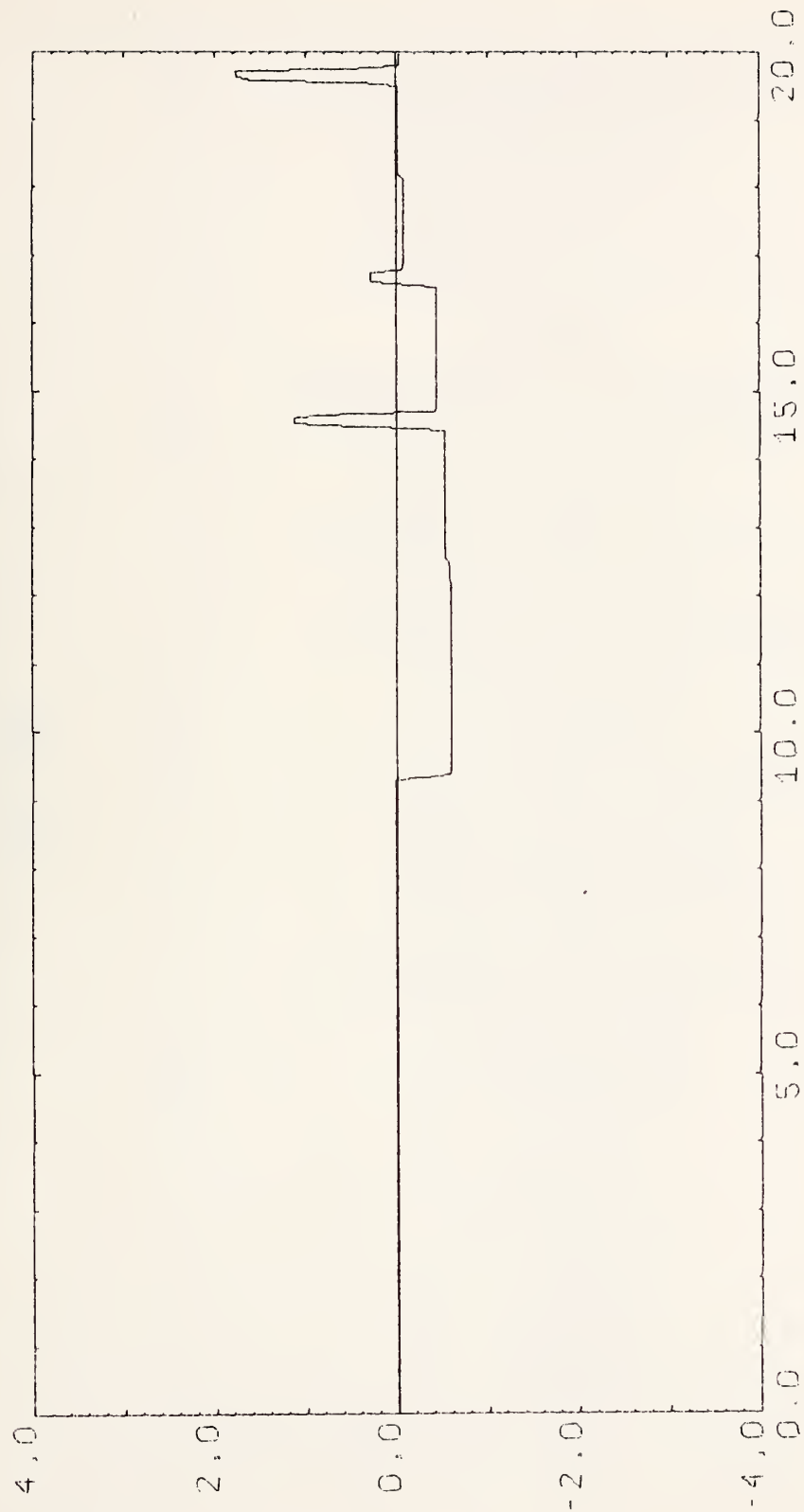
TIME (SEC)

Nonlinear Longitudinal Rotational Deformation at Base of Column - Bent 4

Bridge 1 - Case 5



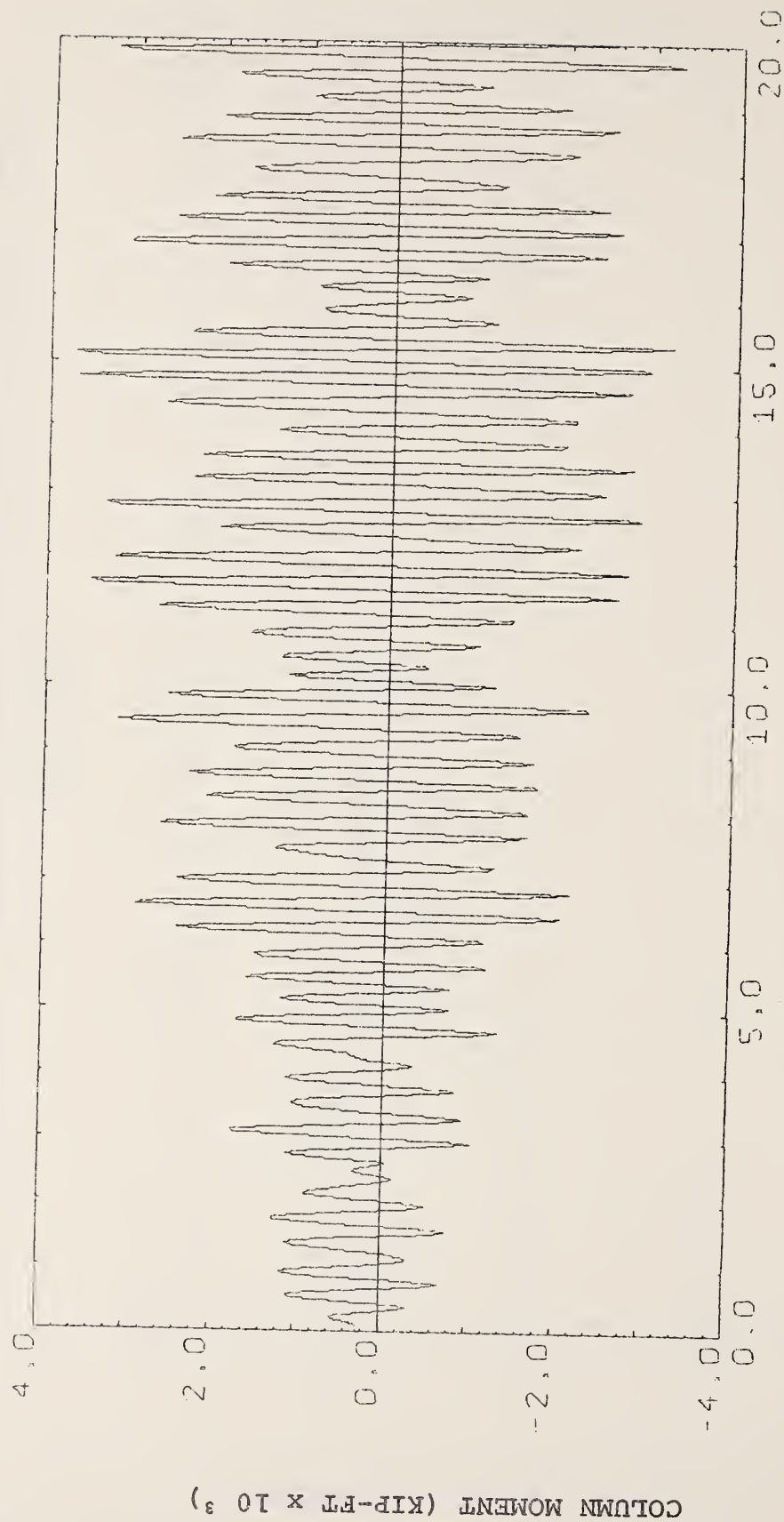
Longitudinal Moment at Base of Column - Bent 4
Bridge 1 - Case 6



TIME (SEC)

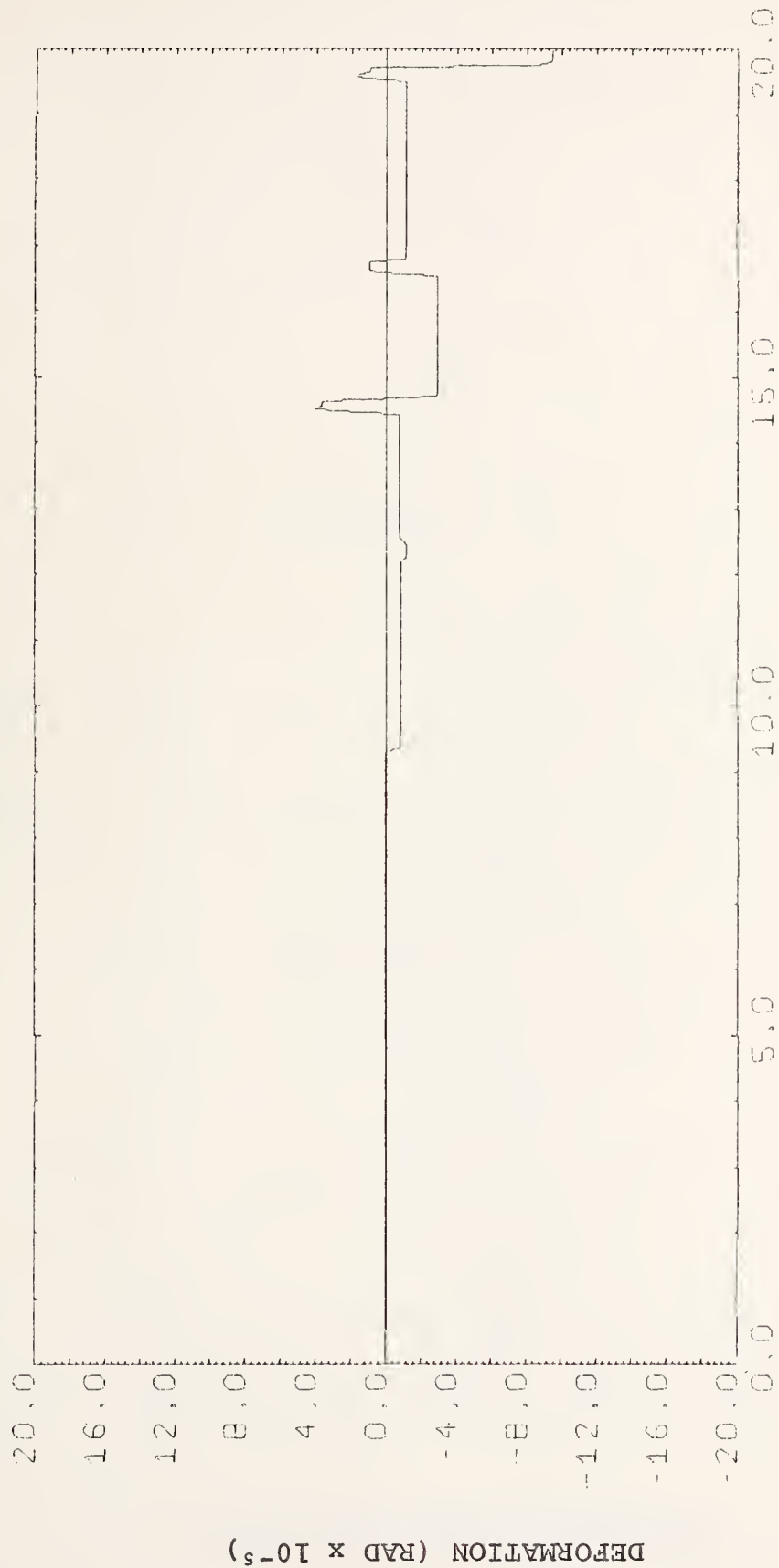
Nonlinear Longitudinal Rotational Deformation at Base of Column - Bent 4

Bridge 1 - Case 6



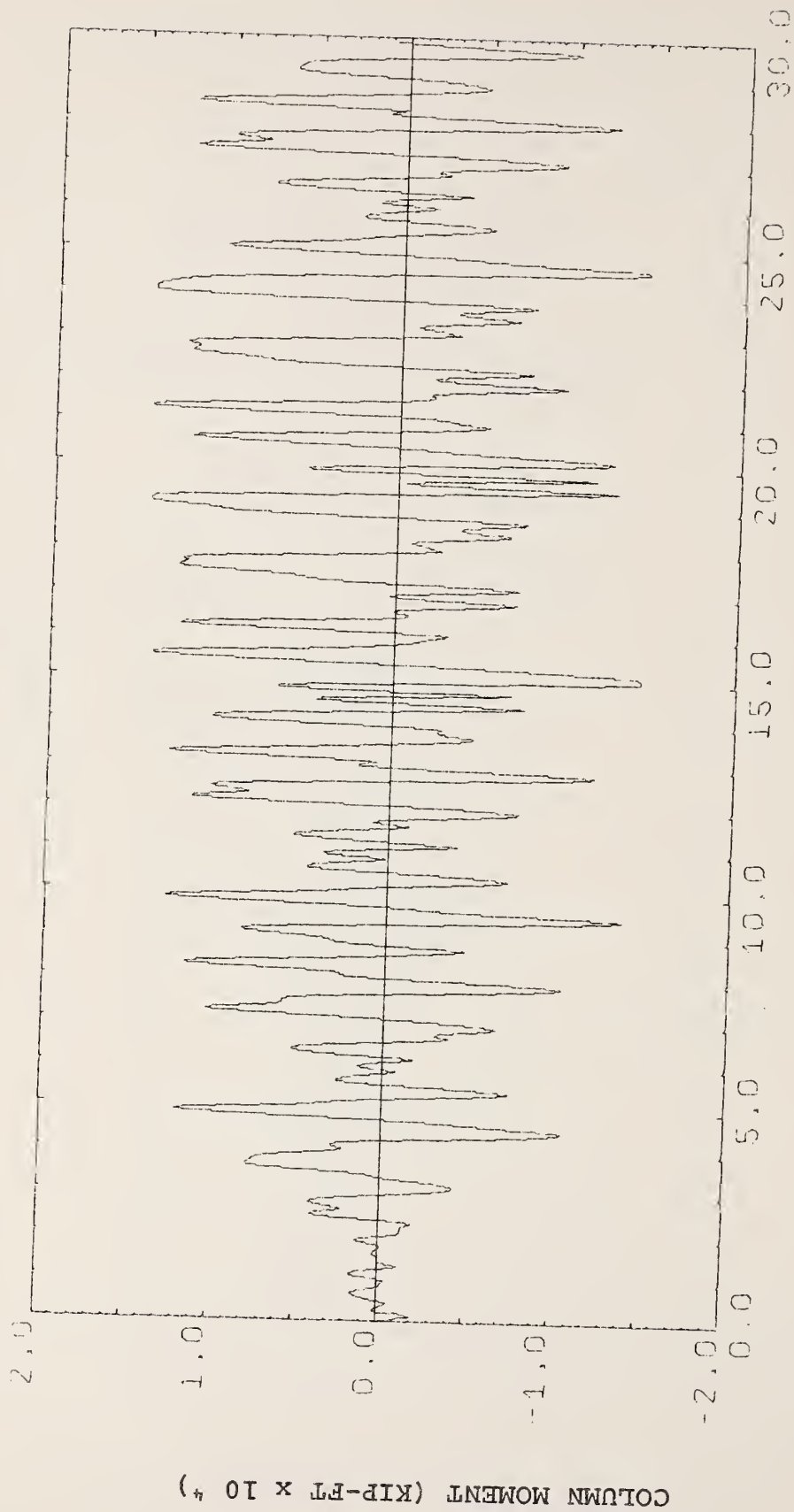
Transverse Moment at Base of Column - Bent 4

Bridge 1 - Case 6

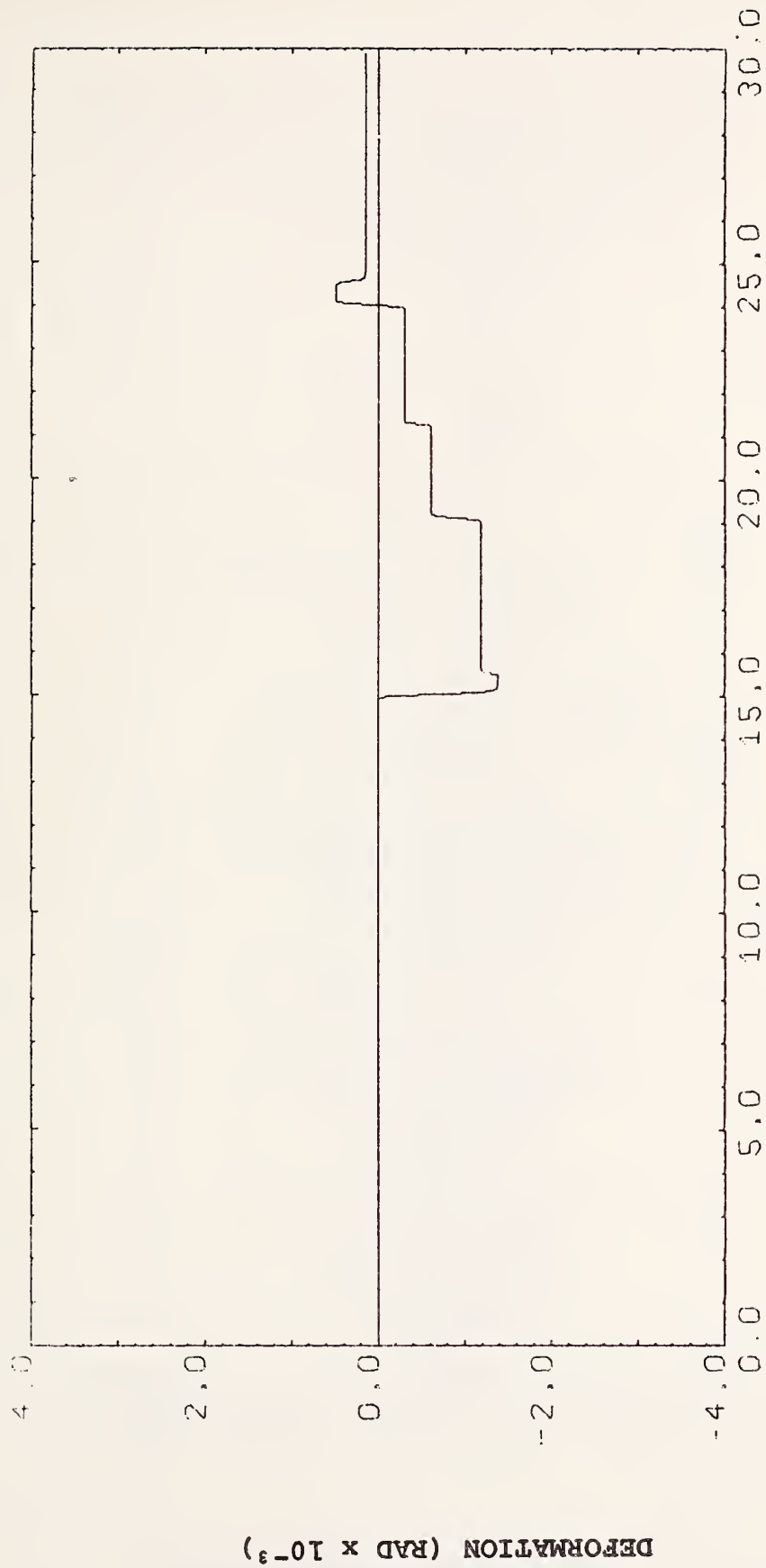


Nonlinear Transverse Rotational Deformation at Base of Column - Bent 4

Bridge 1 - Case 6



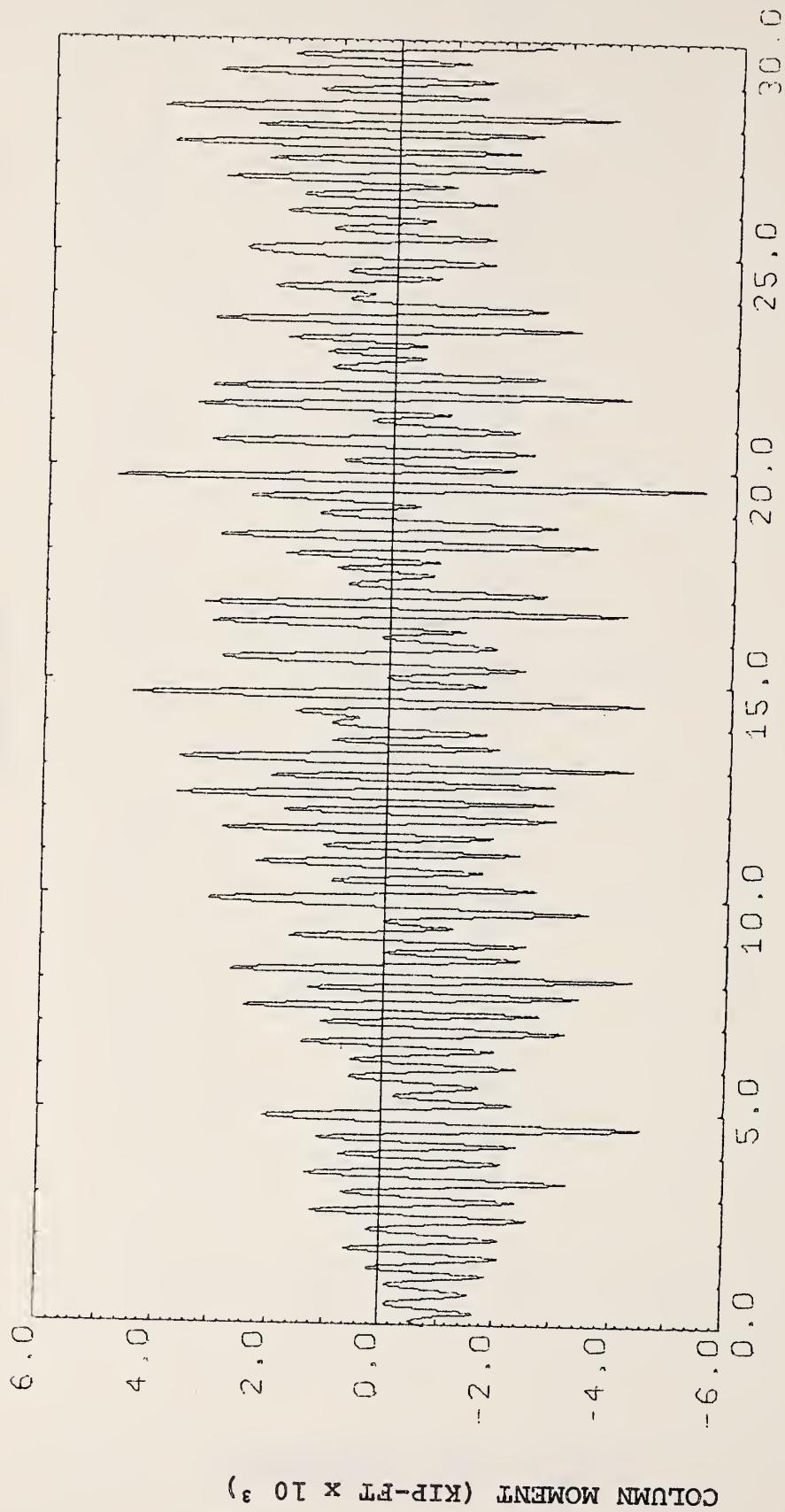
Transverse Moment at Base of Column - Bent 5
Bridge 2 - Case 11



TIME (SEC)

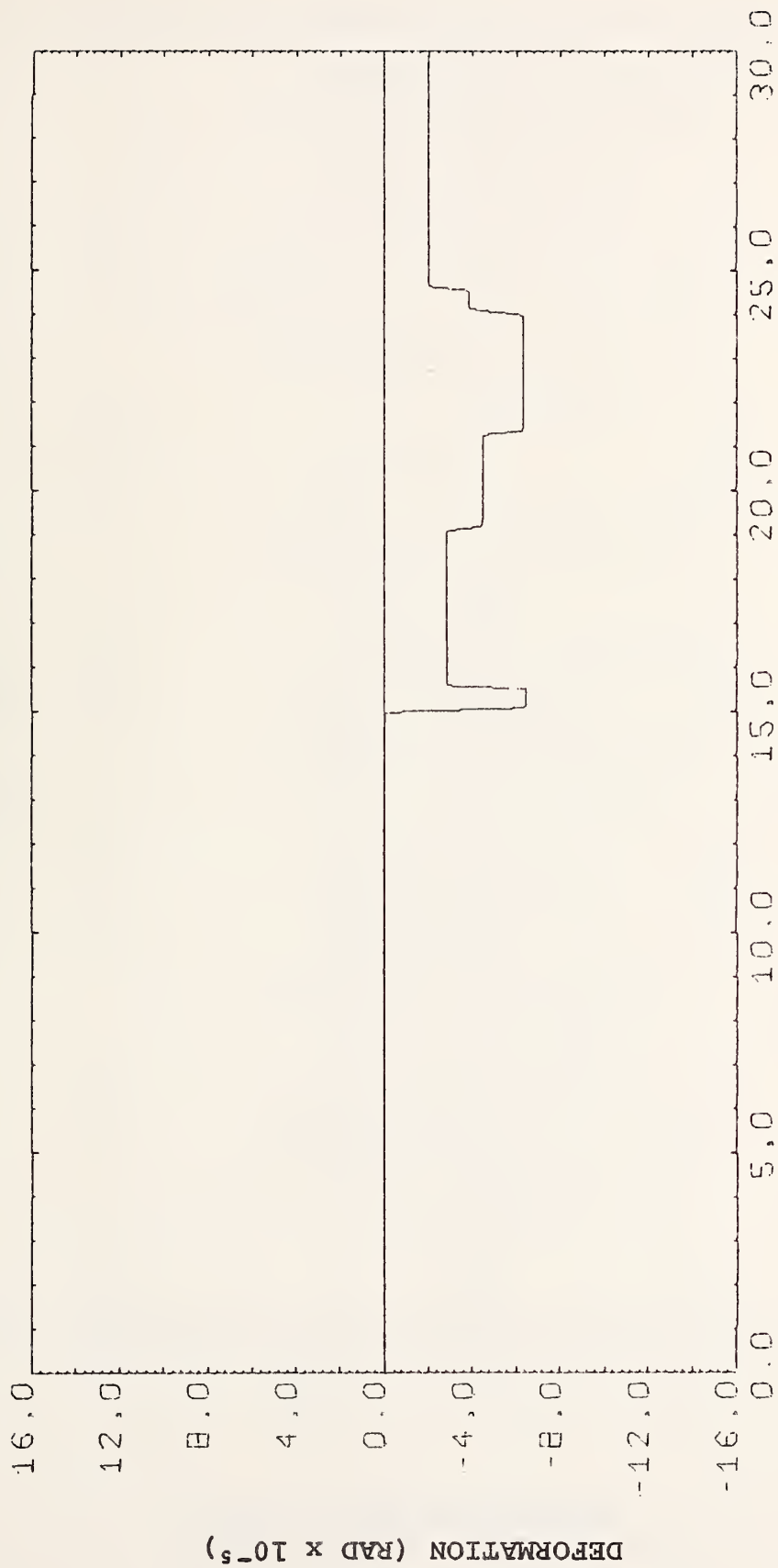
Nonlinear Transverse Rotational Deformation at Base of Column - Bent 5

Bridge 2 - Case 11



Longitudinal Moment at Base of Column - Bent 5

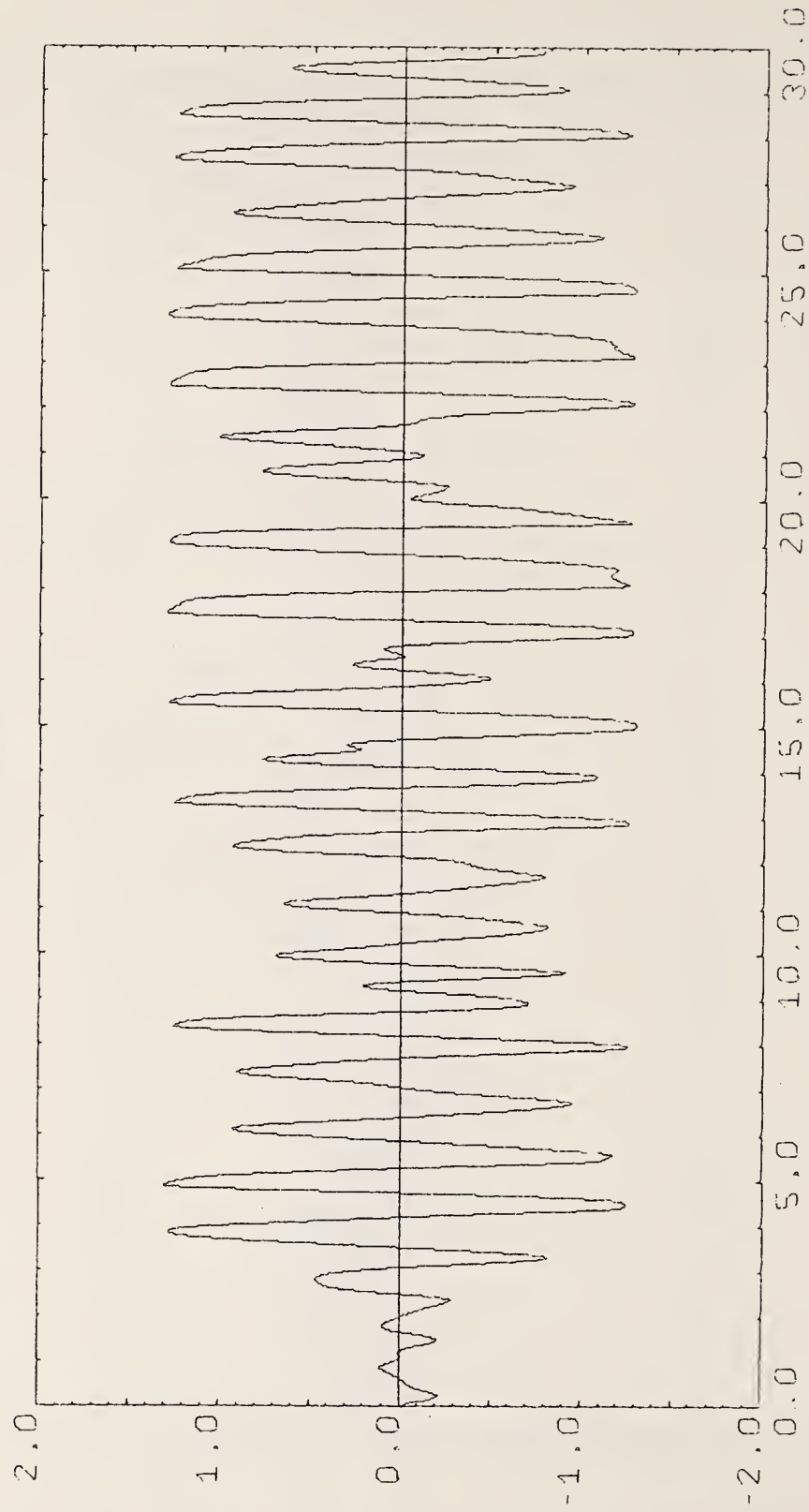
Bridge 2 - Case 11



TIME (SEC)

Nonlinear Longitudinal Rotational Deformation at Base of Column - Bent 5

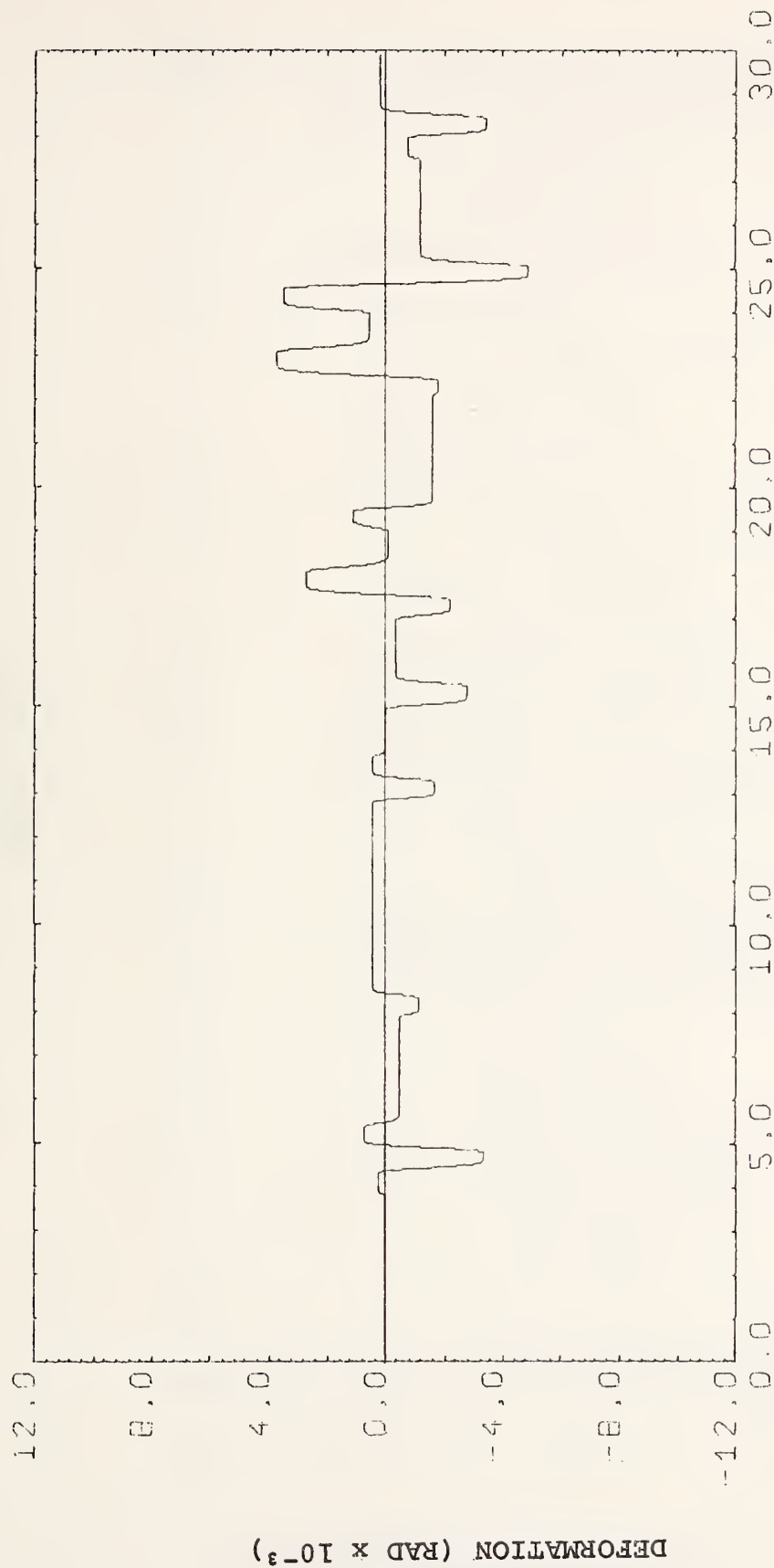
Bridge 2 - Case 11



TIME (SEC)

Transverse Moment at Base of Column - Bent 6

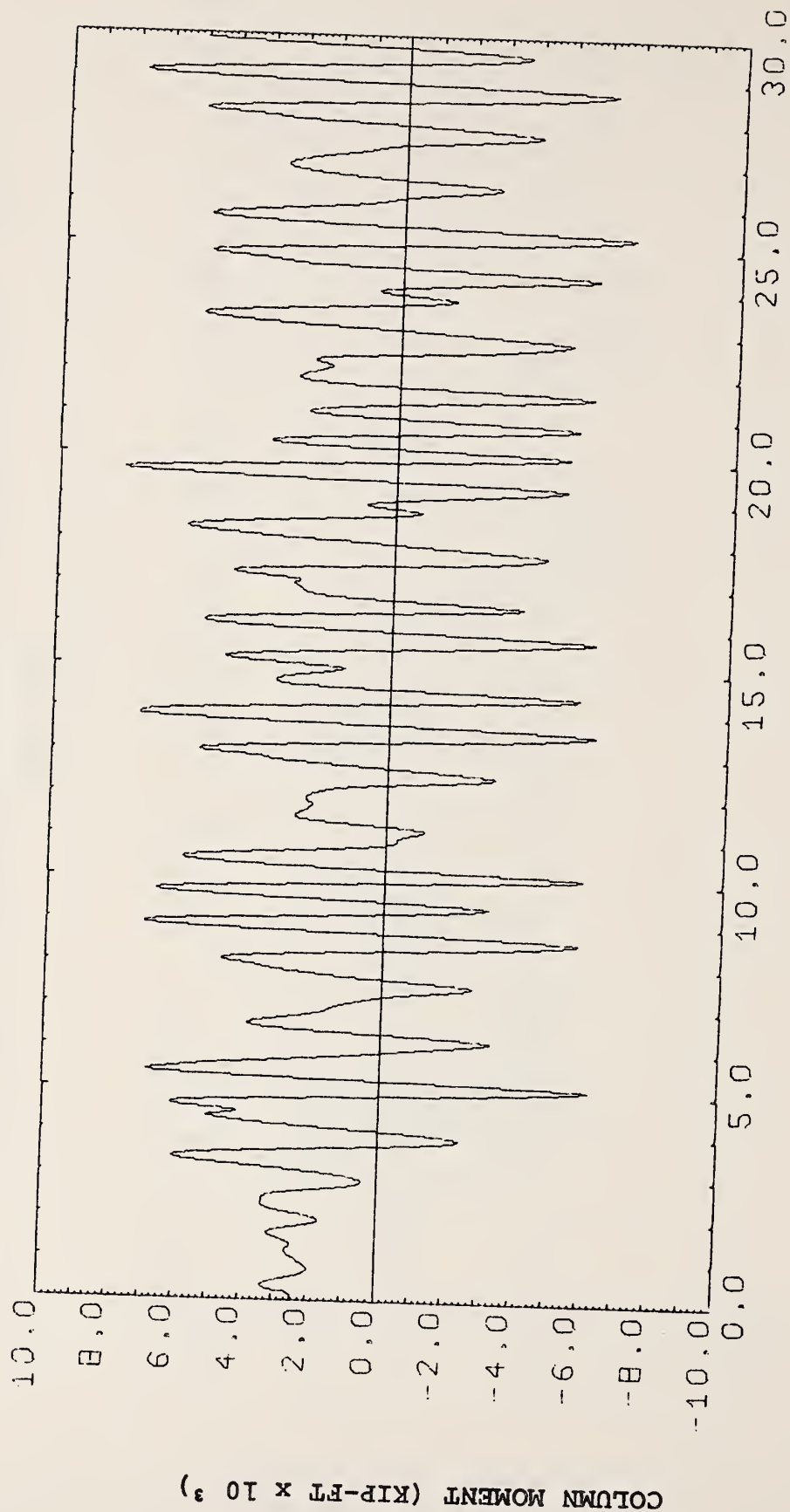
Bridge 2 - Case 11

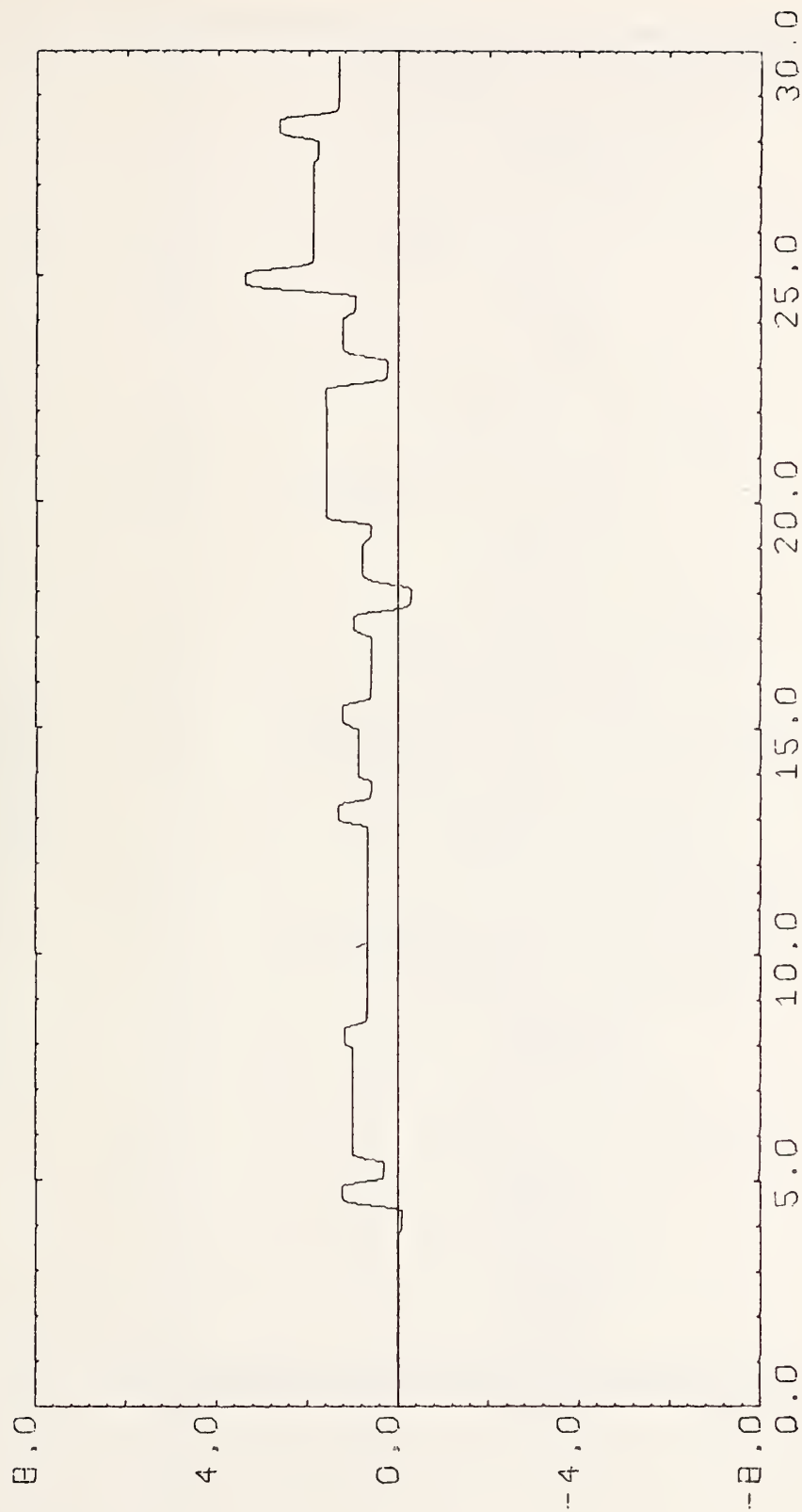


TIME (SEC)

Nonlinear Transverse Rotational Distortion at Base of Column - Bent 6

Bridge 2 - Case 11

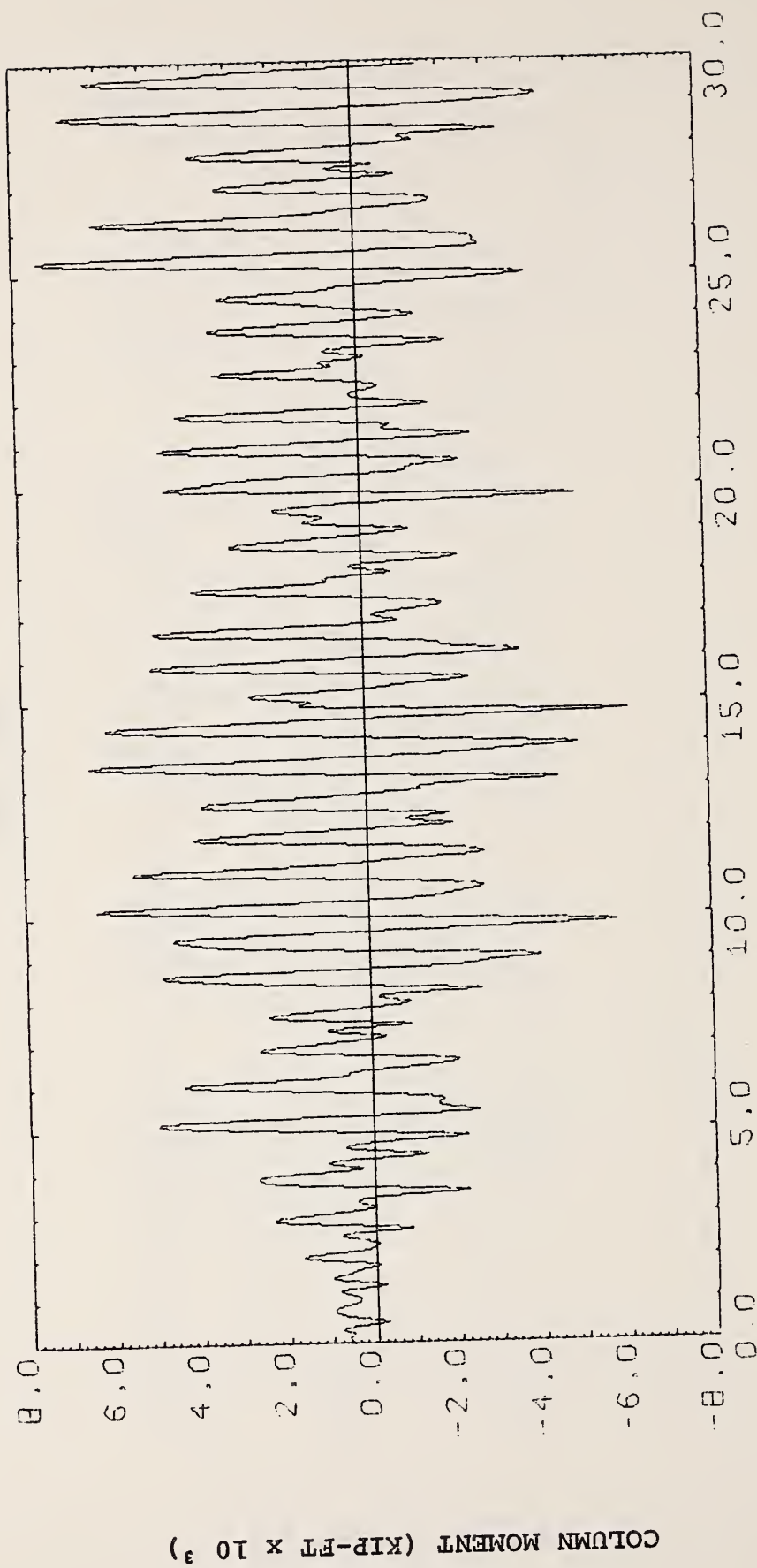




TIME (SEC)

Nonlinear Longitudinal Rotational Deformation at Base of Column - Bent 6

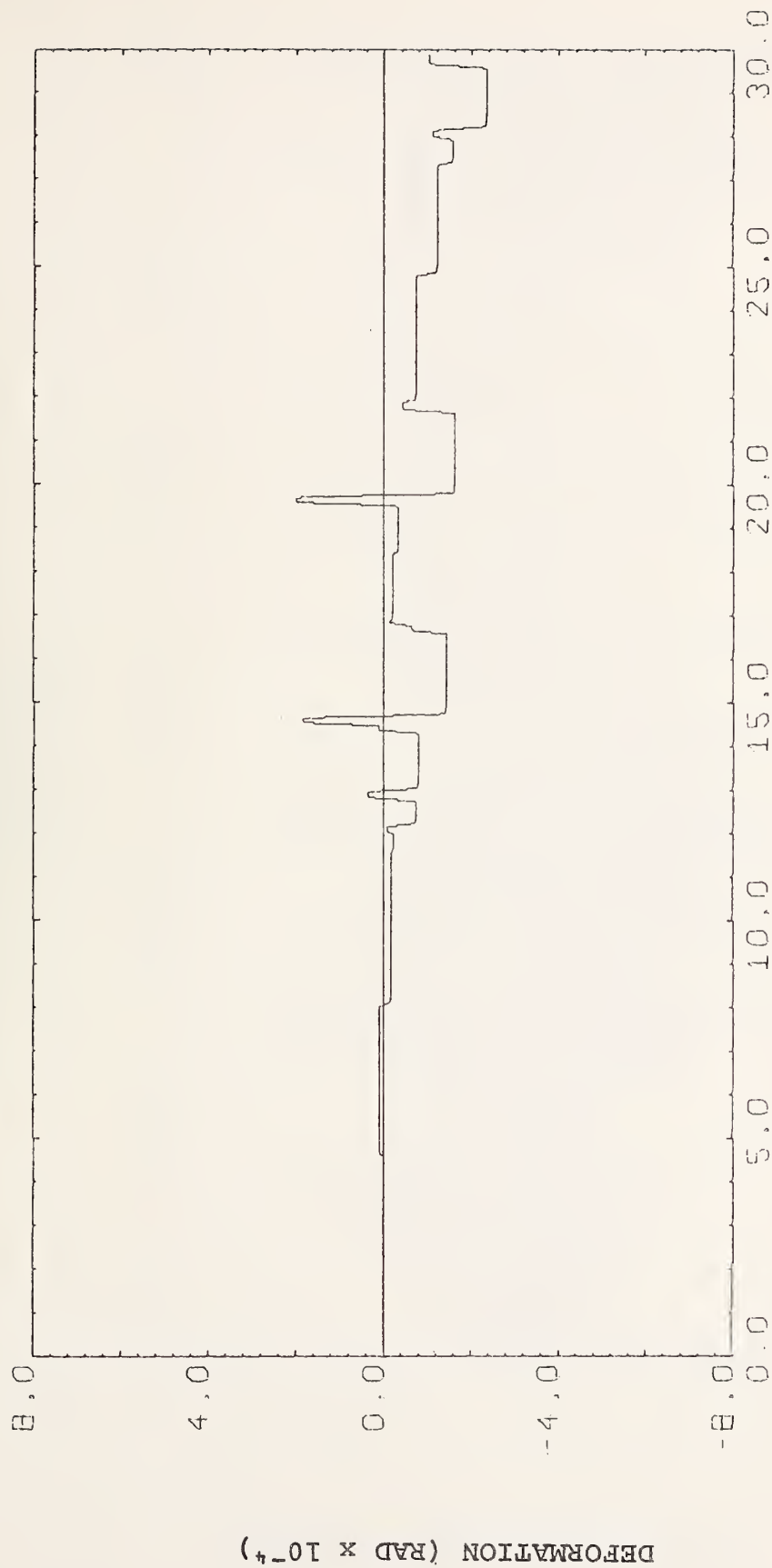
Bridge 2 - Case 11



TIME (SEC)

Transverse Moment at Base of Column - Bent 5

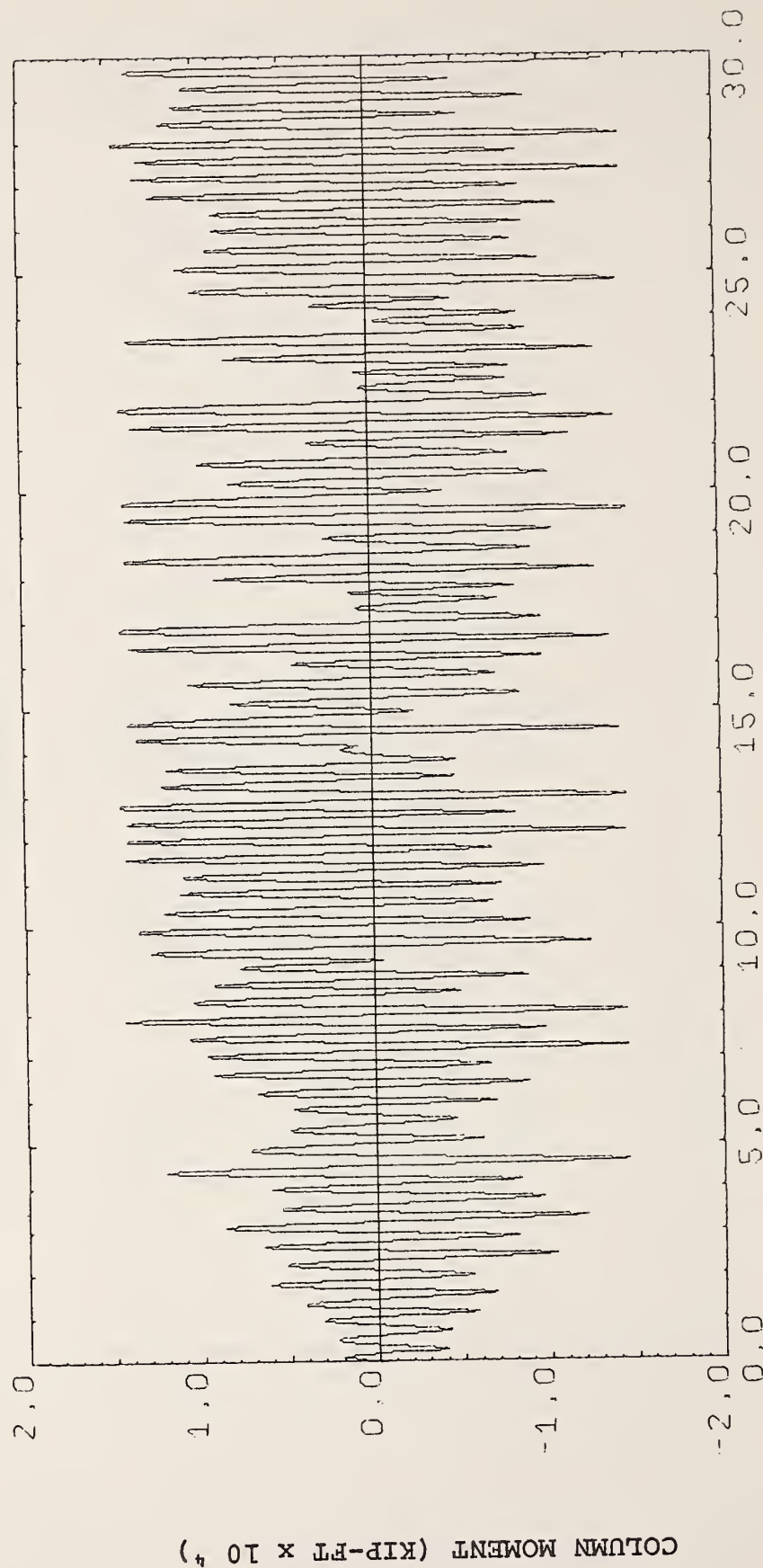
Bridge 2 - Case 12



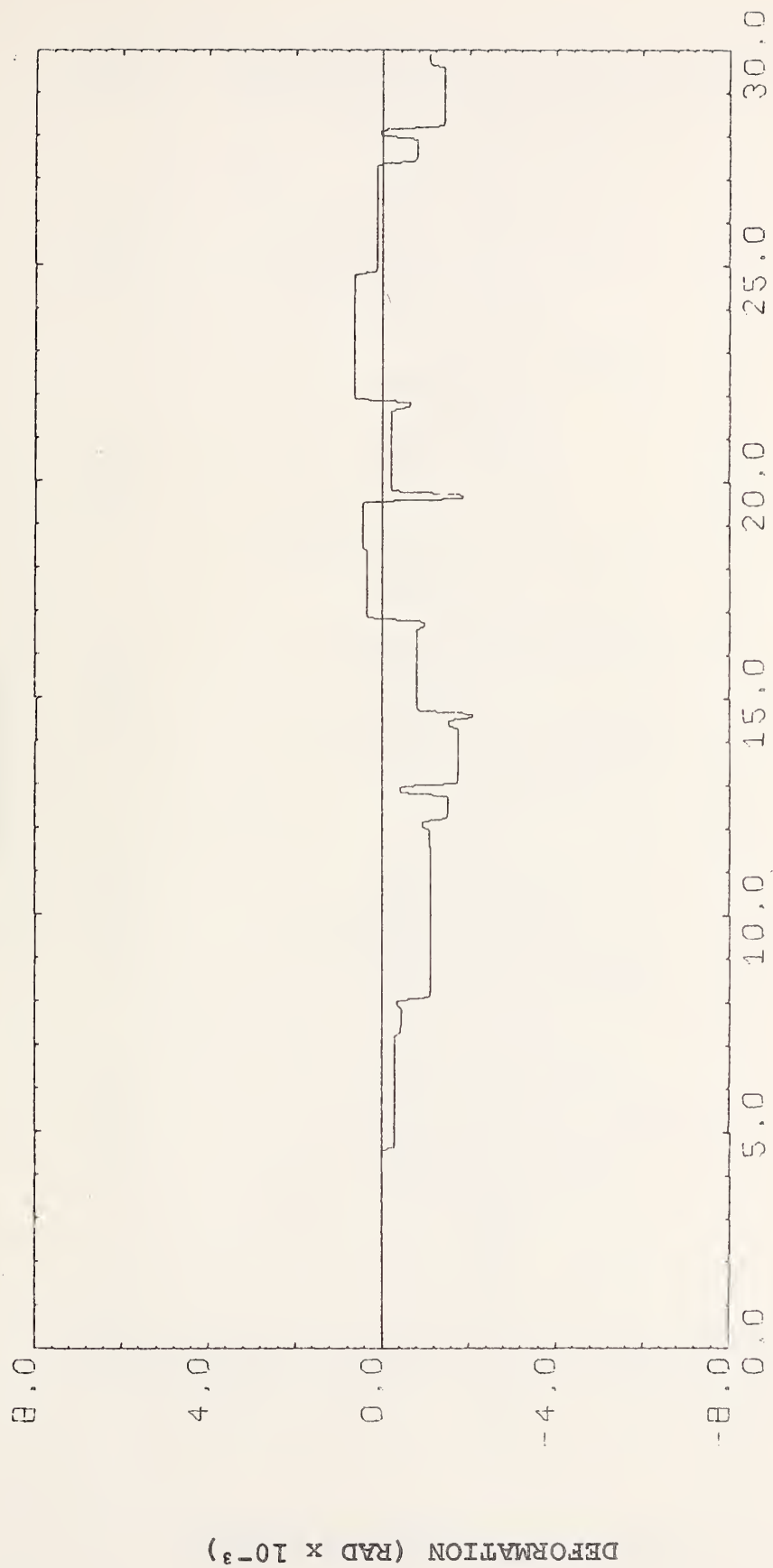
TIME (SEC)

Nonlinear Transverse Rotational Deformation at Base of Column - Bent 5

Bridge 2 - Case 12



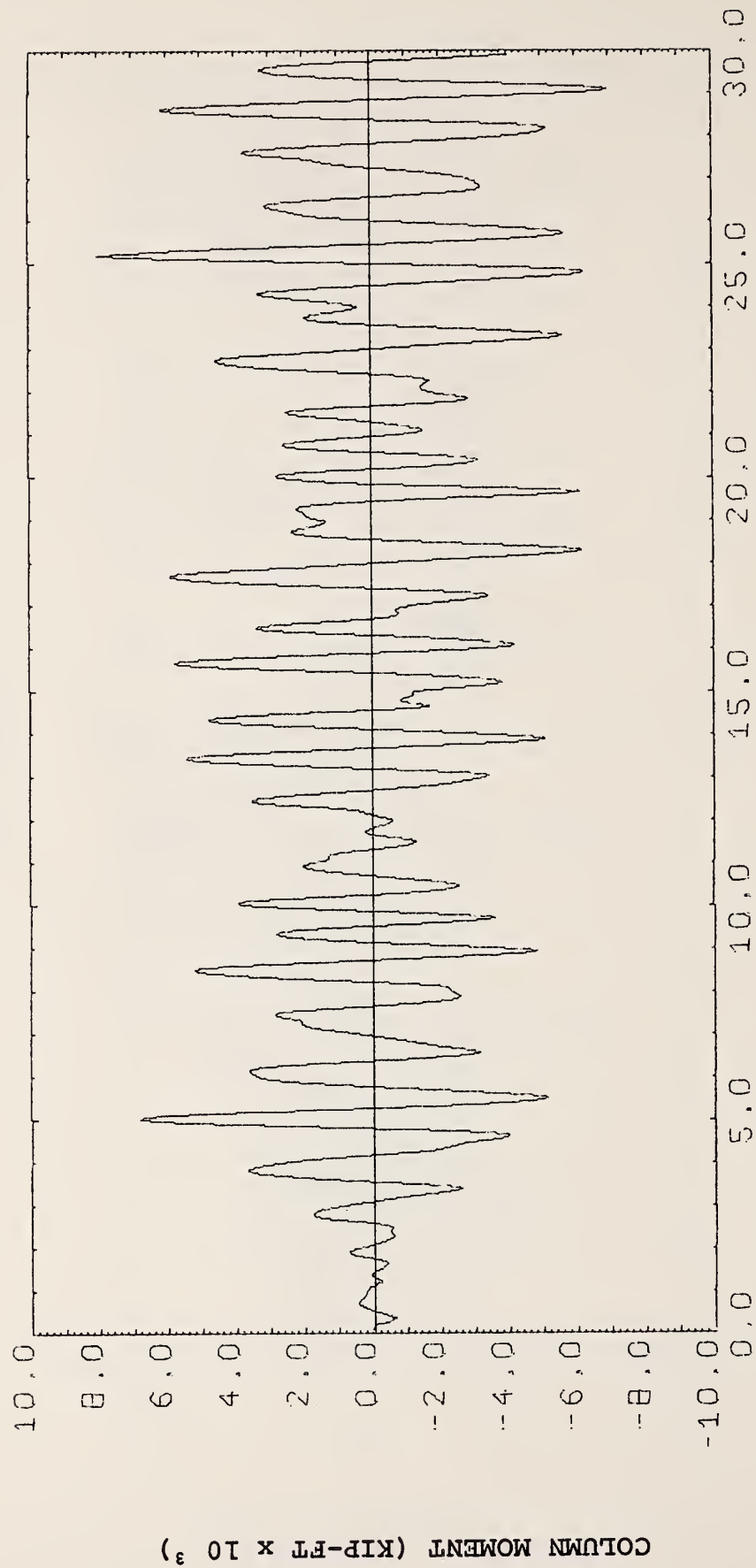
Longitudinal Moment at Base of Column - Bent 5
Bridge 2 - Case 12



TIME (SEC)

Nonlinear Longitudinal Rotational Deformation at Base of Column - Bent 5

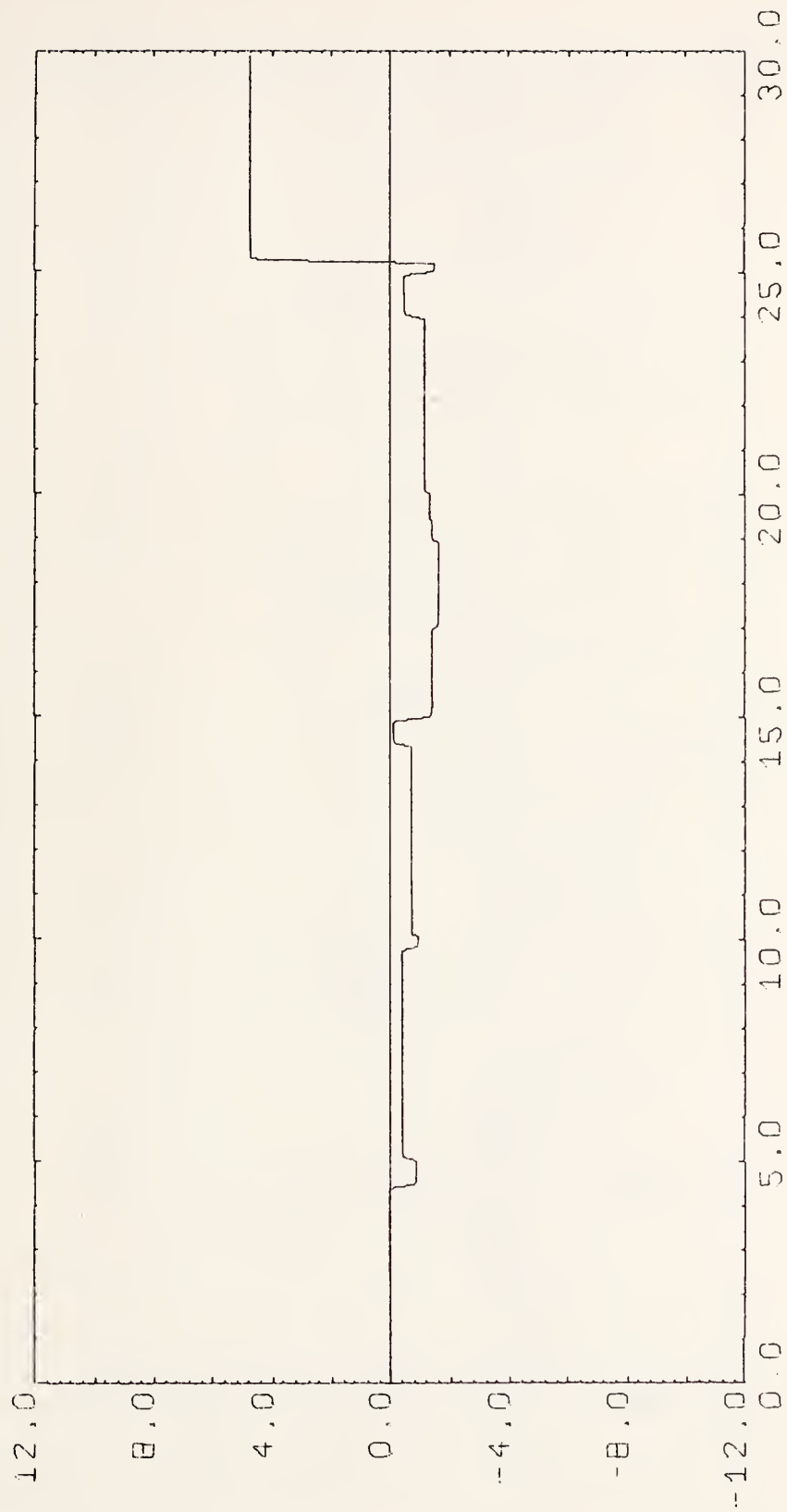
Bridge 2 - Case 12



TIME (SEC)

Transverse Moment at Base of Column - Bent 6

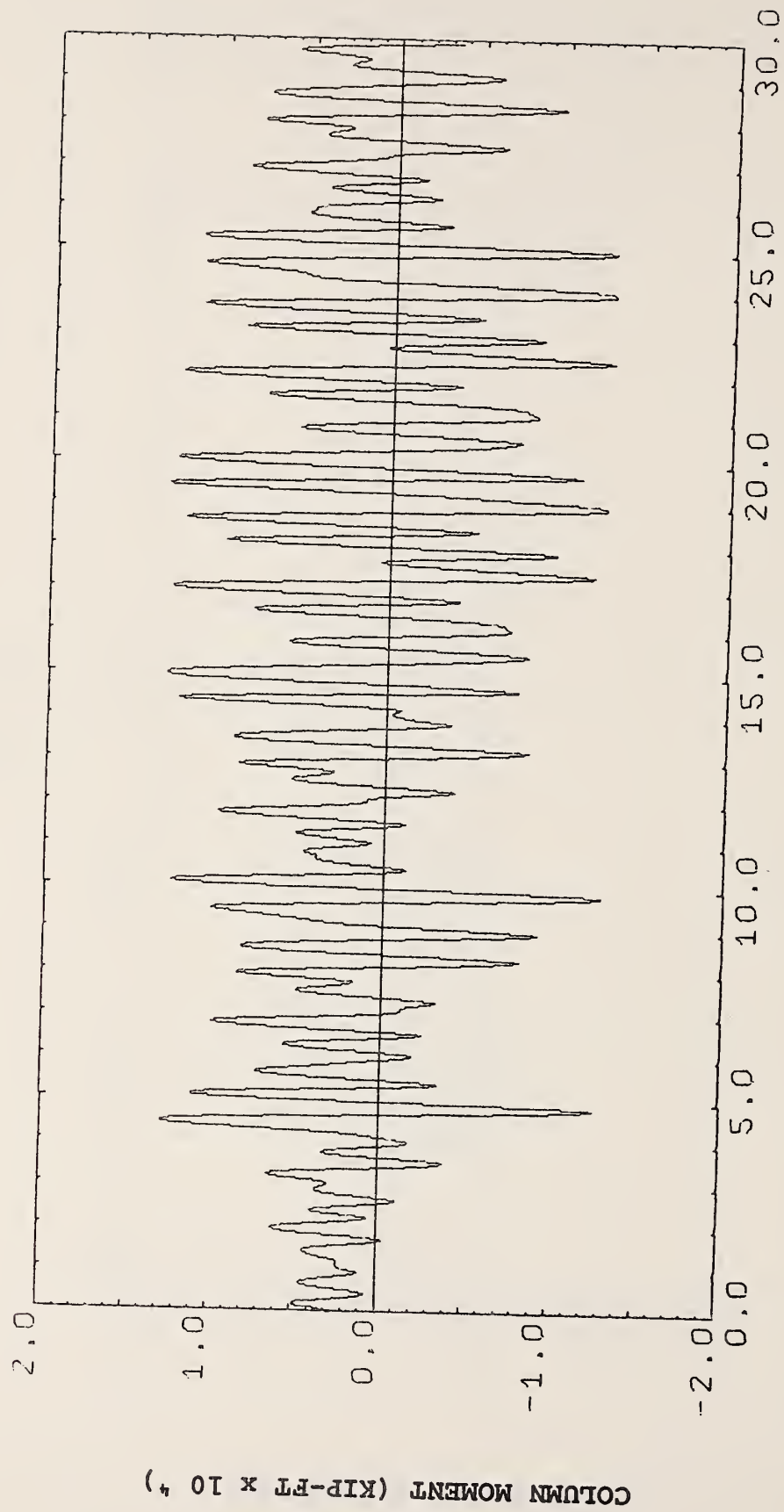
Bridge 2 - Case 12



TIME (SEC)

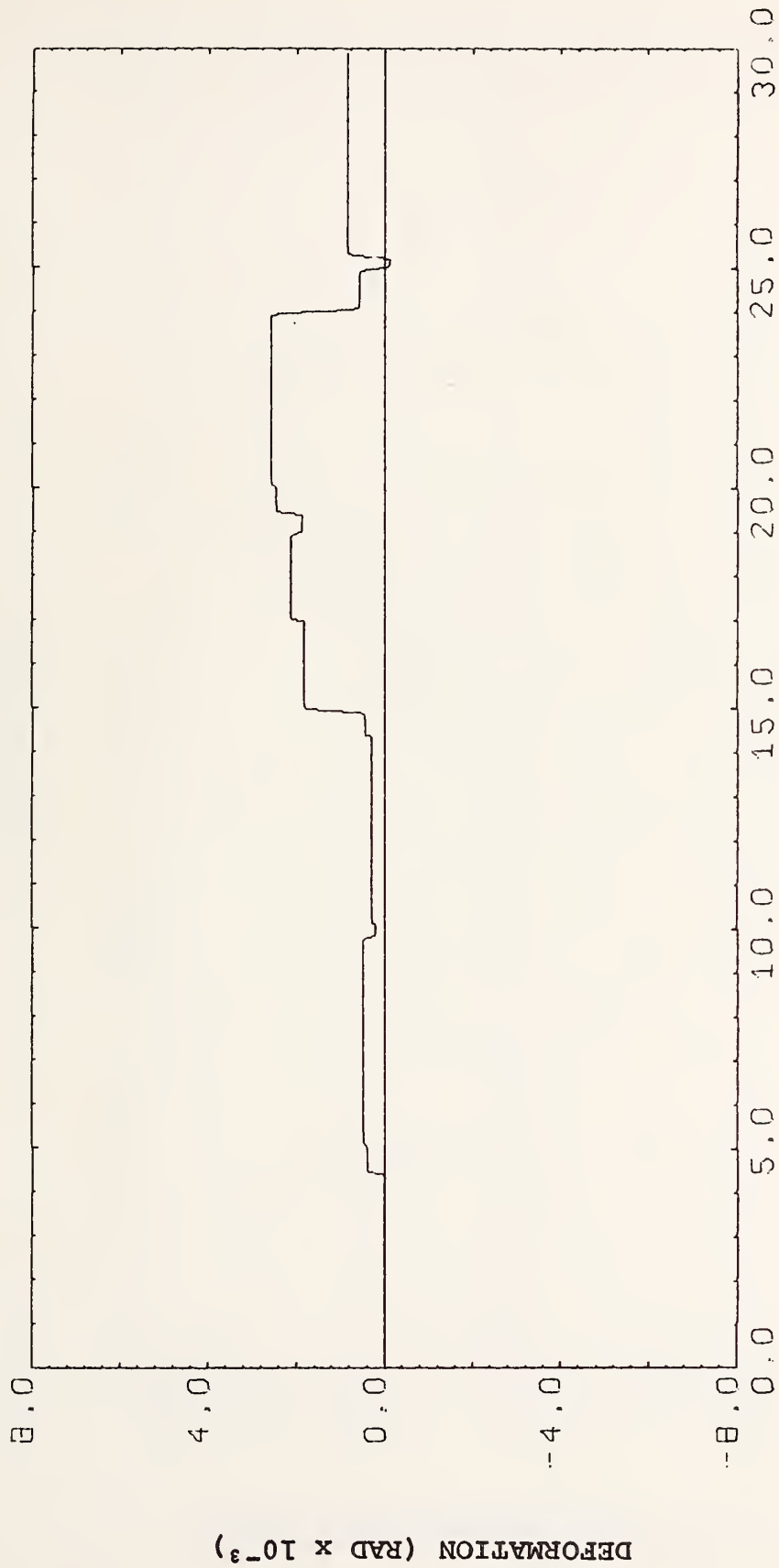
Nonlinear Transverse Rotational Deformation at Base of Column - Bent 6

Bridge 2 - Case 12



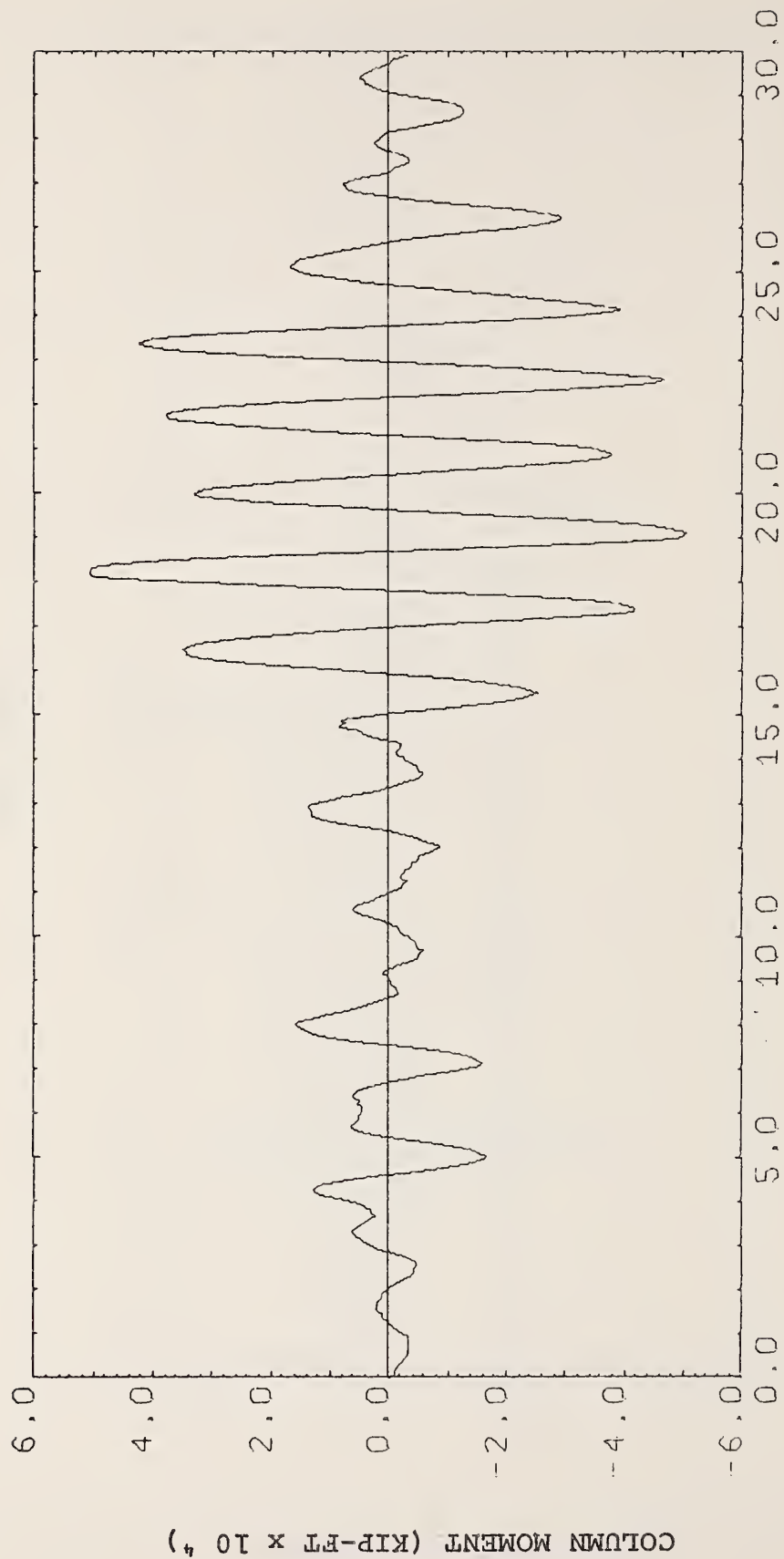
Longitudinal Moment at Base of Column - Bent 6

Bridge 2 - Case 12



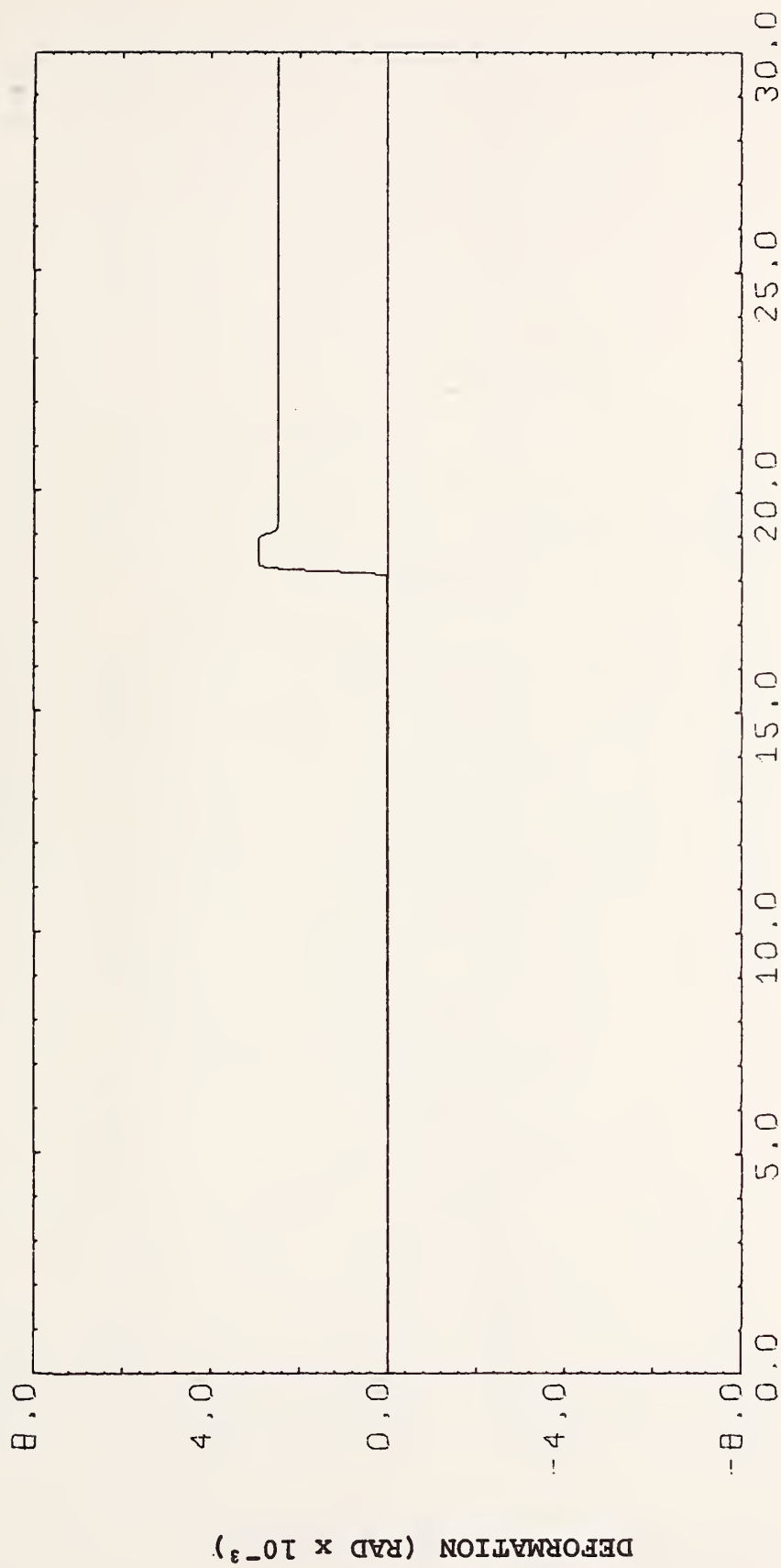
Nonlinear Longitudinal Rotational Deformation at Base of Column - Bent 6

Bridge 2 - Case 12



Transverse Moment at Base of Column - Bent 4

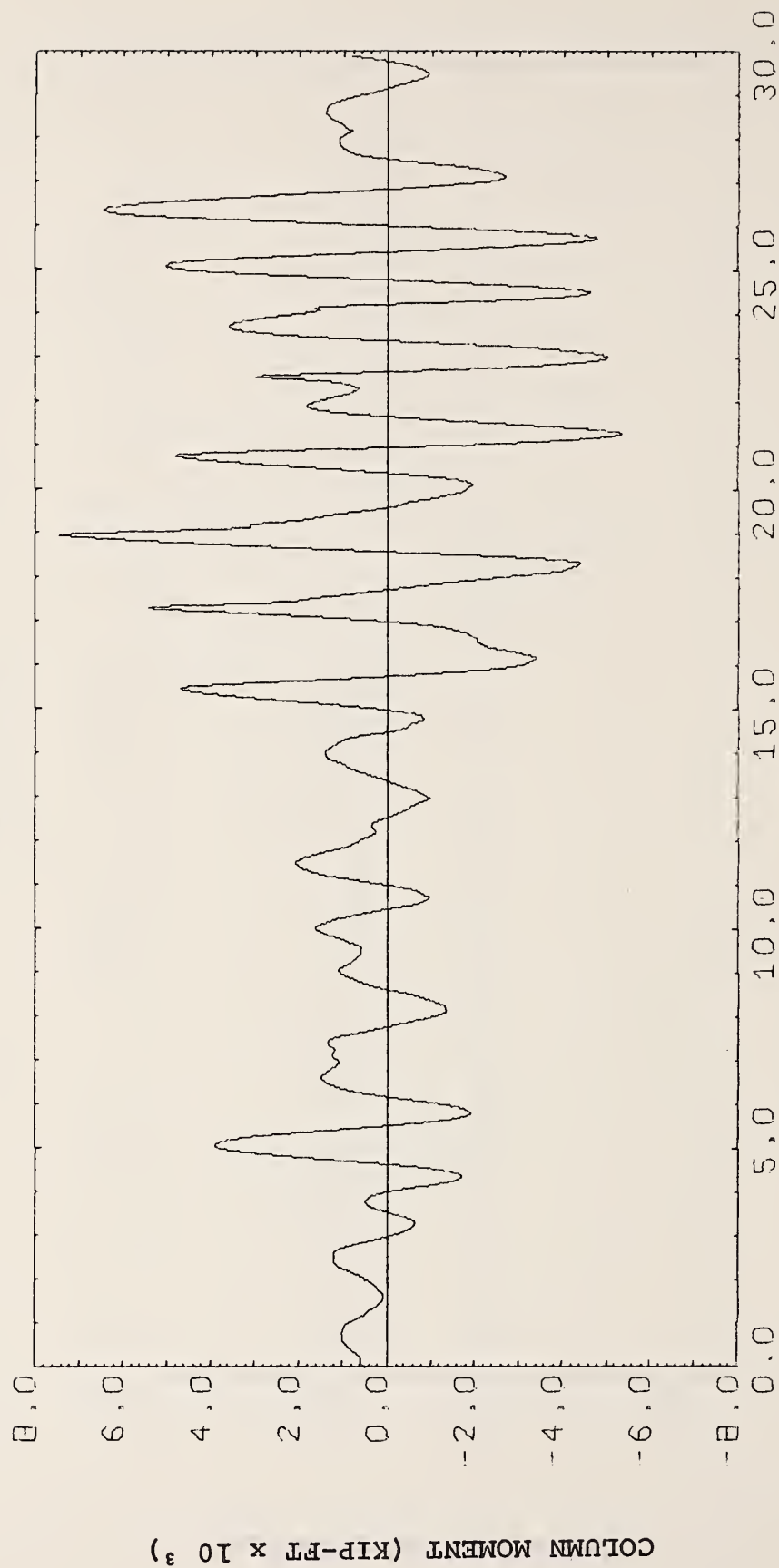
Bridge 3 - Case 17



TIME (SEC)

Nonlinear Transverse Rotational Deformation at Base of Column - Bent 4

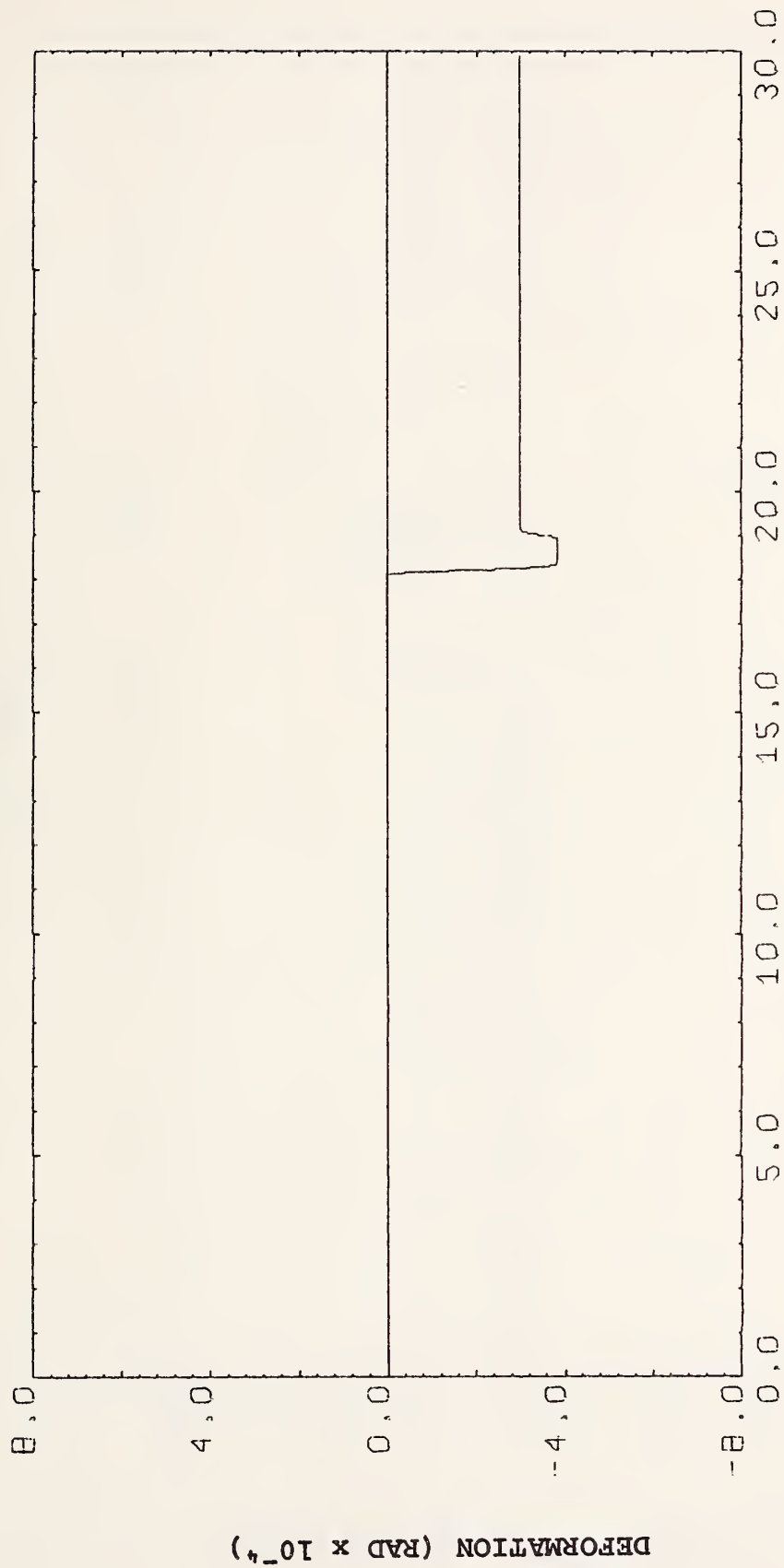
Bridge 3 - Case 17



TIME (SEC)

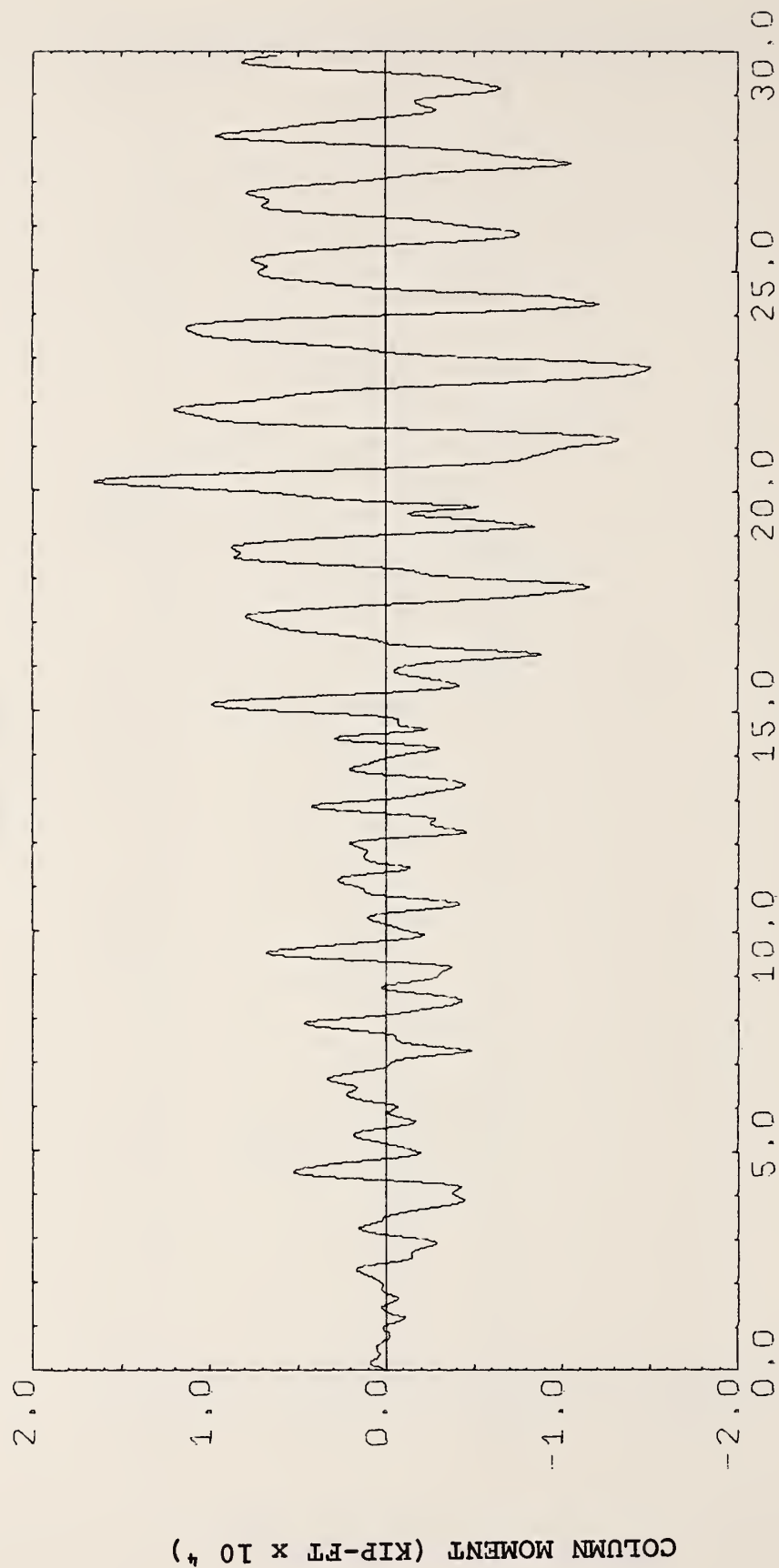
Longitudinal Moment at Base of Column - Bent 4

Bridge 3 - Case 17



Nonlinear Longitudinal Rotational Deformation at Base of Column - Bent 4

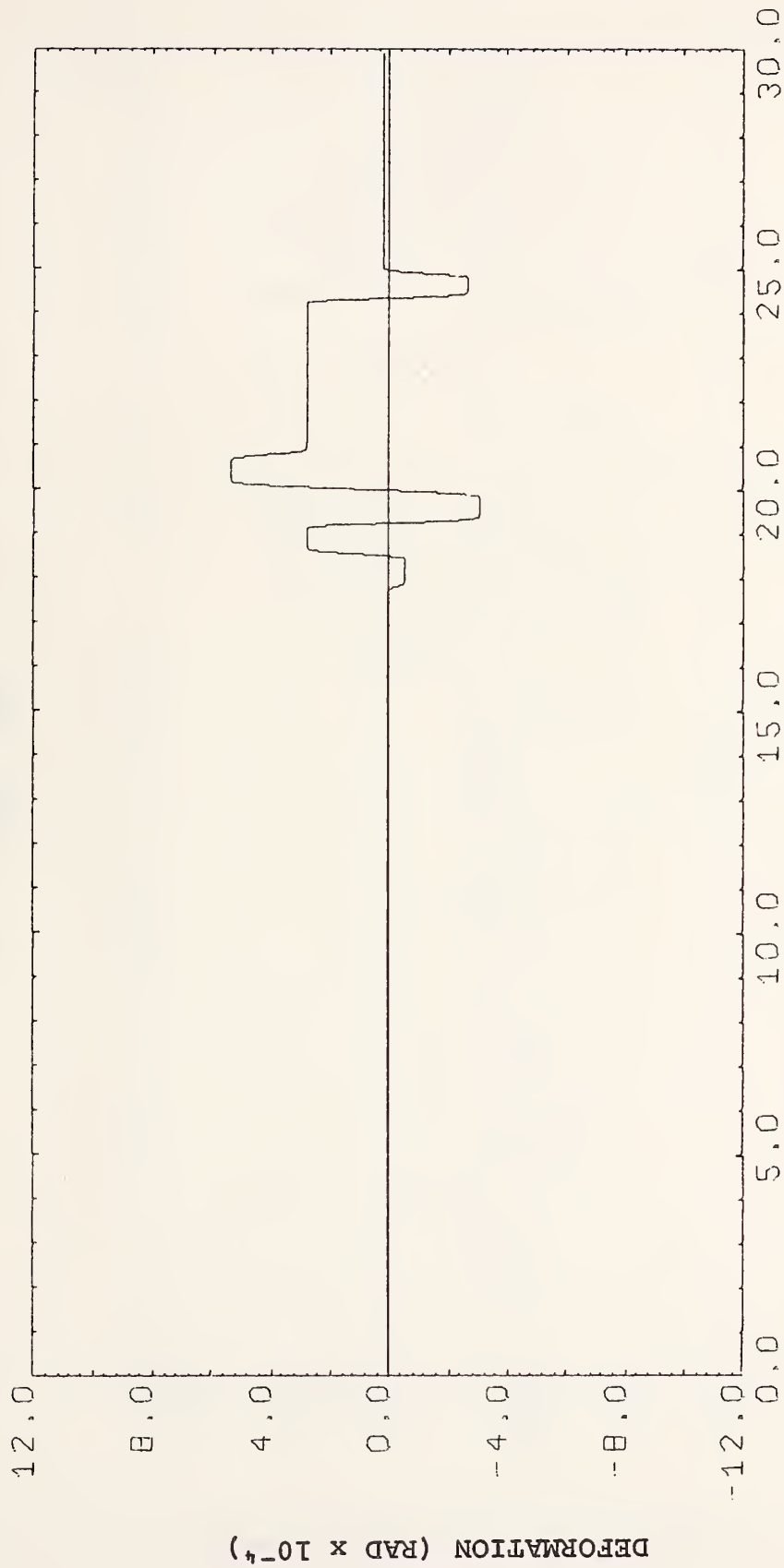
Bridge 3 - Case 17



TIME (SEC)

Transverse Moment at Base of Column - Bent 2

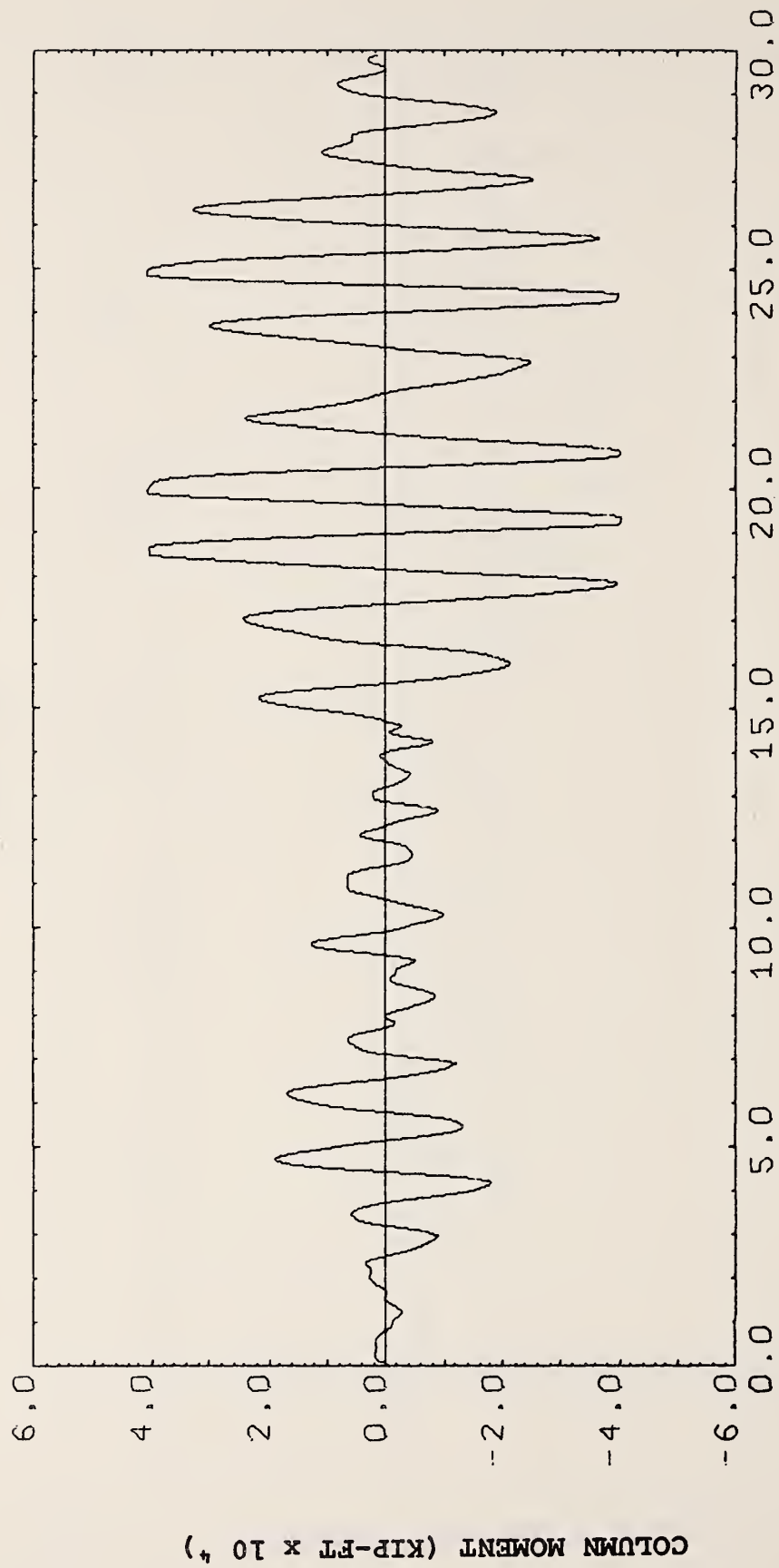
Bridge 3 - Case 18



TIME (SEC)

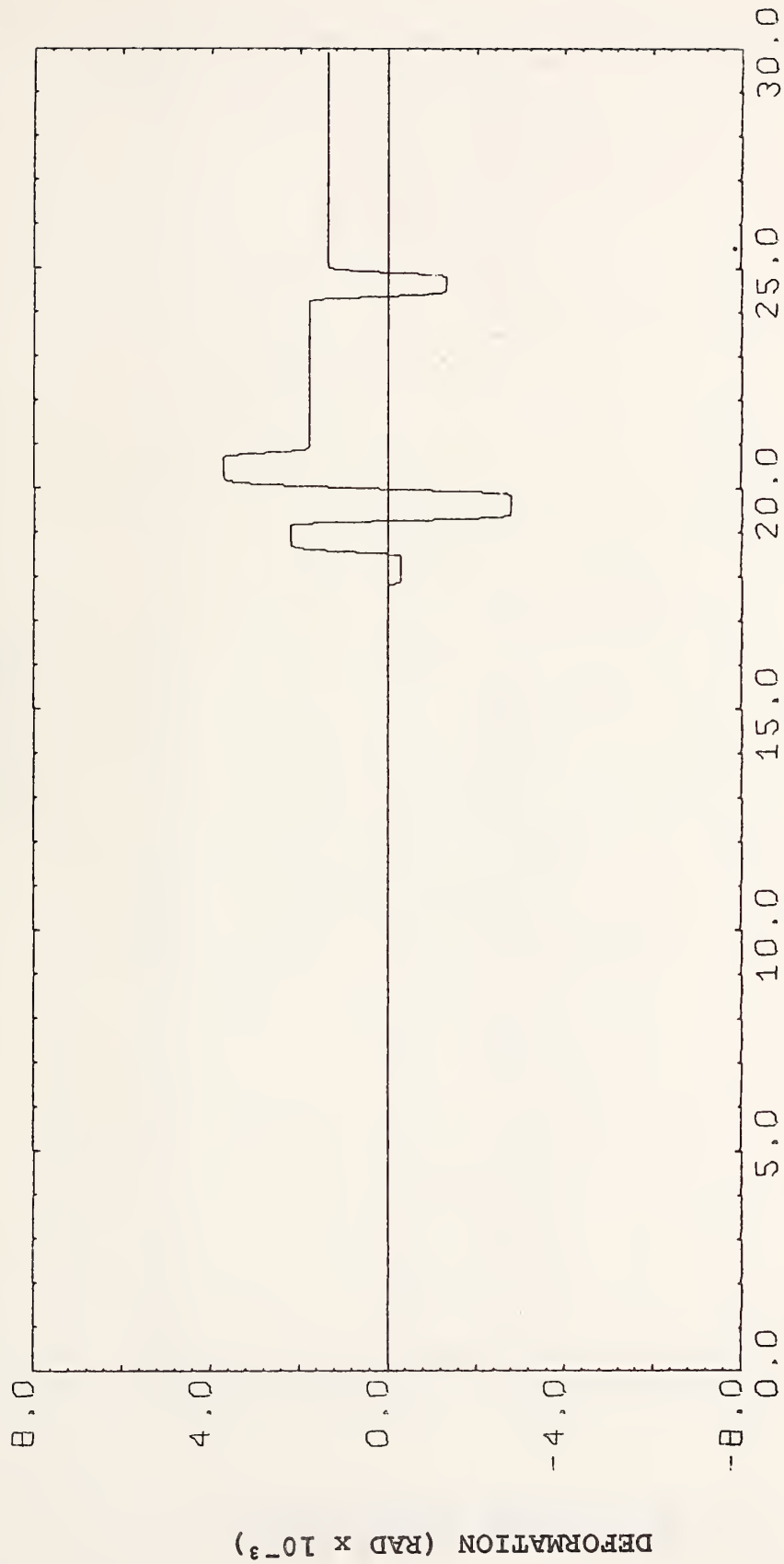
Nonlinear Transverse Rotational Deformation at Base of Column - Bent 2

Bridge 3 - Case 18



Longitudinal Moment at Base of Column - Bent 2

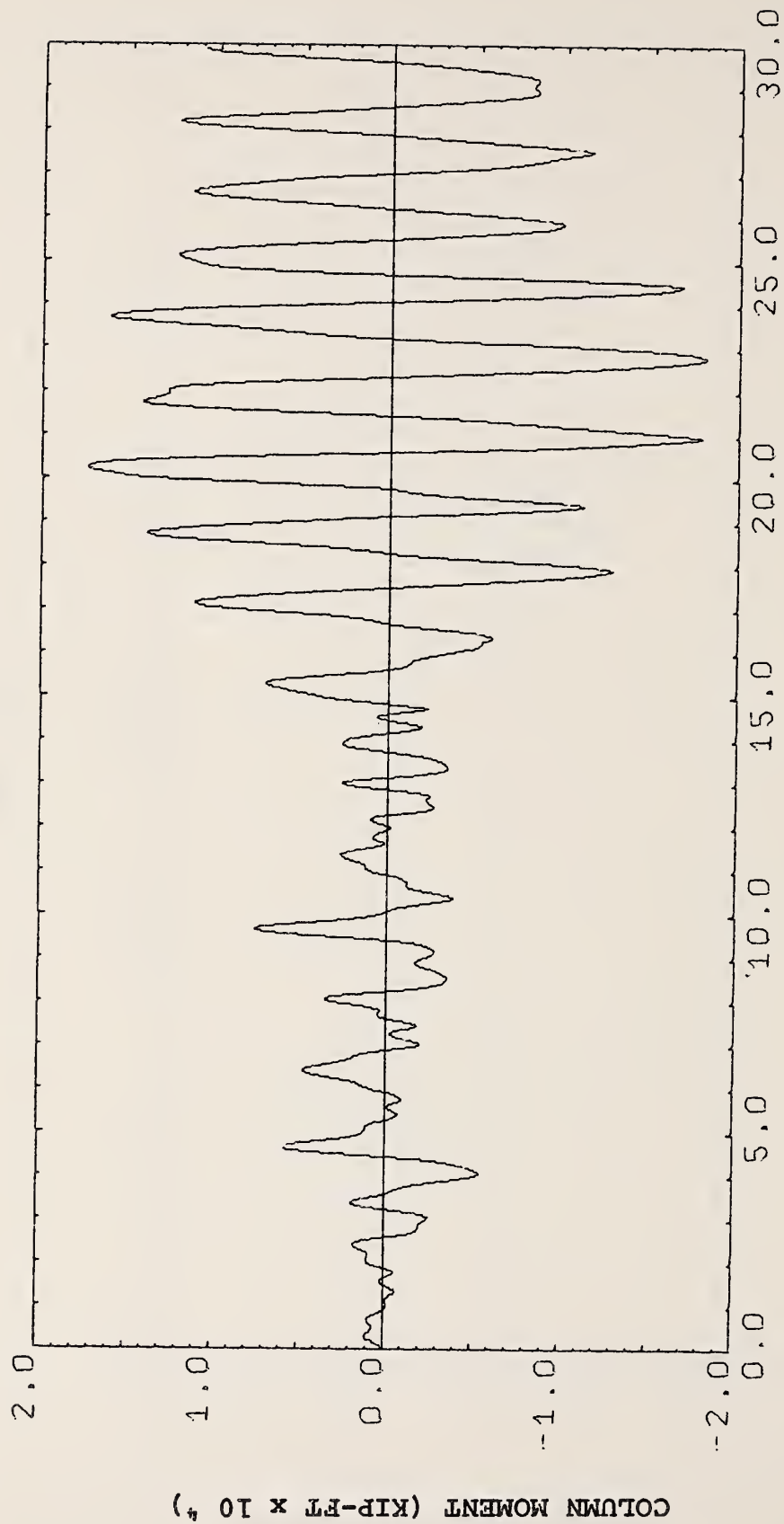
Bridge 3 - Case 18



TIME (SEC)

Nonlinear Longitudinal Rotational Deformation at Base of Column - Bent 2

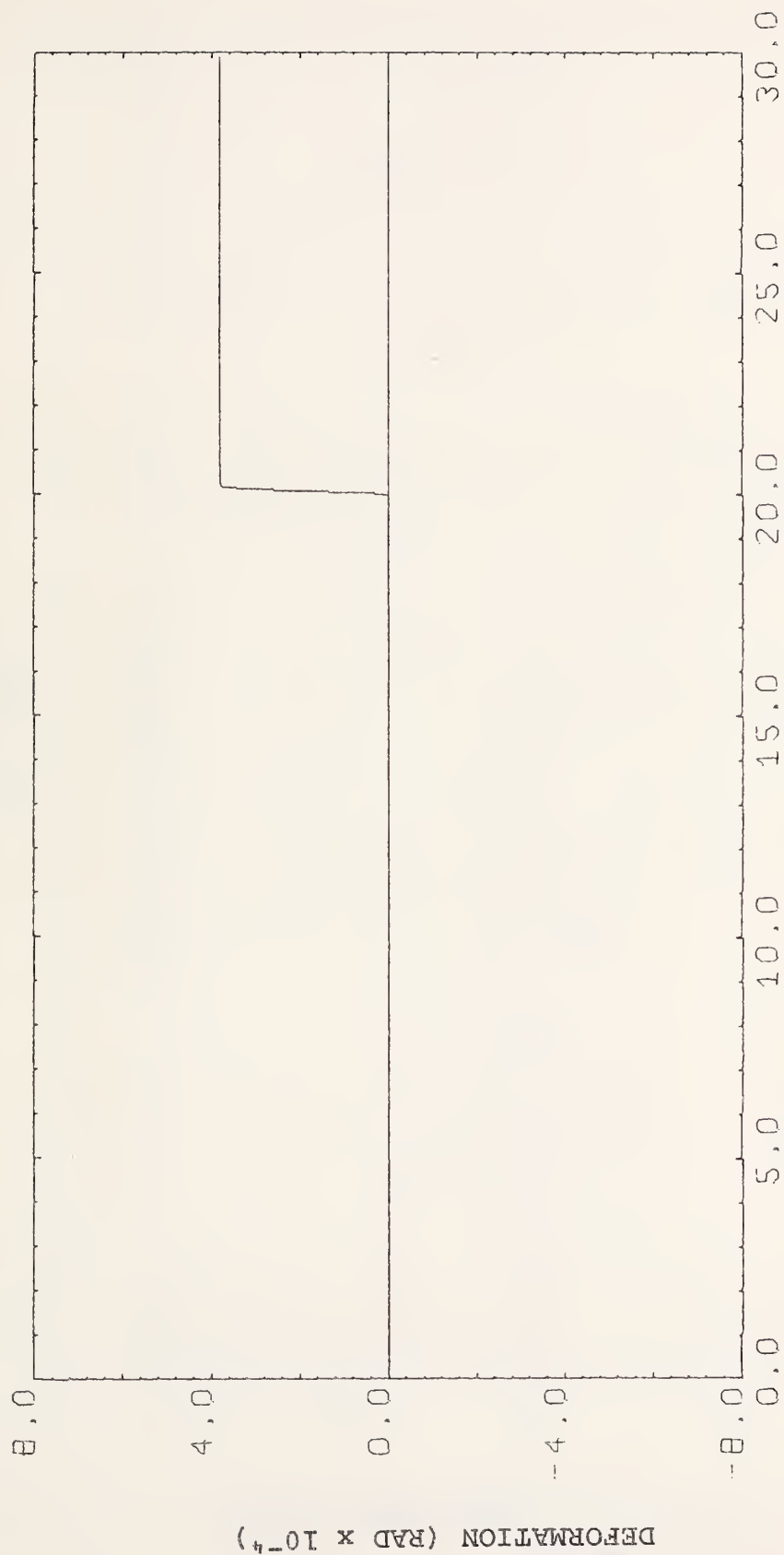
Bridge 3 - Case 18



TIME (SEC)

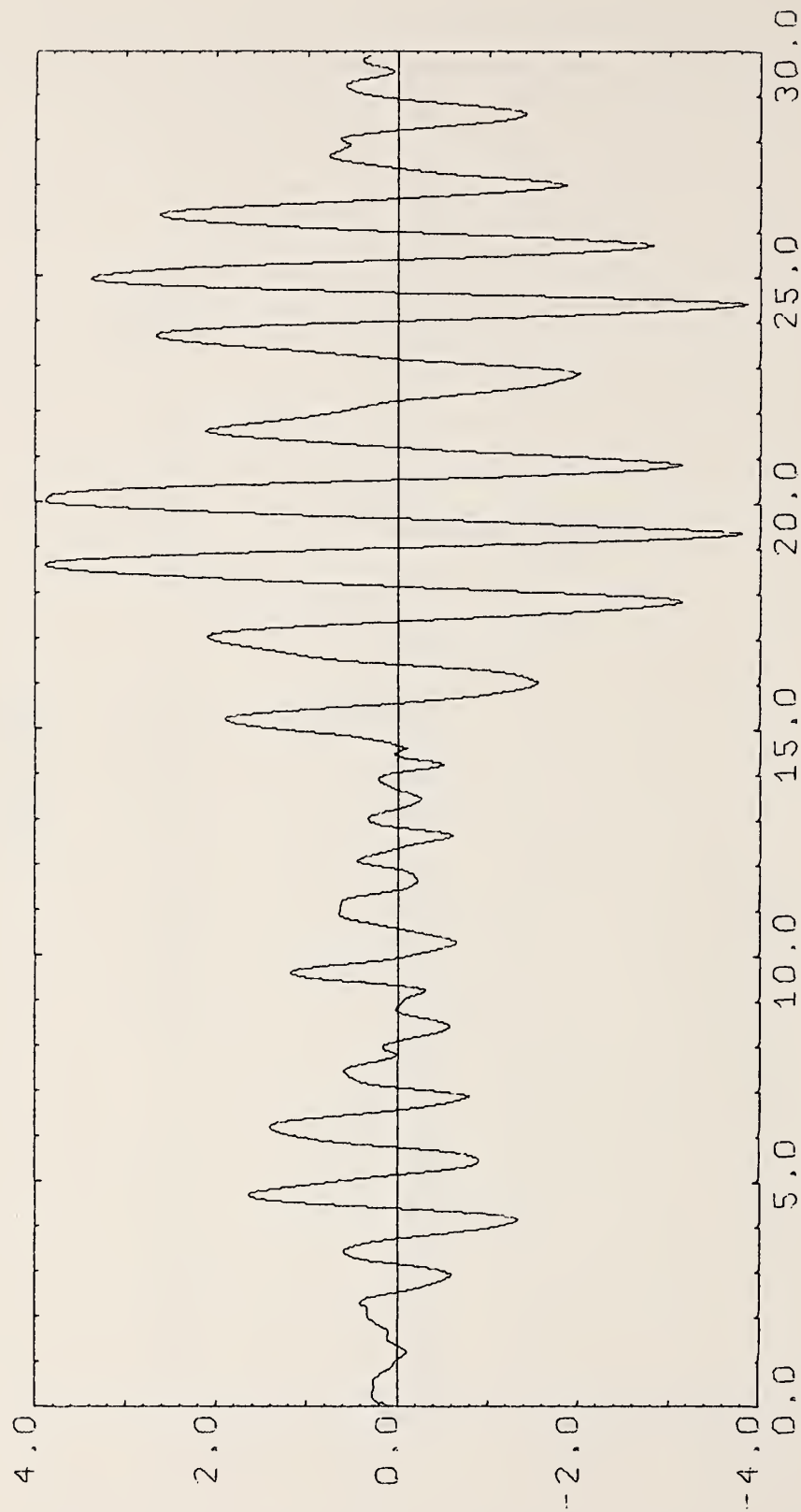
Transverse Moment at Base of Column - Bent 3

Bridge 3 - Case 18



Nonlinear Transverse Rotational Deformation at Base of Column - Bent 3

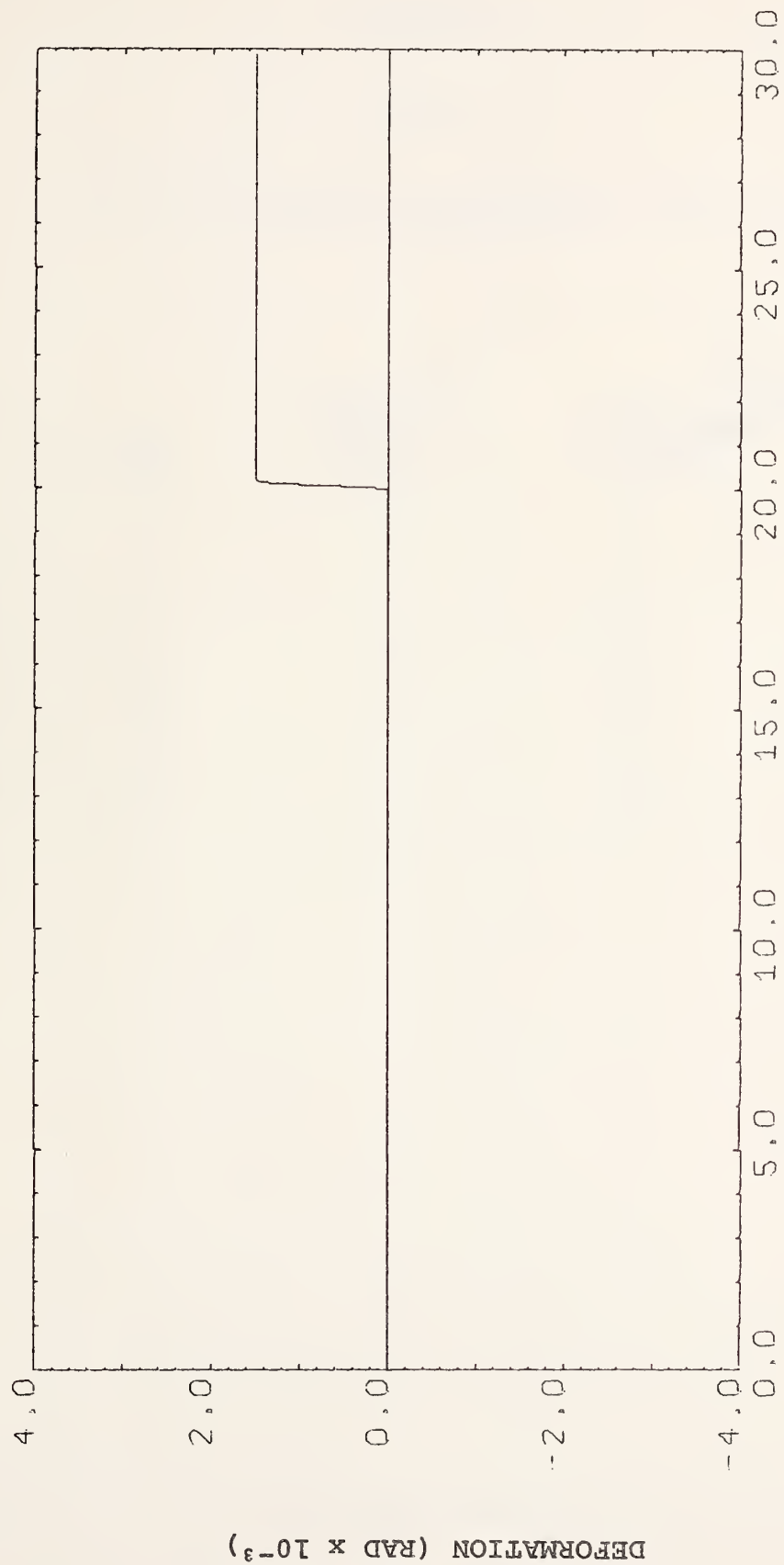
Bridge 3 - Case 18



TIME (SEC)

Longitudinal Moment at Base of Column - Bent 3

Bridge 3 - Case 18



Nonlinear Longitudinal Rotational Deformation at Base of Column - Bent 3

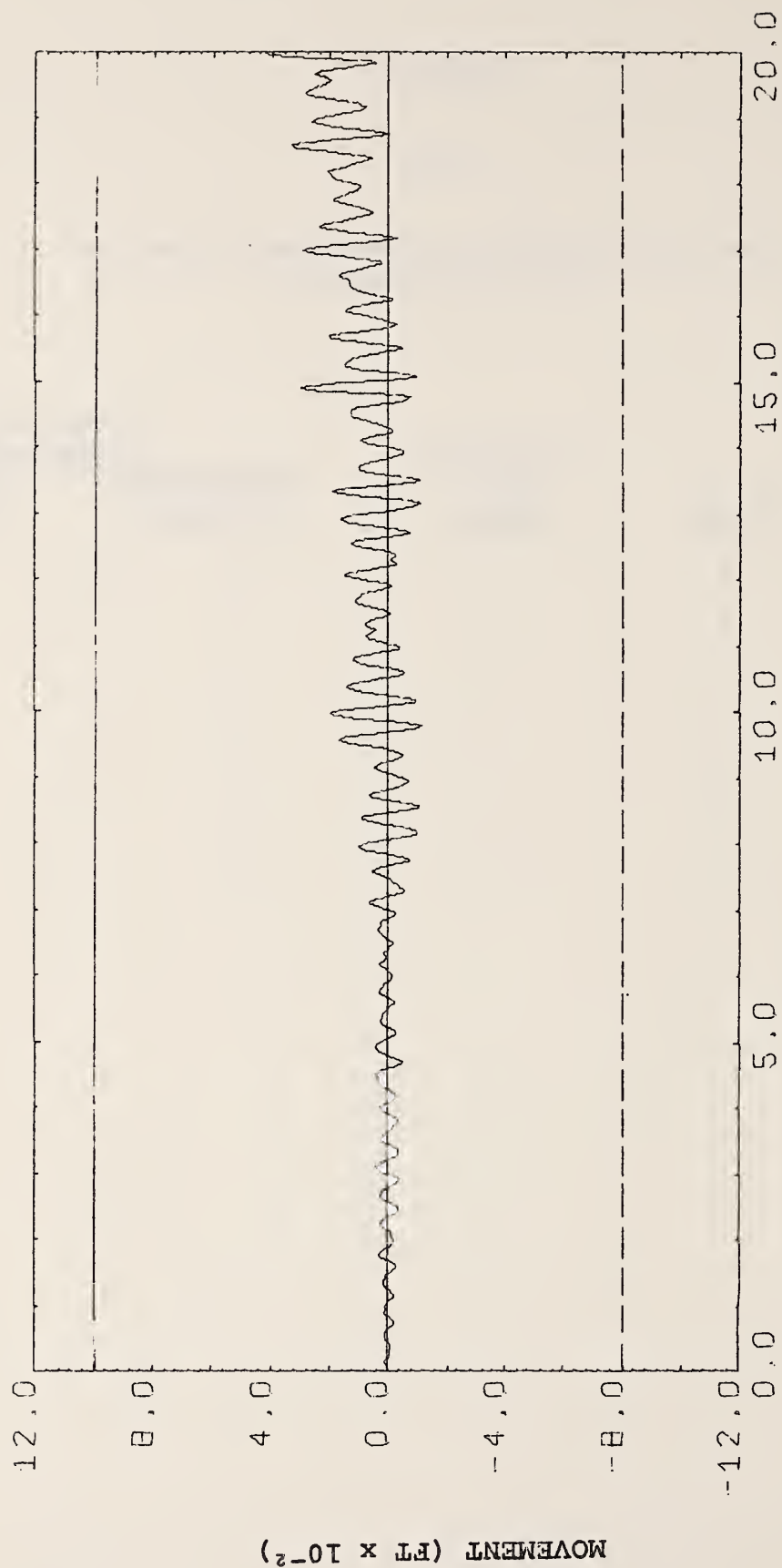
Bridge 3 - Case 18

APPENDIX C

NEABS

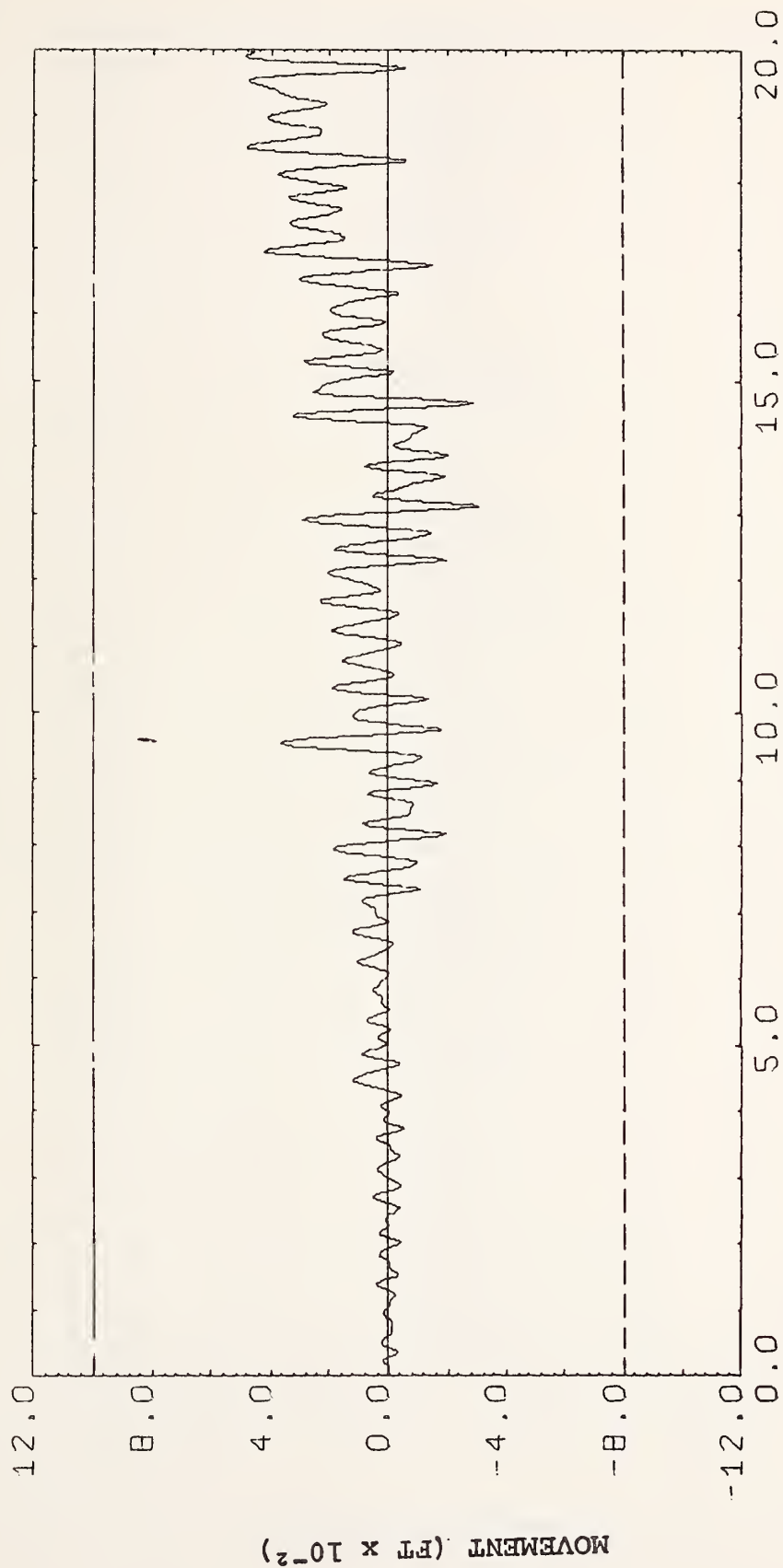
Time History Plots of Selected Expansion Joint Deformations

<u>Bridge</u>	<u>Case</u>	<u>Expansion Joint Span</u>	<u>Restrainer Location</u>	
			<u>Right Edge of Deck</u>	<u>Left Edge of Deck</u>
1	5	3	C-	C-
1	6	3	C-	C-
3	17	3	C-	C-
3	17	7	C-	C-
3	18	3	C-	C-
3	18	7	C-	C-



Expansion Joint Movement at Right Edge of Deck - Span 3 Joint

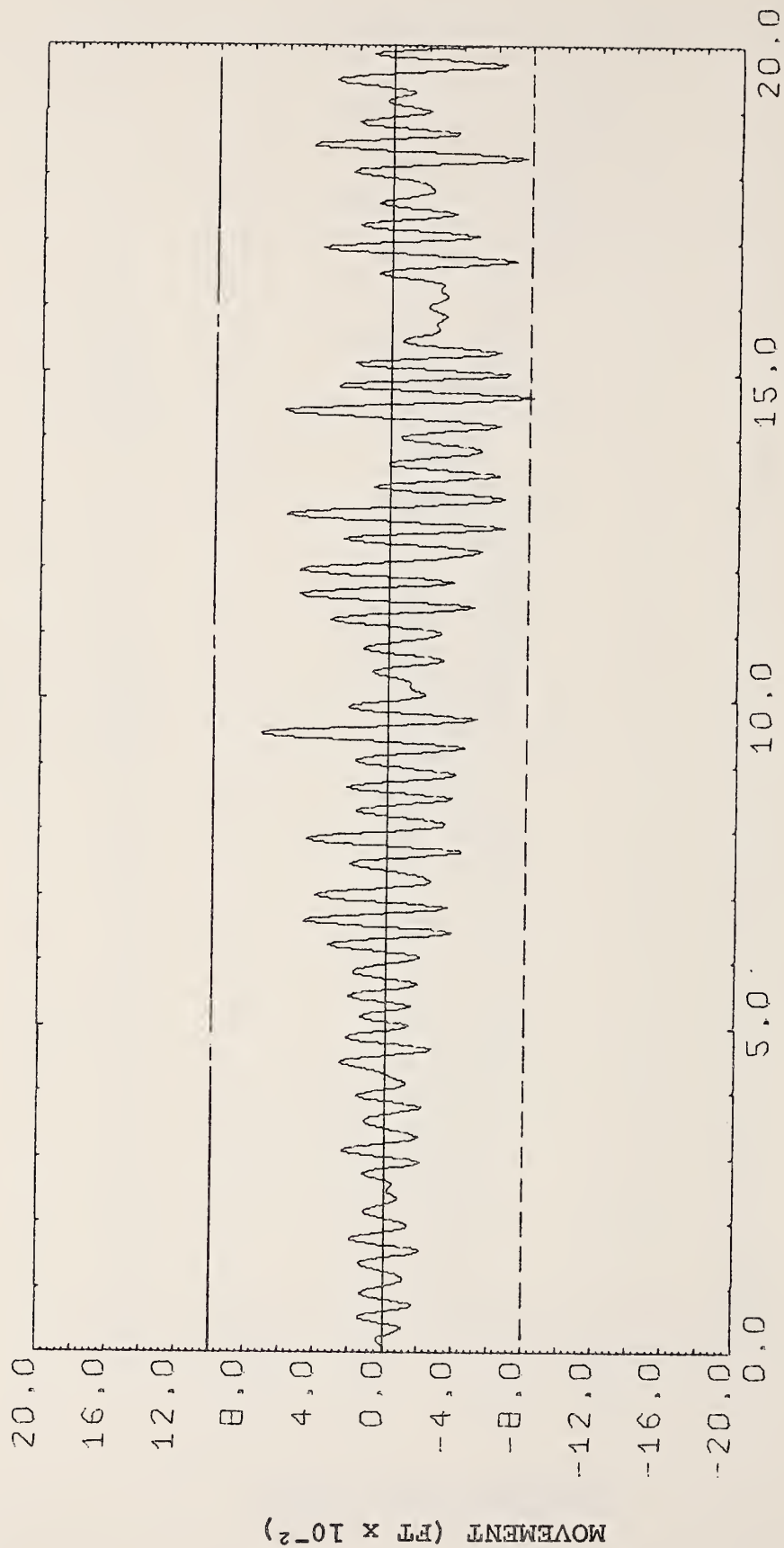
Bridge 1 - Case 5



TIME (SEC)

Expansion Joint Movement at Left Edge of Deck - Span 3 Joint

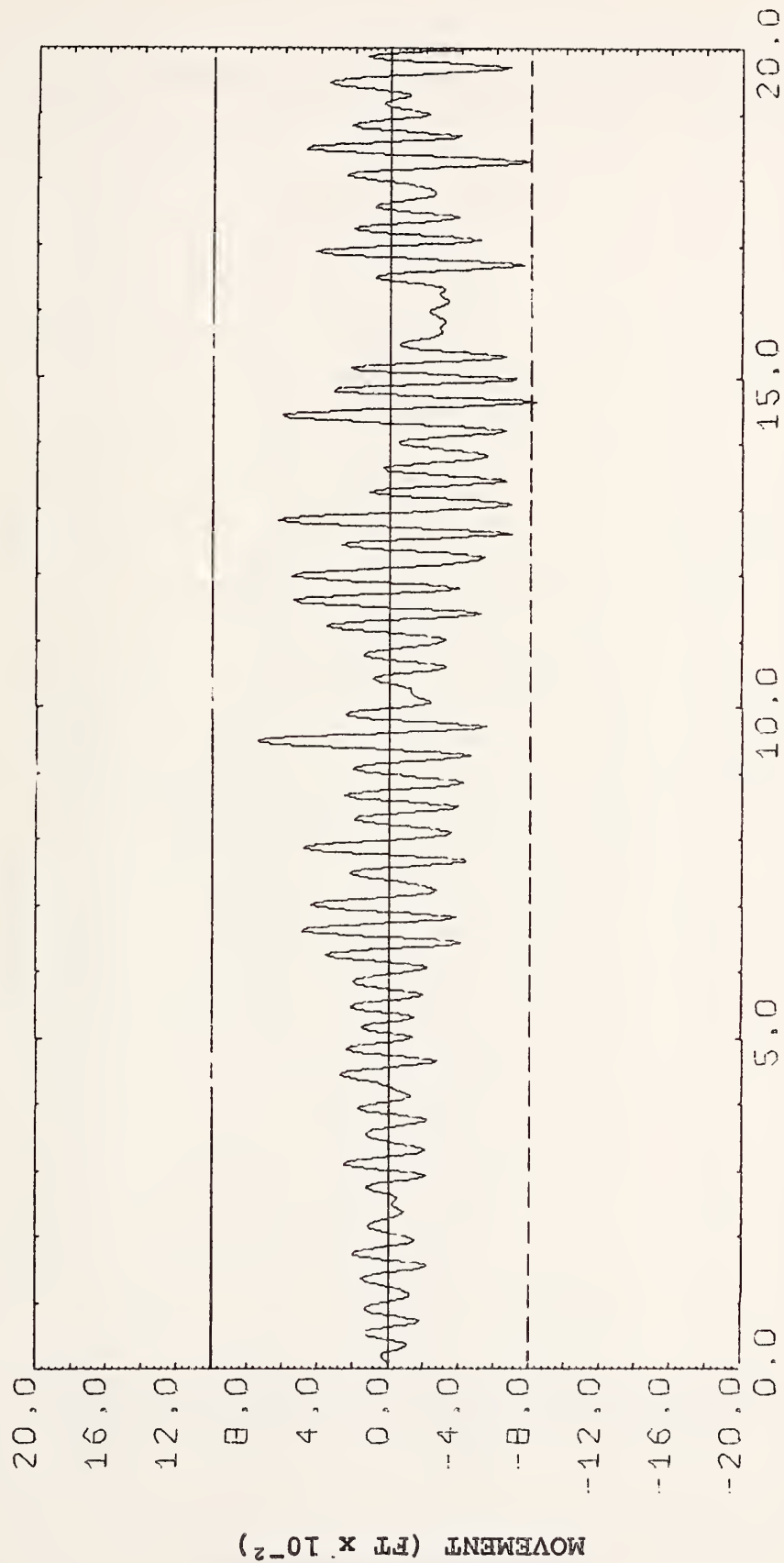
Bridge 1 - Case 5



TIME (SEC)

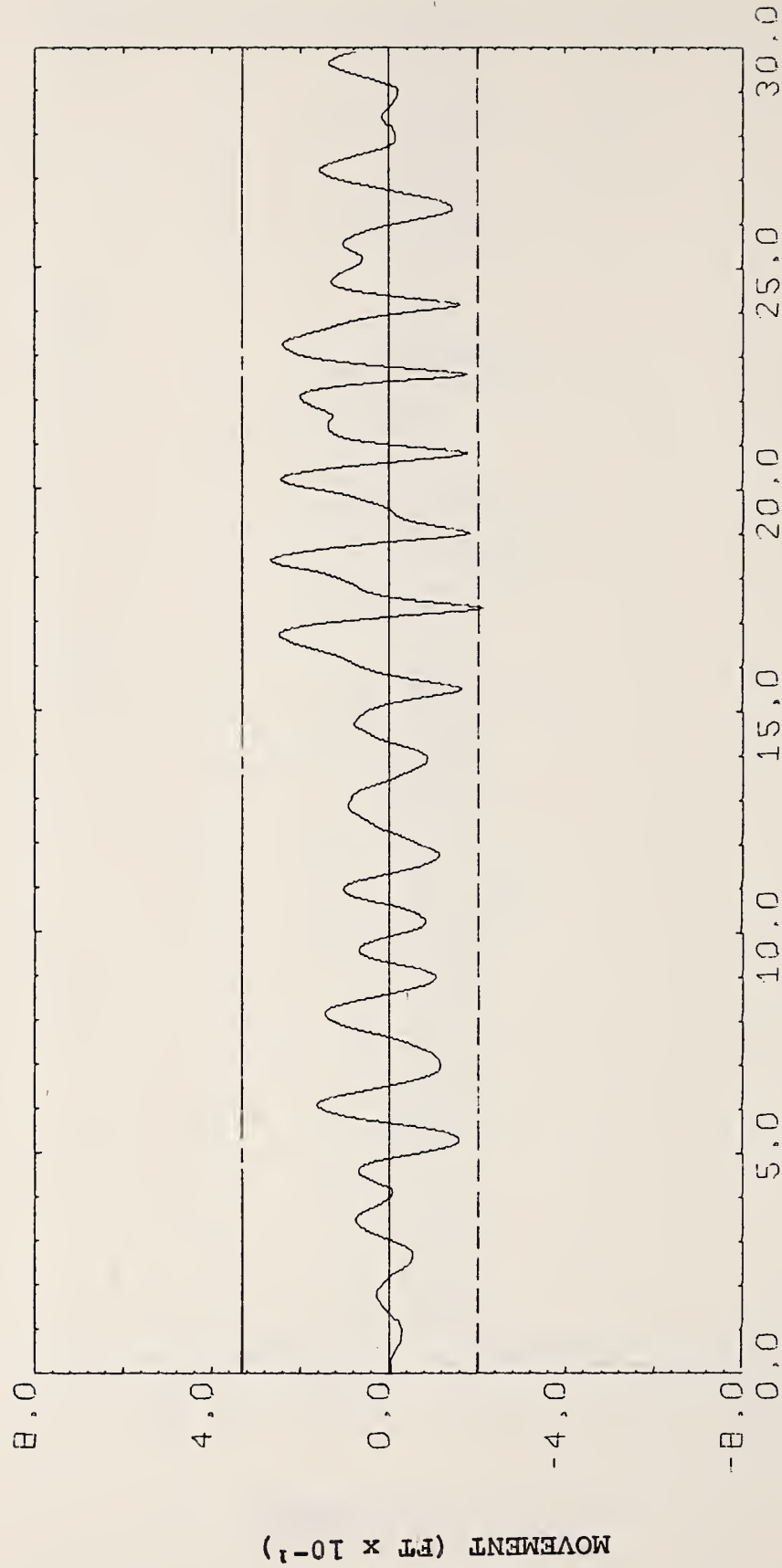
Expansion Joint Movement at Right Edge of Deck - Span 3 Joint

Bridge 1 - Case 6



Expansion Joint Movement at Left Edge of Deck - Span 3 Joint

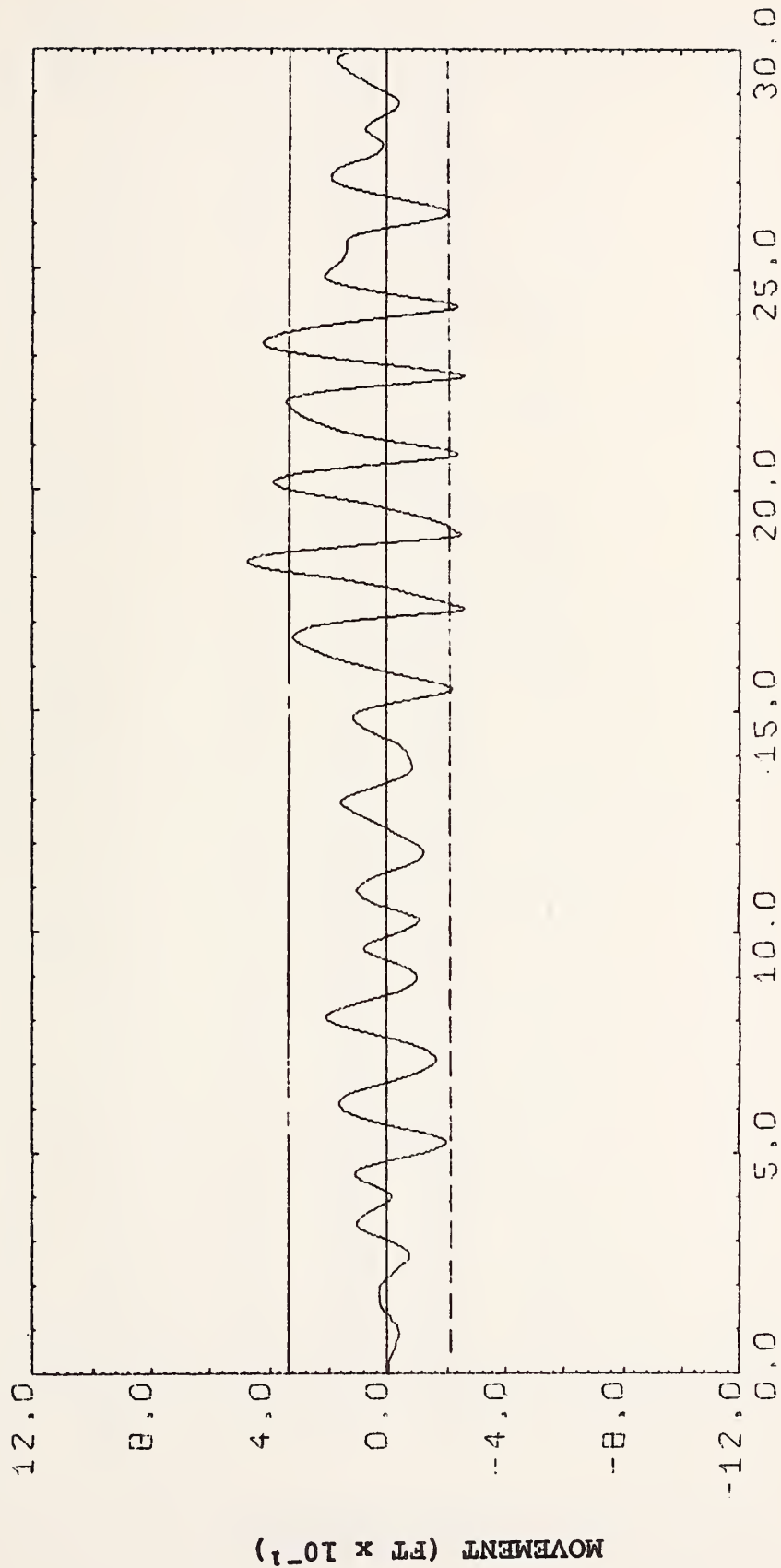
Bridge 1 - Case 6



TIME (SEC)

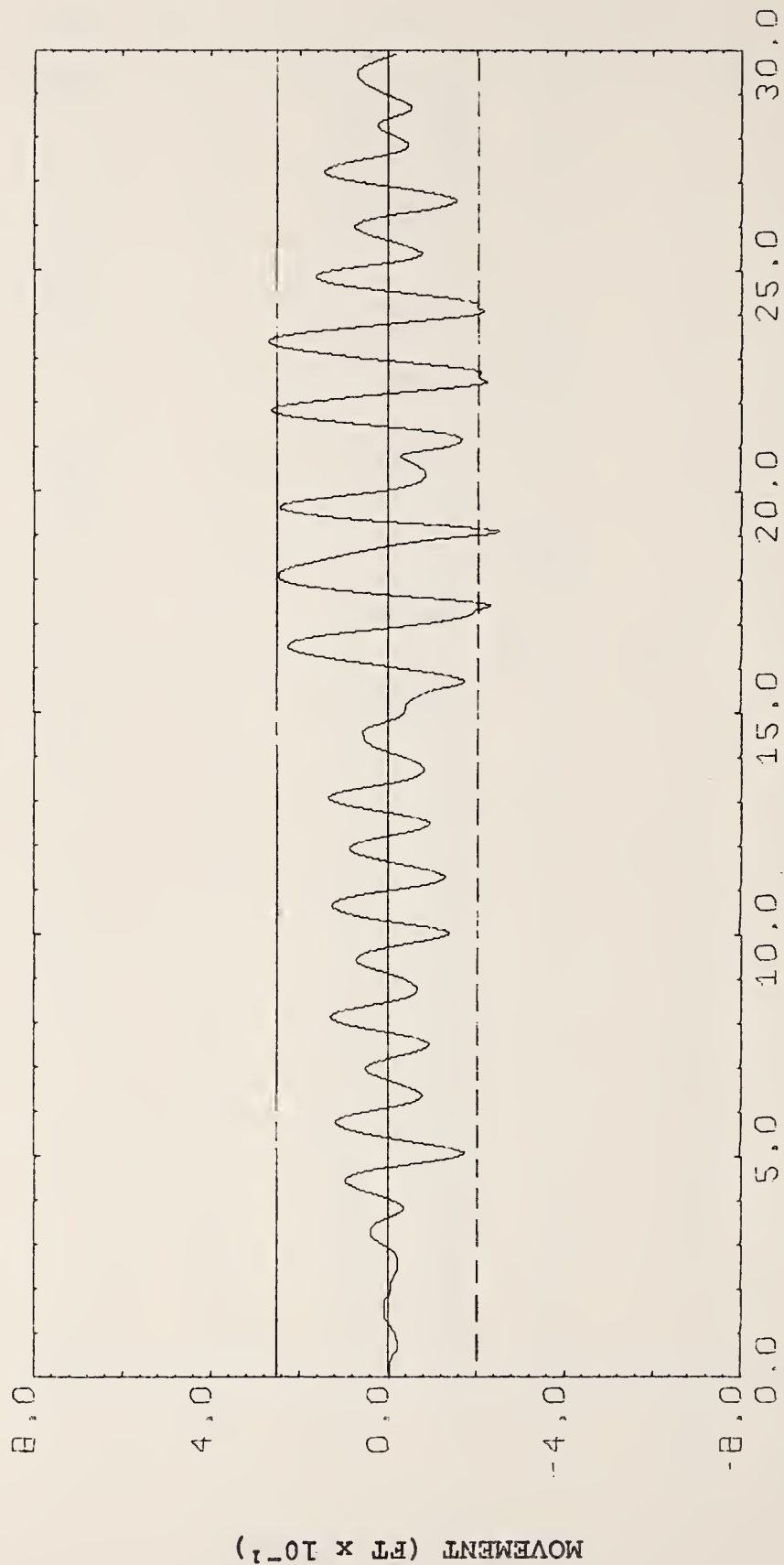
Expansion Joint Movement at Right Edge of Deck - Span 3 Joint

Bridge 3 - Case 17



Expansion Joint Movement at Left Edge of Deck - Span 3 Joint

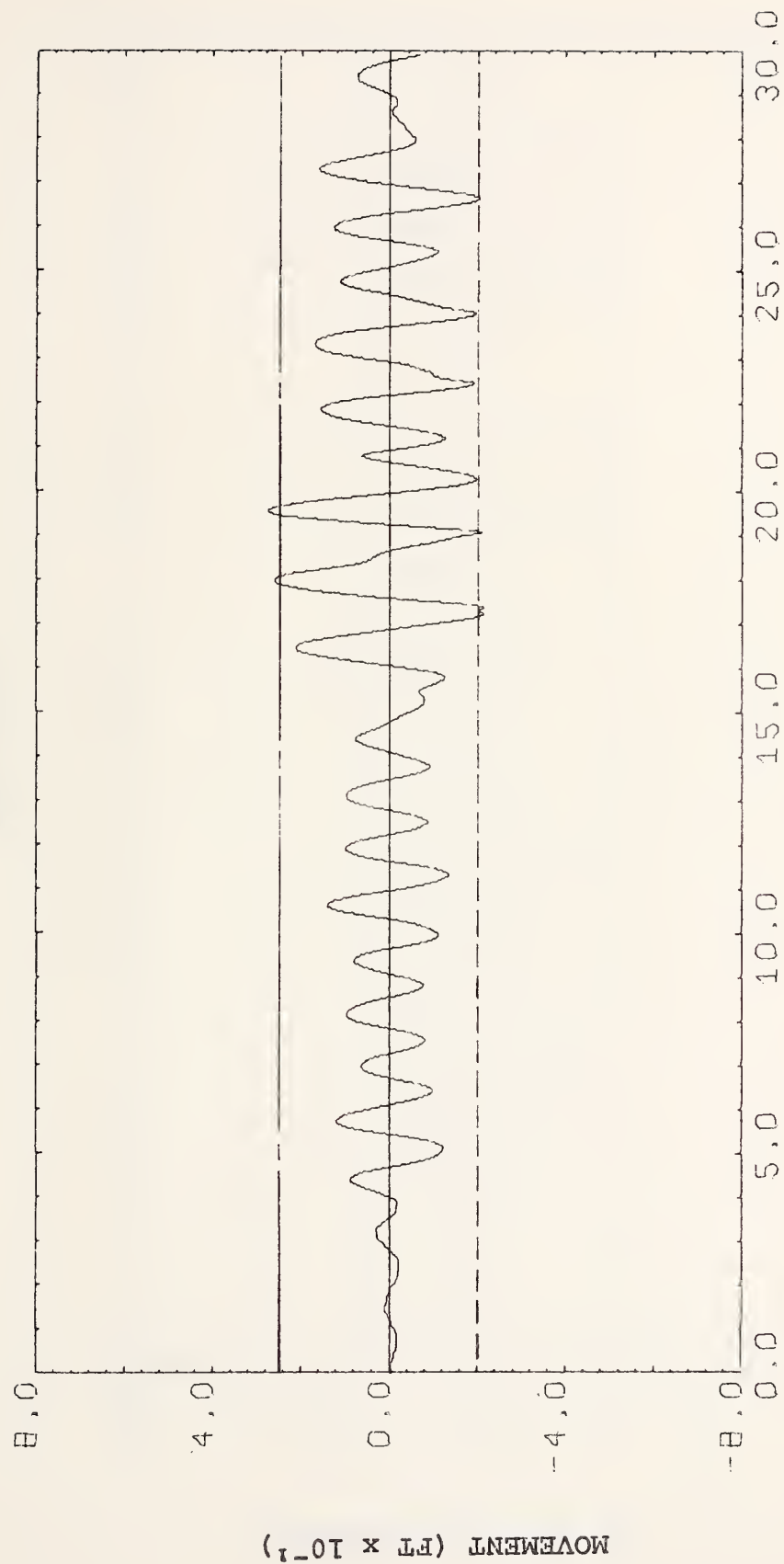
Bridge 3 - Case 17



TIME (SEC)

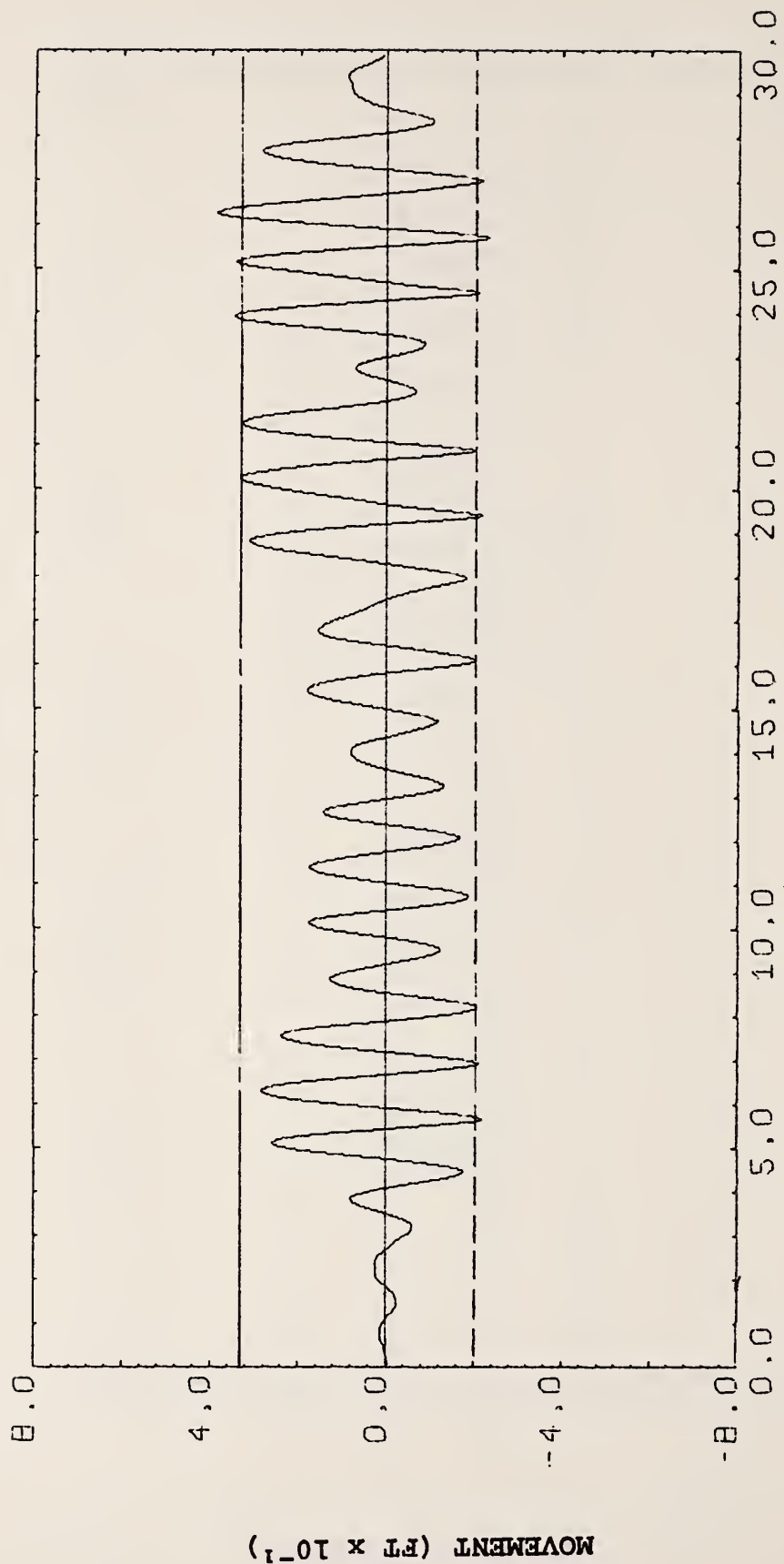
Expansion Joint Movement at Right Edge of Deck - Span 7 Joint

Bridge 3 - Case 17

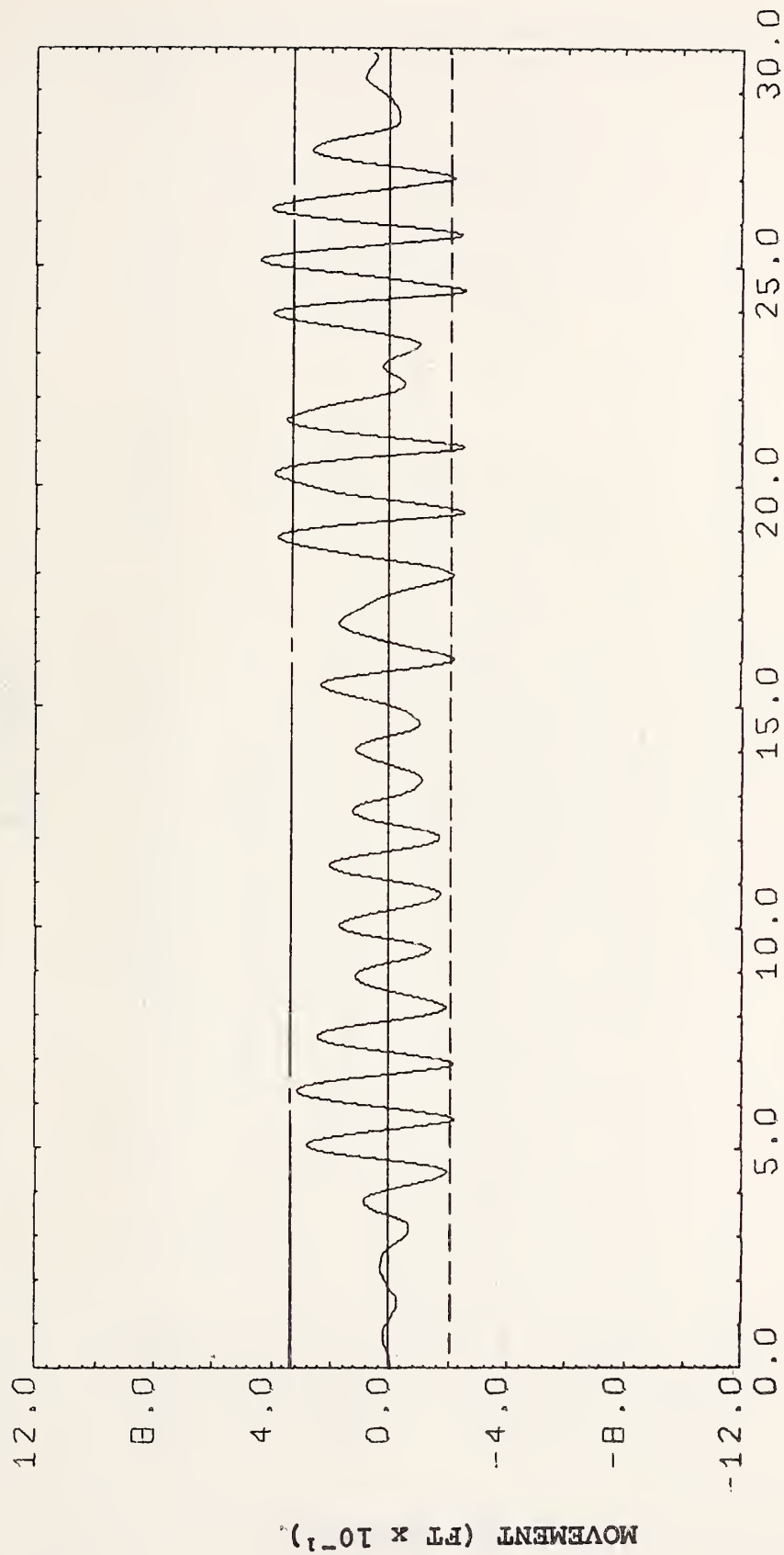


Expansion Joint Movement at Left Edge of Deck - Span 7 Joint

Bridge 3 - Case 17



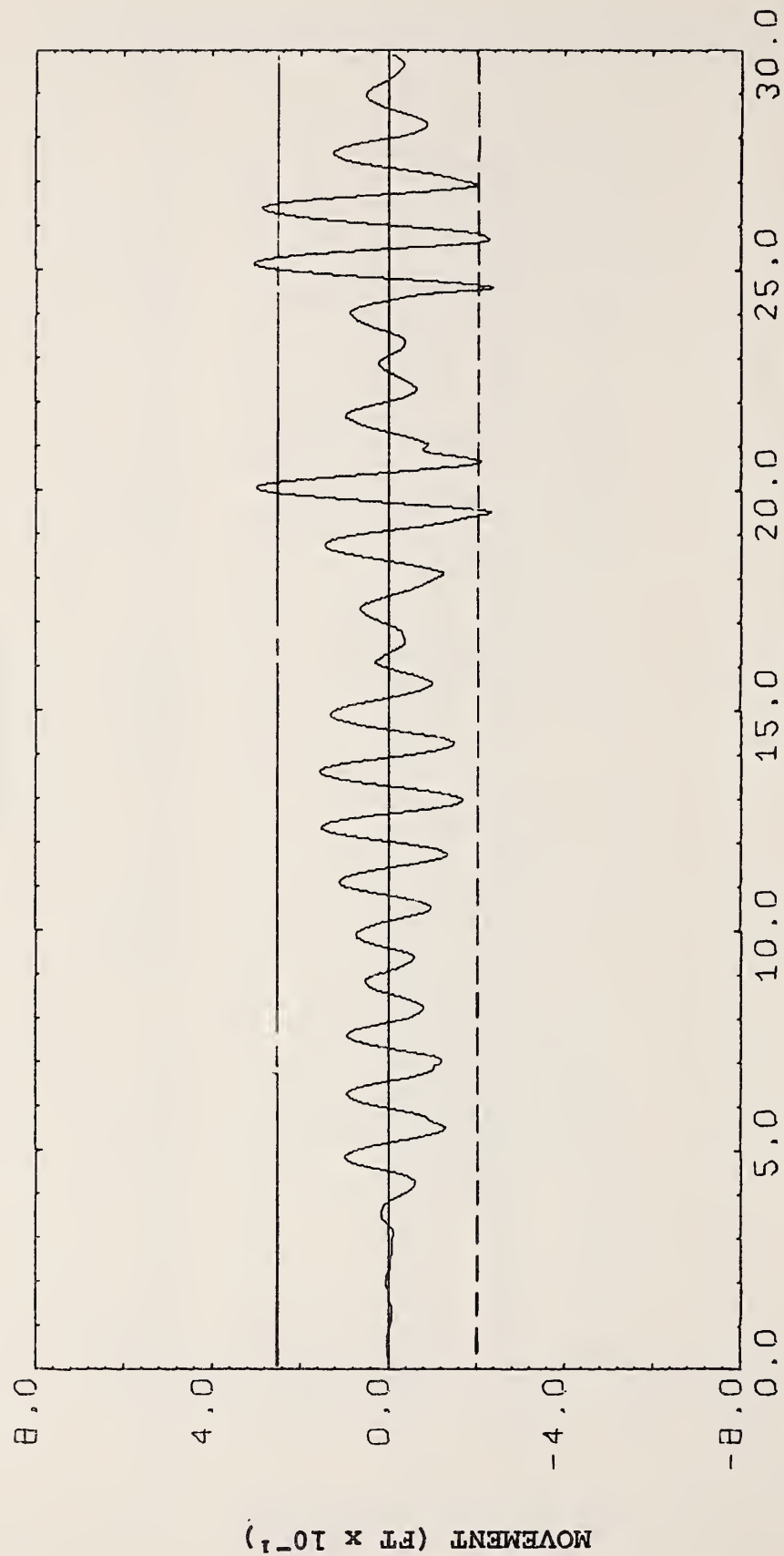
Expansion Joint Movement at Right Edge of Deck - Span 3 Joint
Bridge 3 - Case 18



TIME (SEC)

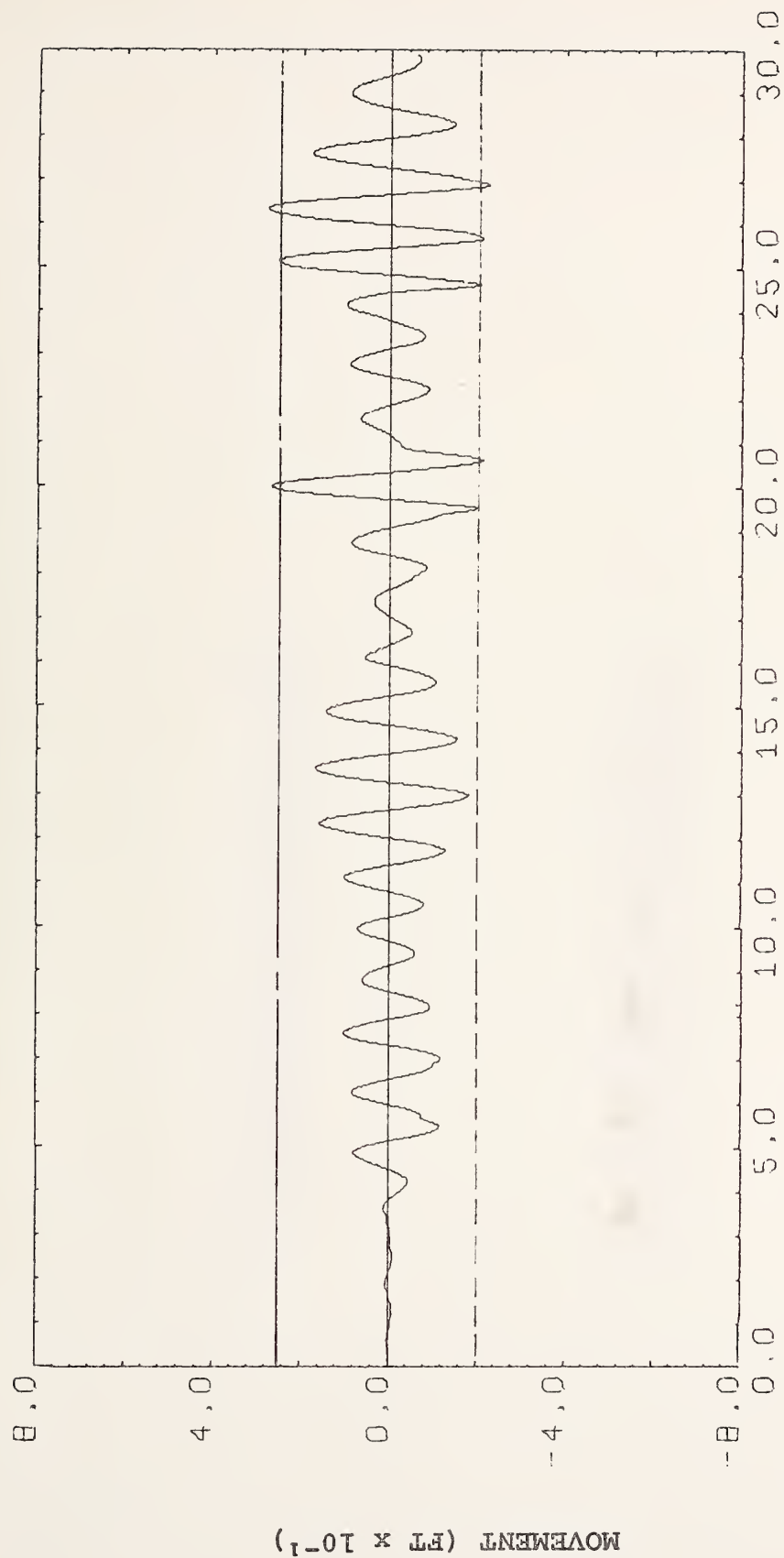
Expansion Joint Movement at Left Edge of Deck - Span 3 Joint

Bridge 3 - Case 18



Expansion Joint Movement at Right Edge of Deck - Span 7 Joint

Bridge 3 - Case 18



TIME (SEC)

Expansion Joint Movement at Left Edge of Deck - Span 7 Joint

Bridge 3 - Case 18

TE 662

U

.A3
no. FHWA-RD-

BORROWER

78-157

Michael

FEDERALLY COORDINATED PROGRAM OF HIGHWAY RESEARCH AND DEVELOPMENT (FCP)

The Offices of Research and Development of the Federal Highway Administration are responsible for a broad program of research with resources including its own staff, contract programs, and a Federal-Aid program which is conducted by or through the State highway departments and which also finances the National Cooperative Highway Research Program managed by the Transportation Research Board. The Federally Coordinated Program of Highway Research and Development (FCP) is a carefully selected group of projects aimed at urgent, national problems, which concentrates these resources on these problems to obtain timely solutions. Virtually all of the available funds and staff resources are a part of the FCP, together with as much of the Federal-aid research funds of the States and the NCHRP resources as the States agree to devote to these projects.*

FCP Category Descriptions

1. Improved Highway Design and Operation for Safety

Safety R&D addresses problems connected with the responsibilities of the Federal Highway Administration under the Highway Safety Act and includes investigation of appropriate design standards, roadside hardware, signing, and physical and scientific data for the formulation of improved safety regulations.

2. Reduction of Traffic Congestion and Improved Operational Efficiency

Traffic R&D is concerned with increasing the operational efficiency of existing highways by advancing technology, by improving designs for existing as well as new facilities, and by keeping the demand-capacity relationship in better balance through traffic management techniques such as bus and carpool preferential treatment, motorist information, and rerouting of traffic.

3. Environmental Considerations in Highway Design, Location, Construction, and Operation

Environmental R&D is directed toward identifying and evaluating highway elements which affect the quality* of the human environment. The ultimate goals are reduction of adverse highway and traffic impacts, and protection and enhancement of the environment.

4. Improved Materials Utilization and Durability

Materials R&D is concerned with expanding the knowledge of materials properties and technology to fully utilize available naturally occurring materials, to develop extender or substitute materials for materials in short supply, and to devise procedures for converting industrial and other wastes into useful highway products. These activities are all directed toward the common goals of lowering the cost of highway construction and extending the period of maintenance-free operation.

5. Improved Design to Reduce Costs, Extend Life Expectancy, and Insure Structural Safety

Structural R&D is concerned with furthering the latest technological advances in structural designs, fabrication processes, and construction techniques, to provide safe, efficient highways at reasonable cost.

6. Prototype Development and Implementation of Research

This category is concerned with developing and transferring research and technology into practice, or, as it has been commonly identified, "technology transfer."

7. Improved Technology for Highway Maintenance

Maintenance R&D objectives include the development and application of new technology to improve management, to augment the utilization of resources, and to increase operational efficiency and safety in the maintenance of highway facilities.

* The complete 7-volume official statement of the FCP is available from the National Technical Information Service (NTIS), Springfield, Virginia 22161 (Order No. PB 242057, price \$45 postpaid). Single copies of the introductory volume are obtainable without charge from Program Analysis (HRD-2), Offices of Research and Development, Federal Highway Administration, Washington, D.C. 20590.

DOT LIBRARY



00056140

